UNDERSTANDING THE RELEVANCE OF EPIGENETIC REPROGRAMMING FOR RESISTANCE TO HDAC INHIBITORS IN CANCER CELLS

Thesis submitted in accordance with the

requirements of the University of Liverpool for

the degree of Doctor in Philosophy

by

Venkateswarlu Perikala

December 2016

This thesis is dedicated to my mother who passed away during my PhD studies.

Table of Contents

Abstract

Therapeutic responses to Histone deacetylase (HDAC) inhibitors (HDACi) in many cancers are well described but development of resistance to HDACi is a major stumbling block. Whether HDACis induce epigenetic reprogramming and how this contributes to relapse is not reported. A CTCL cell line HuT78, and a CLL cell line MEC1, were used to develop HDACi resistant clones (RHuT78 and RMEC1 respectively) that persistently grow in the presence of the clinically used HDAC inhibitor Romidepsin. RHuT78 cells show perturbed trimethylation of histone H3 lysine K4 on Romidepsin treatment which linked to higher protein expression levels of the implicated demethylase KDM5A. Following on from these experiments, a qRT-PCR epigenetic gene expression array was used to quantify levels of 84 epigenetic gene transcripts in RHuT78 cells and significantly altered genes were taken forward for further investigation. Studies of gene expression patterns in parental, resistant and 'drug holiday' cell lines of both HuT78 and MEC1 led to particular interest in HDAC8, DNMT3A and DNMT3B. Functional studies showed that HDAC8 overexpression increased proliferation and resistance of HuT78 cells to Romidepsin. Parallel observations suggested an increase in proliferation of resistant cell lines cultured in the presence of the HDACi. This increased proliferation was seen even with lower concentrations of Romidepsin and argues against prolonged monotherapy using HDACis. Significantly, inhibitors of DNA methyltransferases synergised with Romidepsin in a dose and schedule dependent manner, reversing the changes in epigenetic gene expression associated with resistance and causing increased apoptosis in RHuT78 cells. Taken together this thesis identifies and characterises an unacknowledged contribution of epigenetic reprogramming to drug resistance and provides insights into the effects of Romidepsin on the epigenome that could potentially contribute to HDACi resistance.

List of figures

List of tables

List of appendix figures

List of appendix tables

Acknowledgements

I would like to take this chance to express my deepest respect and gratitude to my primary supervisor Dr. Nagesh Kalakonda for giving me the chance to join his lab. Also, for his endless support, advice and encouragement that he gave me throughout my study. I also give thanks to my secondary supervisor Dr. Joseph Slupsky for his constant help and support.

I deeply thank my colleagues and friends Dr. Andrew Duckworth and Dr. John Allen for their constant day to day support, experimental discussion and critical reading of my thesis.

I also extended my acknowledgements to the rest of my friends and colleagues: Dr. Mark Glenn (help with Lentiviral knockdown work); Dr Lakis Liloglou (providing progress reports, cytogenetic analysis and the drug Decitabine); Dr. Jemma Blocksidge (proof reading my thesis); Anil Kumar Mondru (Proof reading introduction and constant support); Dr. Alix Bee (help with tissue culture); Dr. Mosavar Farahani (advise related to PCR arrays); Dr Gillian Johnson (supplying PI and DioC6); Sofia Karatasaki (help with Western blotting); Dr. Al-sanabra Ola (transfections); A Ahmed Al-Shantti; Faris Tayeb; Dr. Omar Alishlash; Moses Lucas (access to flow cytometer); Dr Monday Ogese (use of qRT-PCR machine and reagents); Dr Athina Giannoudis (supply of resistant cell lines); Dr. Imad Malki (supply of antibodies); Jehad Alhmoud; and Alzahra Alshayeb; Sozan Karim and indeed many others.

I would like to take this chance to thank the Government of India for sponsoring my project, and Celgene for supplying the drug Romidepsin.

Finally, I would like to give special thanks to my family, especially my wife, brother, and sister back in India for their eternal support and encouragement.

Declaration

I, Venkateswarlu Perikala, declare that all of the data presented in this thesis is a result of my own work and efforts and was generated from the experiments that I have performed during my PhD, apart from the Lentivirus shRNA knockdown transductions that were performed by Dr Mark Glenn.

Abbreviations

ABC transporter	ATP-binding cassettes transporter
AML	Acute myeloid leukaemia
ALL	Acute lymphocytic leukaemia
ATCC	American type culture collection
5-Aza	5-Azacytidine
CpG	Cytosine and guanine nucleotides
CBP	CREB-binding protein
cDNA	Complementary deoxyribonucleic acid
CTCL	Cutaneous T-cell lymphoma
DLBCL	Diffuse large B-cell lymphoma
DMEM	Dulbecco's modified eagle's medium
DNMT	DNA methyltransferase
DNMTi	DNA methyltransferase inhibitor
DMSO	Dimethyl sulfoxide
ΔCT	Threshold cycle
ECL	Enhanced chemi-luminnescence
E. coli	*Escherichia coli*
EDTA	Ethylenediaminetetraacetic acid
EtBr	Ethidium bromide
FACS	Fluorescence-activated cell sorting
FBS	Fetal bovine serum

FDA	Food and drug administration
FL	Folicular lymphoma
GAPDH	Glyceraldehyde3-phosphate dehydrogenase
GFP	Green fluorescent protein
HAT	Histone acetyltransferase
HATi	Histone acetyltransferase inhibitor
HDAC	Histone deacetylase
HDACi	Histone deacetylase inhibitor
HDM	Histone demethylase
HMT	Histone methyltransferase
HRP	Horseradish peroxide
IC_{50}	Inhibitory concentration 50
IMDM	Iscove's Modified Dulbecco's Medium
mA	Milliamperes
MAPK	Mitogen activated protein kinase
MDR	Multidrug resistance
MDS	Myelodysplastic syndrome
MM	Multiple myeloma
mL	Millilitre
mRNA	Messenger ribonucleic acid
mg	Milli-gram
mins	Minutes
miRNA	MicroRNA
µg	Micro-gram

µl	Micro-litre
µM	Micro-molar
NaB	Sodium Butyrate
NES	Nuclear export signal
NLS	Nuclear localisation signal
nM	Nanomolar
PBS	Phosphate buffer saline
PCR	Polymerase chain reaction
P-gp	P-glycoprotein
PRC1/2	polycomb-group repressive complex1
PTM	Post translational modification
PVDP	Polyvinylidene difluoride
qRT-PCR	Quantitative real time polymerase chain reaction
Romi	Romidepsin
RT	Room temperature
SAM	S-adenosylmethionine
SEM	Standard error of mean
siRNA	Small interfering RNA
shRNA	Short hairpin RNA
SDS	Sodium dodecyl sulphate
PAGE	polyacrylamide gel electrophoresis
SWI/SNF	SWItch/Sucrose Non-Fermentable
T0	Initial time or Time=0
TBE	Tris borate buffer

TBST	Tween-Tris buffered saline
TSS	Transcription start site
UV light	Ultraviolet light
U	Unit
UK	United Kingdom
USA	United States of America
WB	Western blotting
WCL	Whole cell lysate
WT	Wild type

Chapter 1

General Introduction

1.1 Overview of thesis

This thesis is focused on histone deacetylase (HDAC) inhibitors (HDACi) and the way in which these drugs reprogram the 'epigenome' in normal and drug resistant settings. As HDACis are currently used in the clinical treatment of relapsed cutaneous T cell lymphoma (CTCL), the CTCL derived cell line HuT78 was predominantly employed in most experiments. Primarily the introduction will therefore provide a background into epigenetics, with a particular emphasis on histone post translational modifications (PTMs) and DNA methylation, and the enzymes that control these processes. The introduction will also address HDACis, with an emphasis on Romidepsin as this drug was the main compound used to investigate effects on the epigenome. DNA methyltransferase (DNMT) inhibitors (DNMTis) were used during my fourth experimental chapter and therefore an introduction into this family of drugs is also provided. As the development of resistance towards HDAC inhibitors in CTCL is closely linked to my work, this topic will be introduced.

Thus, the introduction has the following main topics:

- Definition of Epigenetics and processes
- DNA methylation
    - Including enzymes and inhibitors
- Histone PTMs
    - Histone Acetylation including HDACs and histone acetyltransferases (HATs), and their inhibitors
    - Histone methylation including lysine and arginine methylation and the respective enzymatic activities
- Background of CTCL
- Aims and Hypotheses of this thesis

1.2 Definition of Epigenetics and processes

Epigenetics is broadly defined as the study of heritable changes in gene expression that are brought about without perturbation of the underlying nucleotide sequence[1]. Conrad Waddington coined the term "Epigenetics'' to define the various genetic interactions between phenotype and genotype. Known epigenetic mechanisms include transcriptional alteration of mRNA and protein expression by DNA methylation[2], post translational modifications (PTMs) of histone proteins[3] and chromatin remodelling[4], mRNA alternative splicing and

microRNA (miRNA) expression mediated mRNA translational regulation. **Figure 1.1**[5] depicts how the interplay between epigenetics and genetics impacts on gene regulation and protein expression. Because this thesis does not investigate splice variants or miRNA, these subjects will not be discussed further.

1.3 DNA methylation

DNA methylation is an 'epigenetic' mark found in both unicellular and multicellular organisms. In a multicellular genome, DNA methylation occurs on cytosine residues by the covalent attachment of a methyl group from the methyl donor S-adenosylmethionine (SAM) to the carbon-5 position of cytosine to form 5-methyl cytosine[6] (**Figure 1.2**)[5]. This change is catalysed by DNA methyltransferases (DNMT). DNA methylation is reversible either by DNA replication in the absence of DNMTs or can occur as a consequence of deglycosylation of the cytosine base, with subsequent excision and repair mechanisms[7].

Many methylated cytosine residues lie within repeat sequences in the genome. However, groups of cytosine and guanine nucleotides, called "CpG islands", are also found predominantly

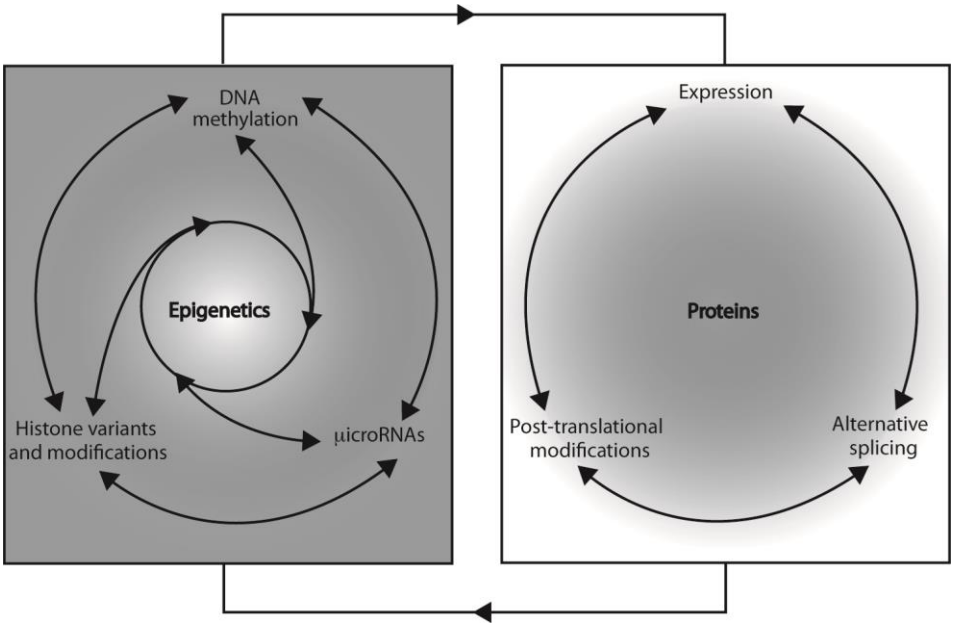

Figure 1.1 - Overview of epigenetic and its effects on protein regulation.

This figure illustrates the fundamentals of how epigenetics can interplay with protein expression and function, and vice versa. Three major forms of epigenetics (DNA methylation, histone PTMs and microRNA) are shown in the box on the left, with each form shown to regulate one another. The right box highlights protein regulation and the three forms of control which are protein expression levels, alternative transcript splicing and PTMs. Again, each mechanism of control can regulate other forms of regulation. Finally, the two boxes are joined by reciprocal arrows which highlight that these mechanisms control and regulate one another in a dynamic fashion (adapted from *Mark Glenn et al.*[5]).

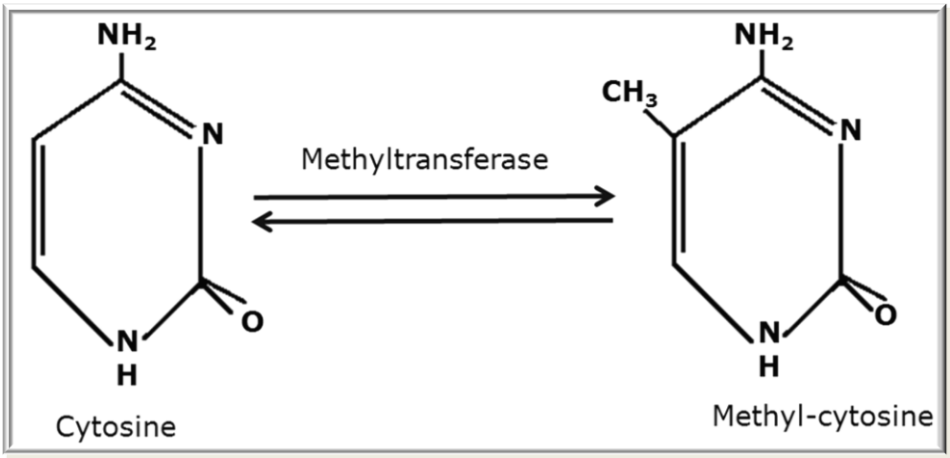

Figure 1.2 - Diagram illustrating the biochemical conversion of cytosine to 5-methyl–cytosine by DNA methyltransferases.

---

within gene promoter regions and are targets and hot-spots for DNA methylation[8]. Methylation of these regions represses gene transcription by hindering binding of transcriptional activators and regulators, and by recruiting DNA methylation binding proteins (e.g. MeCP2[9-11]) leading to chromatin condensation. Examples of cellular effects of DNA methylation include inactivation of the X-chromosome and genomic imprinting[12].

1.3.1 Classification of DNA methyltransferases (DNMT)

DNA methylation is catalysed by two different classes of enzymes known as 'maintenance' (the methylation of new

daughter strands after DNA replication) and *de novo* DNMTs. To date, three identified DNMT enzymes are described which are DNMT1, DNMT3A, and DNMT3B[13-15]. A DNMT3-like regulatory protein (DNMT3L) is also required for correct function of DNMT3A/B, but does not encode DNA methyltransferase activity and therefore will not be further discussed. (N.B. DNMT2 is now classified as a tRNA aspartic Acid methyltransferase and hence is not reviewed).

DNMT1 was first identified as an enzyme containing 1620 amino acids composed of a C-terminal catalytic domain and N-terminal regulatory domain with different functions[6,16]. DNMT1 plays a major role in 'maintenance' methylation[13] due to its preference for a hemi-methylated DNA substrate[17] and therefore has major roles during embryonic development, genomic imprinting, and inactivation of the X-chromosome[18,19]. Alongside these functions, it is also believed to contribute to *de novo* methylation by interacting with DNMT3A and DNMT3B (see below).

DNMT3A and DNMT3B are *de novo* methyltransferases. The important function of these enzymes is to bind to CpG regions and establish the methylation patterns of pre-replicated DNA[14]. The *de novo* methyltransferases first methylate the nascent

strand of DNA, producing hemi-methylated DNA. Subsequently, DNMT1 maintains existing methylation patterns of the hemi-methylated DNA and copies methyl groups to the newly synthesised complementary strand of DNA[20]. This phenomenon is observed both during embryogenesis and in adult tissues. DNMT3A methylates DNA at specific sites of the genome by interacting with unmethylated lysine 4 on histone H3 (see section 1.6.1 on histone post translational modifications below)[21]. DNMT3A interacts with histone modifying proteins SUV39H1, SETDB1 and G9A which are linked to lysine 9 methylation on histone H3 causing transcriptional repression by promoting a condensed chromatin structure[21]. Several studies suggest that DNMT3A also methylates non-CpG sequences of T, C and A, where it referred to as CpH methylation but the functional consequences and significance remains controversial[22].

1.3.2 DNA methylation and cancer

The study of DNA methylation has found genome-wide and locus-specific hyper- and hypo-methylation patterns that are characteristic of tumour cells[23]. In cancer, hyper-methylation of promoters is often found at tumour suppressor genes and is accompanied with the down regulation or silencing of their

expression; In contrast, hypo-methylation is associated with oncogenes causing their up-regulation and overexpression[24]. Aberrant DNA methylation patterns are linked to various types of human malignancies (**Table 1**)[5]. Also, numerous studies have identified that the hyper-methylation of certain genes is a prognostic marker in different types of cancer such as lung, gastric, oesophageal, colon, pancreatic, acute lymphoblastic (ALL) and acute myeloid leukaemia (AML)[25,26]. Such genes are involved in apoptosis, cell cycle regulation, drug resistance, differentiation and DNA repair[23].

Alongside changes in methylation, accumulating evidence suggests that up-regulation of DNMTs leads to neoplastic transformation of the cell[23]. Methyltransferases are highly expressed in different tumour types, particularly DNMT3B, which is commonly overexpressed in many cancers including leukemia[27]. Recent studies have revealed that DNMT3A mutations are not uncommon in both myeloid and lymphoid malignancies[22]. Other investigations have also identified additional mutations in DNMT1 and DNMT3A genes in various types of cancers, including colorectal, adenocarcinoma, prostate and haematological malignancies[22]. For example, loss of function mutations in DNMT3A leads to adverse clinical outcomes in AML[28].

Table 1 - Prevalence of single gene DNA methylation aberrations in mature lymphoid neoplasms.

Disease	Gene	Prevalence (%)	Function
CLL	CALC1	100	Calcium metabolism
	DAPK1	100	Cell death
	PCDHGB7	100	Cell adhesion
	SFRP1	100	Wnt signaling
	HOXC10	79	Homeobox gene
	APC2	77	Wnt signaling
	POU3F3	77	Homeobox gene
	ADAM12	72	Protease
	LHX2	69	Homeobox gene
	sFRP2	69	Wnt signaling
	RLN2	63	Hormone
	CDH1	60	Adhesion
	HOXA5	59	Homeobox gene
	CD38	58	Adhesion
	LRP1B	56	LDL receptor
	CDKN2B	50	G1–S cell cycle control
	ZAP-70	50	Kinase
	RASSF10	50	Tumor suppressor
MCL	DBC-1	100	Tumor suppressor
	SHP1	85	Phosphatase
	p16	82	Cell cycle control
FL	SHP1	100	Phosphatase
	DBC-1	100	Tumor suppressor
	AR	96	Androgen receptor
	DAPK1	85	Cell death
	ABF-1	60	Transcriptional repressor
	GSTP1	56	Xenobiotic detoxification
	p15	50	Cell cycle control
	p16	50	Cell cycle control
BL	ABF-1	90	Transcriptional repressor
	PLK2	90	Kinase
	BMP6	83	Cytokine
	CD44	62	Adhesion
	DUSP16	60	Phosphatase
	GSTP1	52	Xenobiotic detoxification
DLBCL	DBC-1	100	Tumor suppressor
	SHP-1	93	Phosphatase
	ABF-1	75	Transcriptional repressor
	BMP6	60	Cytokine
	$p57^{KIP2}$	55	Tumour suppressor
MALT	SHP-1	82	Phosphatase
	DAPK1	72	Cell death
	GSTP1	50	Xenobiotic detoxification
MZL	p16	75	Cell cycle control
	MAD2	61	Cell cycle control

Genes with >50% prevalence are listed; CLL: Chronic lymphocytic leukemia; MCL: mantle cell lymphoma; FL: follicular lymphoma, BL: Burkitt's lymphoma, DLBCL: diffuse large B cell lymphoma; MALT: mucosa associated lymphomas; MZL: marginal zone lymphomas(adapted from *Mark Glenn et. al.*[5])

1.3.3 DNA methyltransferase inhibitors

DNA methylation inhibitors (DNMTi) cause re-expression of tumour suppressor genes, induce apoptosis, DNA hypomethylation, degradation of DNMTs and inhibition of proliferation. DNMTis are broadly divided into nucleoside and non-nucleoside inhibitors based on their structure and mode of action[29]. Nucleoside inhibitors include 5-Azacytidine (Vidaza), Decitabine (Dacogen), Zebularine, Cytarabine, and 5-Fluoro-2-deoxycytidine (FdCyd). Non-nucleoside inhibitors include Procaine, MG98, RG-108, Hydralazine, Epigallocatechin-3-gallate and Genistein (**Table 2**)[30-36].

1.3.3.1 Nucleoside DNMTis

The US Food and Drug Administration (FDA) has approved 5-Azacytidine and Decitabine for the treatment of haematological malignancies including AML and myelodysplastic syndrome (MDS) as clinical responses are well documented[37,38]. Both of these drugs target all DNMT isoforms and act as covalent inhibitors of their action. 5-Azacytidine is a pyrimidine nucleoside analogue isolated from *Streptoverticillium ladakanus*[39], which is repeatedly phosphorylated *in vivo* to form 5-Azacytidine triphosphate (by uridine-cytidine and pyrimidine kinases) after which it can then be incorporated into RNA and

Table 2 – Classes of DNA methyltransferase inhibitors and their current status in the FDA clinical drug developmental process.

DNMT analogues	Inhibitors/derivatives	Preclinical phases
Nucleoside analogues	5-Azacytidine	FDA approved in MDS
	Decitabine	FDA approved in MDS
	5,6 dihydroazacytidine	Preclinical
	5-fluro-2'doecytodine	Preclinical
	Zebularine	Preclinical
	NPEO-DAC	Preclinical
	SGI-110	Phase I
	CP-4200	Phase I
Non-Nucleoside analogues	Hydralazine	Preclinical
	Procainamide	Preclinical
	Procaine	Preclinical
	Epigallocatechin-3- Gallate	Preclinical
	Mithramycin A	Phase I/II
	Nanomycin A	Phase I
	RG-108	Preclinical
	SGI-1027	Preclinical
	NSC-14778	Phase II
	NSC-106084	Preclinical

to a lesser extent into DNA[31]. The pharmacological action of 5-Azacytidine mainly depends on the presence of the altered carbon-5 position of the pyrimidine ring[40]. Incorporation of the drug into RNA interrupts protein synthesis[41]. Integration of 5-Azacytidine into DNA results in a covalent complex with the enzyme DNMT1 resulting in its inhibition and degradation of this protein. Subsequently, further conversion of cytosine to 5-methylcytosine in newly replicated DNA is inhibited leading to reduced DNA methylation, induction of DNA damage and consequently cytotoxicity, especially during S phase of the cell cycle[40,42,43].

Decitabine or 5-aza-2-deoxycytidine is an S-phase (cell cycle) specific agent[44]. It is phosphorylated by various kinases and is directly incorporated into replicating DNA (but not into RNA), inactivating the DNMT1 enzyme which results in re-expression of genes silenced by hypermethylation[45]. Comparative studies carried out in animal models suggest that Decitabine produces less toxic effects and is a more effective inhibitor than 5-Azacytidine, therefore providing a high degree of antitumor activity[46].

1.3.3.2 Non-nucleoside DNMTis

Non-nucleoside compounds bind to and directly block the active site of DNMT1 in human cancerous cell lines and cause hypomethylation, reactivating tumour suppressor genes[47]. In breast cancer cells, Procaine competes with DNMT1 at CpG regions causing demethylation[48].

1.4 Histone PTMs

In all eukaryotes, the genetic material is packaged into the nucleus as chromatin. Chromatin is necessary for condensing and organising the long molecules of DNA and therefore controls many of its functional properties. The basic repeating unit of chromatin is the nucleosome, which incorporates ~147 base pairs (bp) of DNA that are tightly coiled around an octameric histone protein core complex. These 8 core proteins consist of 2 copies of the 4 histones: H2A, H2B, H3 and H4. Additional linker histones (H1/H5) couple nucleosomes to each other. The core and linker histones are critical for giving rise to higher order structures to condense the DNA into euchromatin or heterochromatin (**Figure 1.3**)[49]. This complex mechanism plays a crucial role in gene regulation[50,51]. In addition, the flexible amino-terminal "tail" of each of the 4 core histone proteins extends outside of the nucleosome and contributes to

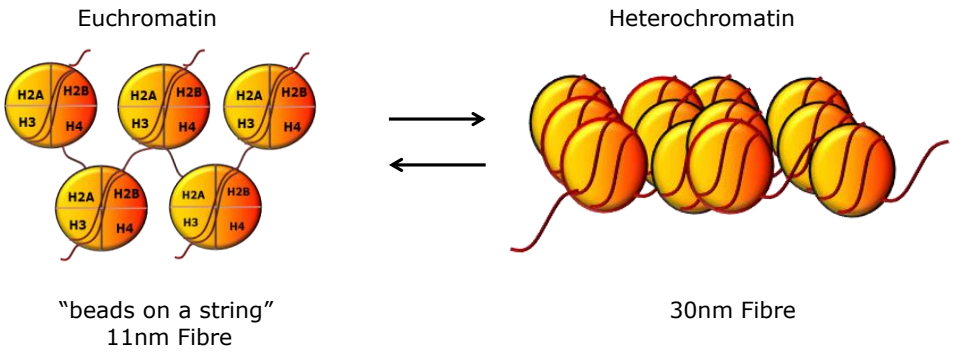

Figure 1.3 – Structural differences in euchromatin and heterochromatin.

This diagram describes how DNA is organised by histones into either euchromatin or heterochromatin. Euchromatin, also known as "beads on a string" (11 nm fibre), allows binding of transcriptional regulators due to its open structure and the accessibility to the DNA filament. In contrast, heterochromatin is a condensed form of chromatin (30 nm fibre) that restricts the access of transcriptional regulators to DNA binding sites and is associated with transcriptional repression. The two forms of chromatin are interchangeable and are tightly controlled by epigenetic histone PTMs (adapted from *Victoria Valinluck Lao et al*.[49]).

the regulation of chromatin structure. The amino acid sequence of these tails is highly conserved in all eukaryotes and is enriched with basic amino acid residues such as lysine (K) and arginine (R) that can be post-translationally modified.

Post-translational modification of histone tails modulates the access of proteins (e.g. transcription factors and the transcription initiation complex) to the DNA molecule. Examples of these are acetylation and methylation (of K and R residues), phosphorylation (of serine (S) and threonine (T) residues), ubiquitination, citrullination etc. (**Figure 1.4**)[52]. Enzyme families that catalyse these PTM are summarised in **Figure 1.5**. Because only acetylation and methylation of histone residues are discussed in this thesis, only these modifications will now be discussed in greater detail.

1.5 Histone Acetylation

In 1964, Allfrey and co-workers were the first to discover the acetylation of histones within chromatin[51]. Normally, most genes are hypoacetylated and are in a silenced or inactivated state. When a gene undergoes transcriptional activation, transcription factors trigger acetylation of histone proteins in nucleosomes of regulatory regions such as promoters. Therefore, histone acetylation is associated with activation of

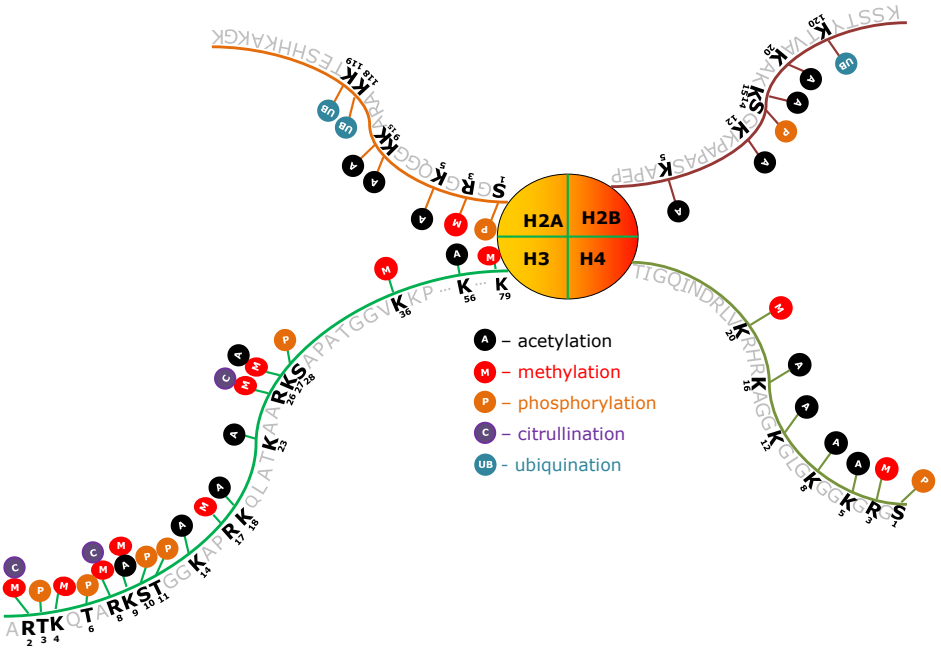

Figure 1.4 - Known PTMs of core histone protein tails.

Schematic figure showing known PTMs on histones tails of H2A, H2B, H3 and H4. The five major PTMs are shown. Amino acids that are modified are highlighted in black. Certain amino acids may have more than one possible modification - acetylation and methylation are exclusive marks on lysine residues, while citrullination and methylation can be present on the same arginine residue (adapted from *Tony Kourazides et al.*[53-56]).

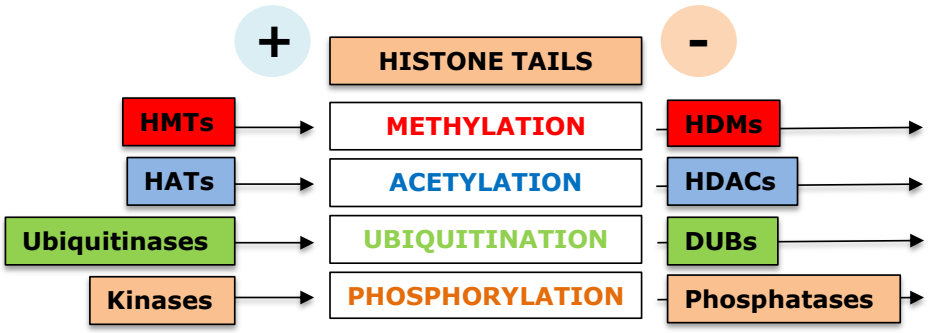

Figure 1.5 – Writers and Erasers of Histone PTMs.

The figure illustrates the general enzyme families that write (on the left) or erase (on the right) the histone PTMs of methylation, acetylation, ubiquitination and phosphorylation. HMT, histone methyltransferase; HDM, histone demethylase; HAT, histone acetyltransferase; HDAC, histone deacetylase; DUB, deubiquitinase.

transcription and can affect this process in two major ways. Firstly, acetylation of the amino groups of histone-tail lysines neutralises their positive charge and therefore reduces the attraction of the tail to the negatively charged DNA. This in turn reduces the interaction between DNA and histone proteins, relaxing chromatin structure and providing accessibility to the DNA for additional activating factors and transcriptional machinery[57-59]. Secondly, acetylation of histone tail lysines provides docking sites for bromodomain containing proteins. To maintain acetylation levels, a delicate balance is required between histone acetylation and deacetylation which is catalysed by the two opposing enzymes namely histone acetyltransferases (HATs) and histone deacetylases (HDACs).

1.5.1 Histone acetyltransferases (HATs)

HATs (also known as lysine acetyltransferases (KATs) due to their ability to target non-histone proteins), are enzymes that form multi subunit protein complexes that catalyse the transfer of an acetyl group from acetyl-coenzyme A cofactor, to the amino group of an internal protein lysine side chain[57]. HATs can be classified into two major classes (Types A and B). These classes are segregated according to their cellular localisation, catalytic targets, and functional similarities. Type A HATs are

heterogenic enzymes found in the nucleus where they acetylate chromatin. In contrast, Type B HATs are restricted to the cytoplasm where they acetylate newly synthesised histone proteins and then transport *de novo* translated histones to the nucleus. HAT1 (KAT1) was the first identified HAT B catalytic protein and participates in a complex with HAT2 and RbAp46/48 protein found in chromatin. The HAT1 protein complex is involved in histone deposition and DNA repair[60,61].

Type A HATs can be organised into several families according to their structural homology (e.g. all MYST family members contain a MYST domain), target sites, and biochemical mechanism (**Table 3**)[60,61].

1.5.1.1 HATs and cancer

During normal cellular development, HATs play a crucial role in numerous biological processes such as cell proliferation, growth, and differentiation by interacting with transcriptional activators. Alterations of these enzymes disturbs the balance of acetylation state which is in general associated with numerous diseases particularly cancer[62]. Mutations in p300 and CBP genes have been reported in several cancers[63] and these result in p300/CBP tumour suppressor gene inactivity. Similarly, PCAF regulates various cellular pathways through acetylating

Table 3 - HAT families, functions and substrates.

HAT family	HAT complexes	KAT	Function	Organism	Histone Substrates
GNAT	Gcn5	KAT2A	Transcriptional activation, DNA repair	Yeast- human	H3K9,14,18,36
	PCAF (PCAF)	KAT2B		Yeast	H3K9,14,18,36
	Elp3	KAT9			
MYST	Tip60	KAT5	Transcriptional activation, DNA repair, replication, dosage compensation	Yeast	H4K5,8,12,16
	MOZ/MYST3	KAT6A		Yeast	H3K14
	MORF/MYST4	KAT6B			H3K14
	HBO1/MYST2	KAT7		Yeast	H4K5,8,12
	HMOF/MYST1	KAT8			H4K16
p300/CBP	CBP	KAT3A	Transcriptional activation	Worm to human	H2AK5, H2BK12,15 H4K14, 18, H4K5,8
	p300	KAT3B			H2AK5, H2BK12,15 H4K14,18 H4K5,8
$TAF_{II}250$	TAF1/TBP	KAT4	Transcriptional activation, Pol III transcription	Yeast to human	
	TFIIIC90	KAT12			H3K914, 18
SRC	SRC-1	KAT13A	Transcriptional activation	Mice to human	
	AIB1/ACTR/SRC3	KAT13B		Mice to human	
	P160	KAT13C			
	CLOCK	KAT13D			
HAT1	HAT1			Yeast to human	
	ATF-2				

histones and non-histone proteins by interacting with acetyl-lysine residues[64]. Overexpression of PCAF in glioblastoma results in increased cell proliferation and tumour formation by increasing acetylation and activity of Akt1[65]. Elevated endothelial growth factor signalling activity has been observed in many cancers which could be the result of GCN5 mutation[66].

1.5.1.2 HAT inhibitors

In order to regulate HAT activities several small molecules have been identified from natural sources and high throughput screening methods. These are mainly responsible for inhibiting cell proliferation and induction of apoptosis in various cell lines.

HAT inhibitors can be classified into natural products, synthetic derivatives and bi-substrate inhibitors[67-69]. HAT inhibitors obtained from natural sources are Anacardic acid, Curcumin, Garcinol and Epigalactocatechin-3-gallate. Anacardic acid is isolated from the cashew nut shell and has significant antitumor activity. It non-competitively inhibits both p300 and PCAF with an IC_{50} of 8.5μM and 5μM respectively[70]. Specifically, HAT dependant transcription is strongly inhibited but does not affect direct DNA transcription[71]. Previous studies have shown that Anacardic acid also inhibits the MYST family member Tip60[72]. Similarly, Curcumin is a polyphenolic derivative

obtained from rhizomes of *Curcuma longa.* It inhibits p300 and PCAF acetylation of histone H3 and histone H4 with an IC_{50} of 25μM[73]. It mainly inhibits cell proliferation and induces apoptosis in tumour cells. In addition to HAT inhibition, Curcumin also interacts with other epigenetic enzymes, namely DNA methyltransferases and HDACs. Currently it is under clinical development for the treatment of cancer, fibrosis and rheumatoid arthritis[70].

C646 is a recently identified small molecule which has selective and competitive inhibitory activity against p300. It also shows potent anti-cancer activity in melanoma and non-small cell lung cancer cell lines[74]. In AML cells, C646 suppresses histone acetylation and causes cell cycle arrest and apoptosis[75]. Currently, no single HAT inhibitor is as yet approved for clinical use.

1.5.2 Histone Deacetylases (HDACs)

HDACs catalyse the removal of an acetyl group from the ε-N-acetyl lysine amino acid. They can be broadly classified into 4 major classes of enzymes based upon sequence homology and domain structure (**Figure 1.6**)[76]. Class I, II and IV are considered as the classical HDAC enzymes as they all require Zn^{2+} as a cofactor and are more closely related. In contrast,

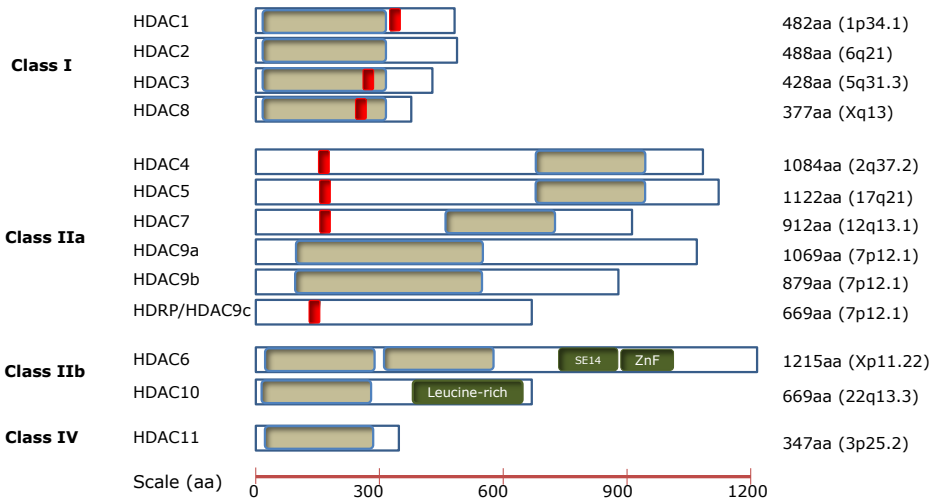

Figure 1.6 – Classification of HDAC members.

This figure shows the 13 major HDAC proteins identified in humans. The diagrams also illustrates catalytic domains (in tan colour), NLS (as non-annotated red boxes), and other domains (annotated green boxes). HDAC9 has 3 major isoforms as shown. aa, amino acids (adapted from *Holger Hess-Stumpp et al)*[76].

class III HDACs, known as the sirtuins, rely on NAD^+ for their catalytic activity. Each class is now described further, with particular focus on HDAC8 and HDAC9, as these were studied in more detail.

1.5.2.1 Class I HDACs

Class I HDACs are expressed ubiquitously in most cell types including yeast, plants, and mammalian cells. They are predominantly found in the nucleus, have a simple structure, and tend to be smaller (40-55kDa) proteins than class II HDACs[58]. In humans, there are 4 identified Class I HDACs that are HDAC1, 2, 3, and 8. These proteins are highly conserved; for example, HDAC1 is a paralogue of HDAC2 and both share >80% sequence homology with the yeast homologue Rpd3[77]. The localisation of HDACs varies depending upon the presence of a nuclear localisation signal (NLS). Interestingly, HDAC1, 2 and 8 have a NLS but do not have a nuclear export signal (NES) so they are restricted to the nucleus[78]. In contrast, HDAC3 is a membrane bound protein which has both a NES and NLS, therefore allowing movement from nucleus to cytoplasm and vice versa[79].

Overexpression and improper recruitment of different Class I HDAC isoforms is linked with various haematological

malignancies, particularly T-cell lymphoma[80,81]. Preclinical and clinical studies suggest that HDAC1, 2 and 3 have elevated expression in colorectal, gastric and pancreatic cancers associated with enhanced tumour cell proliferation with poor prognosis[82]. In addition, overexpression of HDAC2 and acetylated H4 is very common in indolent CTCL[81]. Mutations of HDAC2 have been found in cancer cell lines derived from human epithelial cells, which causes protein truncation and resistance to histone deacetylase inhibition by Trichostatin-A[83]. Knock out studies suggest that class I HDACs play a crucial role in cell proliferation (HDACs and proliferation are discussed in more detail in Section 1.5.2.5), survival and differentiation[82].

1.5.2.1.1 HDAC8

HDAC8 protein is 377 amino acids in length (molecular weight 45kDa) and is expressed ubiquitously in both the nucleus and cytoplasm[84]. Unlike other class I enzymes, HDAC8 has divergent functions and its activity is independent of additional co-factors[85]. However, it still shows a significantly high degree of sequence homology to class I HDACs, and a much lower homology (between 15-40%) to class II enzymes[86]. Several non-histones proteins are targeted by HDAC8 including p53, NCOA3, SMC3 and ARID1A. These genes regulate various

processes such as DNA repair, sister chromatid separation, microtubule integrity, muscle contraction and energy homeostasis[87]. A unique phosphorylation site on serine 39 of HDAC8 decreases the activity of the enzyme; whereas, phosphorylation of HDAC1 and HDAC2 on alternative residues leads to their activation[88]. Whether HDAC8 targets histone proteins *in vivo* remains controversial. Despite this, overexpression studies suggest that HDAC8 can mediate deacetylation of histone proteins *in vivo.* Also, *in vitro* studies show deacetylation of lysines 14, 16 and 20 on peptides of histone H4 by HDAC8[86,89].

Aberrant changes of HDAC8 have been found in different cancers, such as colon, breast, lung, prostate, pancreas and is particularly associated with childhood neuroblastoma as well as T-cell lymphoma[90-92]. HDAC8 protein overexpression significantly correlates with metastasis and poor prognosis[90]. Previous studies suggest that over expression of HDAC8 is linked with poor prognosis in neuroblastoma. In contrast, knock down of HDAC8 in neuroblastoma cell lines results in reduced differentiation, cell cycle arrest and inhibition of proliferation. Taken together these results indicate that increased expression of HDAC8 can lead to tumour cell progression[90].

1.5.2.2 Class IIa and IIb

In mammals, there are 6 different class II HDACs which are HDAC4, 5, 6, 7, 9, and 10[93]. These proteins play a dynamic role in cell differentiation and development processes but, their expression is limited to specific cell types[94]. The molecular masses of class II HDACs are between 120 and 130kDa and they share sequence homology with HDAC1 in mammals and other deacetylase genes in yeast, namely Hda1[58]. Class II HDACs have been further divided into two sub groups: class IIa (HDAC4, 5, 7 and 9) and class IIb (HDAC6 and 10) according to their sequence homology[85,93].

Class IIa HDACs have distinct N-terminal and C-terminal domains[93]. This class of HDACs can be controlled by phosphorylation. Upon becoming phosphorylated, as a result of intracellular signalling pathways, the HDACs can no longer interact with repressive transcription factors and leads to their export from the nucleus and the acetylation and activation of silenced genes[95-99]. Despite containing a conserved deacetylase catalytic domain, it is still unclear whether these enzymes can directly deacetylate protein substrates, including histones. They have unmeasurable activity on histone substrates in vitro, and it has been shown that enzymatic activity is facilitated by their

recruitment to multiprotein complexes that contain HDAC3. It is therefore hypothesised that these proteins are not true enzymes but in fact act more like adapter proteins[100]. Regarding their known roles in disease, mutations of HDAC4 have been found in patients with breast cancer and also elevated expression of HDAC5 and HDAC7 has been identified in cases of colorectal cancer with poor prognosis[82,101].

Class IIb HDACs are specifically found in the cytoplasm[58]. HDAC6 has two catalytic domains and a C-terminal zinc finger which directly binds to ubiquitinated proteins via its ubiquitin binding domain. HDAC6 mediates aggresome formation, regulates heat shock factor-1, and has a role in autophagy[102]. It also binds with several non-histone proteins like α-tubulin, heat shock protein 90 (HSP90), peroxiredoxins and interferon-αR which regulates the functions of cell adhesion and viability[103,104]. HDAC6 levels are high in diffuse large B-cell lymphoma, peripheral T-cell lymphoma, breast and oral squamous cell cancers[105].

HDAC10 has a single catalytic inactive N-terminus domain but its function remains unclear. Notably, it shows approximately 37% structural similarity to HDAC6 and interacts with HDAC1, 2, 3, 4, 5, and 7 but not with HDAC6[106,107].

1.5.2.2.1 HDAC9

There are 2 major splice variants of full length HDAC9 (HDAC9a), which are HDAC9b and HDRP/HDAC9c. These have tissue-specific expression patterns. HDAC9a and HDAC9b possess a deacetylase catalytic domain in the N-terminus, while HDAC9c/HDRP does not[108]. Overexpression of HDAC9 has been associated with poor prognosis in several malignancies including medulloblastoma, lung and cervical carcinomas[109]. Zhao and colleagues found that overexpression of HDAC9 promotes cell proliferation by inhibiting the transcription of p53 in osteosarcoma[110]. Interestingly, drug resistance to HDAC inhibitors in AML cell lines develops by up-regulating HDAC9 expression[111].

1.5.2.3 Class III

Class III HDACs have seven members (SIRT1 to SIRT7) and are widely expressed in different cell types. SIRT1, SIRT 6 and SIRT 7 are localized in the nucleus, SIRT 2 is located in the cytoplasm, and SIRT 3, SIRT 4, and SIRT 5 are found in the mitochondria. This class regulates different cellular functions, especially DNA repair and oxidative stress. These are structurally related to yeast SirT2 proteins and require the co-factor NAD^+ for deacetylase activity[112].

1.5.2.4 Class IV

Class IV has only one known member, HDAC11, found in heart, smooth muscle, kidney and brain, and is closely related to class I and class II. Its binding partners and substrates still remain unclear and have not yet been identified[113].

1.5.2.5 HDACs and their role in cell cycle control

Due to the observed findings in **Chapter 3** and **5** that Romidepsin induces proliferation in resistant HuT78 cells, the regulation of cell cycle by HDACs requires introduction.

The normal cell cycle is tightly regulated by cyclin dependant kinases (Cdks), and their associated cyclins and cell cycle inhibitors. An overview of the cell cycle stages, checkpoints and cell cycle regulators studied in this thesis are given in **Figure 1.7**[114]. The cell cycle inhibitor $p21^{WAF1/CIP1}$ is highlighted due to its regulation by HDACs (see below).

By inhibitor and knockdown/knockout studies, HDACs have been shown to play a major role in inhibiting transcription of tumour suppressor genes resulting in cell cycle progression, proliferation and differentiation. Treatment with HDACis activates these genes promoting the anti-proliferative effects,

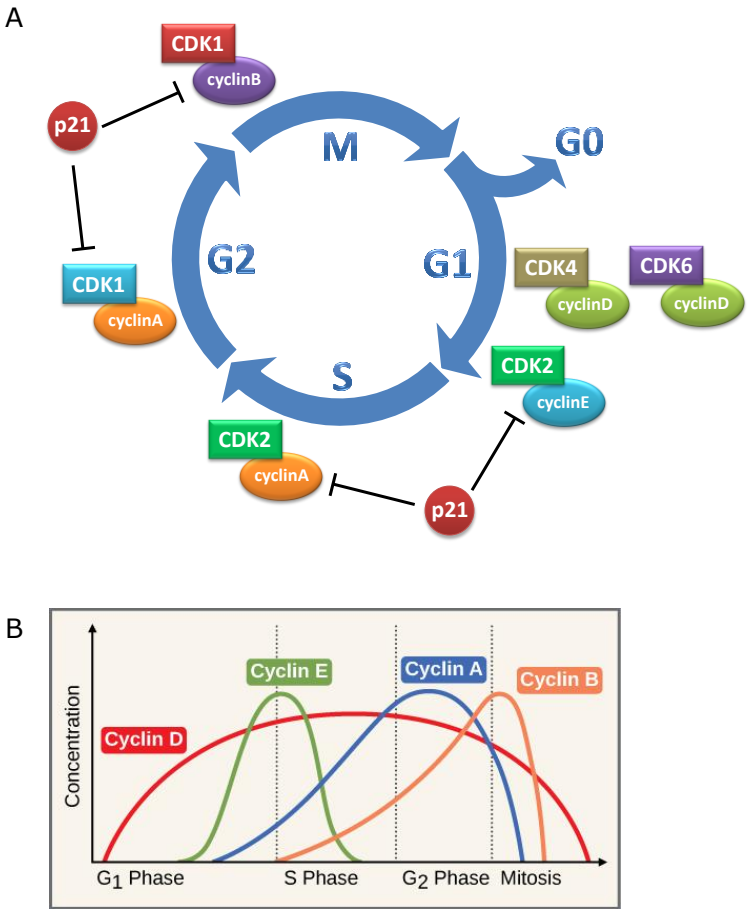

Figure 1.7 – Cell cycle and its control by CDKs and cyclin proteins.

Diagram illustrates cell cycle phases and their regulation by CDK/cyclin complexes and p21 in part A, while part B shows changes in levels of cyclin expression throughout the cell cycle. Briefly, the complex of cyclins with their CDKs drives the cell through cell cycle checkpoints (e.g. G1 to S phase checkpoint) while cell cycle inhibitors (such as the illustrated p21) inhibits this process (Adapted from *Richard G. Pestell et.al.)*[114].

apoptosis, differentiation etc. in both malignant cell lines and primary cells[115,116]. Previous studies suggest that several members of HDACs particularly HDAC1, 2, 3, 4, 5, 6, 8 and 9 are implicated in the regulation of cell cycle progression and proliferation in tumour cells[117,118]. Deletion of certain class I HDACs causes reduced proliferation in human transformed cells and also in murine cells[119]. Accordingly, class I HDACs have emerged as important therapeutic targets for specific inhibitors as anti-cancer drugs. HDAC1 inhibits the cyclin dependant kinase inhibitor $p21^{WAF1/CIP1}$ and therefore acts as a negative regulator of proliferation. Numerous other genes identified as HDAC1 targets also control proliferation[120]. Earlier studies revealed that silencing of HDAC1 gene results in overexpression of HDAC2 in embryonic stem cells (ES) and mouse embryos[121]. Similarly, deletion of HDAC1 gene has been shown to increase proliferation in T cells[122]. Both HDAC1 and HDAC2 have partially redundant functions due to 82% identity in the amino acid sequence. Their loss results in abnormalities in cell cycle progression, cell survival and differentiation[123-125]. Knockdown studies also disclose that both HDAC1 and HDAC2 enzymes enhance the expression $p21^{WAF1/CIP1}$ and induce apoptosis in human osteosarcoma and cervical cell lines respectively[126,127]. Similarly, HDAC3 and HDAC4 also inhibit the expression of

$p21^{WAF1/CIP1}$ in human cancerous cells and affect cell proliferation[128,129]. Ueda et al., reported that these drugs enhance the expression of cyclin dependant kinase inhibitor 1 (p21), cyclin E, and decrease mRNA expression of cyclin D1[130].

1.5.2.6 Histone deacetylase inhibitors

Histone deacetylase inhibitors (HDACi) are promising non-chemotherapeutic drugs and potent anti-cancer agents that are specifically used in the treatment of haematological malignancies such as cutaneous T-cell lymphoma (CTCL), peripheral T-cell lymphoma (PTCL), Hodgkin's and Non-Hodgkin lymphoma and other solid tumours[131] (see **Table 4** for summary)[132]. These agents have two effects. The first is to inhibit the deacetylation of acetylated histones and promote an open chromatin structure which allows gene expression[58]. The second is to inhibit HDAC activity on non-histone proteins which can effect downstream gene expression and cellular biology in a number of ways. The various effects of HDACi in cells, particularly cancer cells, include cell cycle arrest, differentiation, apoptosis, anti-angiogenesis and autophagy[133]. The available compounds mostly affect class I and class II HDACs.

1.5.2.7 Classification of HDAC inhibitors

Currently, several HDACi are under clinical development. These can be categorised into four different classes depending on their chemical structure and properties: Cyclic tetrapeptides; hydroxamic acids derivatives; short chain fatty acids; and Benzamides (see **Table 4**)[132]. These inhibitors only target Zn^{2+} dependant class I and/or class II HDAC proteins due to their ability to chelate this ion from the active site of the enzyme.

1.5.2.7.1 Cyclic tetrapeptides (Romidepsin)

Romidepsin is a naturally occurring cyclic tetrapeptide derivative, isolated from the fermentation product of *Chromobacterium violaceum,* a Gram-negative bacterium[134]. The U.S. FDA has approved Romidepsin for the treatment of patients with relapsed and refractory CTCL and PTCL[135]. Initially, Romidepsin was developed as an anti-Ras compound. It has the ability to reverse Ras oncogene activity which plays a crucial role in tumorigenesis. Later studies revealed that it interacts with mitogen-induced signalling pathways and subsequently it was found to be a histone deacetylase inhibitor[136].

Table 4 - Different classes of HDAC inhibitors currently in clinical trials for cancer.

Class	Compound	Selectivity to HDAC	Clinical status	Clinical indication
Hydroxamic acids	Trichostatin-A (TSA)	I, II	none	
	Vorinostat (SAHA)	I, IIa, IIb, IV	Approved for CTCL	NSCLC
	Belinostat (PXD101)	I, IIa, IIb, IV	Approved for CTCL	Ovarian cancer, CTCL, thymoma or thymic carcinoma myelodysplastic syndrome
	Panobinostat (LBH589)	I, IIa, IIb, IV	Phase II	CTCL, non-hodgkins lymphoma, sickle-cell disease, prostate cancer or small lung cancer
	Resminostat (4SC-201)	I, II	Phase I, II	Hodgkins lymphoma, hepatocellular carcinoma or colorectal cancer
	Dacinostat (LAQ824)	I, IIb	Phase I	Hodgkins lymphoma, refractory leukaemia and myelomas
	Givinostat (ITF2357)	I	Phase I, II	Sarcoma and lymphoma
	PCI-24781 (CRA-024781)	I	Phase I	CTCL, leukaemia myeloid
	JNJ-26481585 (R306465)		Phase I	Prostate cancer and myelofibrosis
	SB939		Phase I	
	Pyroxamide		Phase I	
Short-chain fatty acids	Sodium butyrate	I, IIa	Phase I	Lymphoma and solid tumors
	Valproic acid	I, IIa	Phase I, II, III	Cervical, ovarian, head, neck cancer, leukaemia, lymphoma.
	Pivanex (AN-9)		Phase I, II	Leukaemia, lymphocytic, chronic, lymphoma, small lymphocytic or malignant melanoma
Cyclic peptides	Romidepsin (Despipeptide,FK228, FR901228)	HDAC 1, 2, 4, 6	Approved for CTCL	Relapsed or refractory mantle cell or diffuse large cell non hodgkins lymphoma
	Apicidin	I, II		
Benzamides	Entinostat (MS-275)	HDAC 1, 2, 3, 9	Phase II	Hodgkins lymphoma, lung and breast cancer or melanoma
	Mocetinostat (MGCD0103)	HDAC 1, 2, 3, 9	Phase II	Follicular lymphoma and leukaemia

Romidepsin is a prodrug, which is converted into its active form (RedFK) inside the cell by reduction of the disulphide bond, causing the release of a thiol group. This thiol group can then reversibly bind to the Zn^{2+} ion at the active site of the HDAC and block its catalytic activity. In cell free conditions, RedFK strongly inhibits HDAC1 and HDAC2 at an IC_{50} of 1.6 and 3.9nM respectively[137]. It can also inhibit HDAC4 and HDAC6 at much higher IC_{50} of 25 and 790nM respectively[138]. Some studies have shown that Romidepsin might inhibit HDAC6 by facilitating HSP90 acetylation but the underlying mechanism still remains unclear[139]. Inhibition of HDACs by Romidepsin causes cell cycle arrest at G1 and G2/M phases of the cell cycle and is associated with an increase in $p21^{WAF1/CIP1}$ and cyclinE expression, while decreasing expression of cyclinD1 and c-myc[130]. Romipedsin also induces apoptosis in tumour cells by altering apoptotic gene expression including repression of Bcl2 or Bcl-X_L, and can also mediate differentiation[133].

Clinical data suggest that serum concentration of Romidepsin at a dose of $14mg/m^2$ should be given to patients in 4-hour intravenous infusions per day. The drug is comprehensively metabolised *in vivo* by Cytochrome P450 (CYP) 3A4 enzyme and to a lesser extent by CYP3A5. It has an enormous volume

of distribution and a short half-life (approximately 3.5 hrs), hence the drug is rapidly eliminated from the blood[140].

Romidepsin has little effect on diseases like lung, renal and colon cancer but is being studied as a single agent in CTCL and in AML. Combinational trials with Romidepsin for the treatment of solid tumours are still under development[141]. Combination of Romidepsin along with DNA methyltransferase inhibitors like 5-Azacytidine or Decitabine, potentiate the effect in a synergistic manner. This is thought to be a result of the methyltransferase inhibitor causing demethylation of condensed regions of heterochromatin and facilitating the access of HATs to acetylate and open the chromatin up for transcription[142-144].

1.5.2.7.2 Hydroxamic acids

SAHA (aka Vorinostat, Zolinza), is a class I, II and IV HDAC inhibitor at nanomolar concentrations[145]. It is known to interact with HDAC1 (IC_{50} 10nM), HDAC2, HDAC3 (IC_{50} 30nM), HDAC6, HDAC8 and HDAC11 (IC_{50} 200nM). Vorinostat is the first drug approved for treatment of progressive, recurrent or persistent Cutaneous T-Cell Lymphoma (CTCL), by the U.S. FDA in 2006. It has also been approved for the treatment of other diseases including Sezary syndrome[104,146]. Vorinostat is effective at inducing apoptosis of a variety of tumours, particularly

refractory solid tumours, leukaemias and lymphomas[147,148]. Vorinostat alters gene expression by decreasing HDAC1 and Myc expression but does not impact HDAC2, Brg1, GCN5, P300 and Sp1 proteins in the complex[133].

Like other HDAC inhibitors, it inhibits cell growth and induces apoptosis by increasing the $p21^{WAF1/CIP1}$ activity. However, upon continuous exposure, drug resistance develops[133,149].

Belinostat is a pan HDACi with a sulphonamide-hydroxamide moiety. Its activity is similar to Vorinostat, and inhibits class I, II and IV non-specifically at nanomolar concentrations[150,151]. Belinostat is also approved for the treatment of patients with relapsed and refractory PTCL[152].

Additionally, Panobinostat is also a pan HDACi, currently in phase I and II development for refractory CTCL[153]. It is effective in treating primary chronic myelogenous leukaemia, acute myelogenous leukaemia and multiple myeloma cells *in vitro*[154]. In a phase I trial, Panobinostat has produced objective response in myeloproliferative and leukaemic disorders[155].

1.5.2.7.3 Hydroxamates

Trichostatin A (TSA) is an anti-fungal antibiotic that was isolated from the strains of *Streptomyces hygroscopicus*[156]. TSA is also a potent reversible HDACi structurally related to Vorinostat. It induces potent differentiation and anti-proliferative actions in MEL cells[157]. Like other HDACi, it inhibits the progression of cells through the G1 and G2 phases of cell cycle and development of drug resistance is mediated by over expression of MDR1[158].

1.5.2.7.4 Short chain fatty acids

Sodium butyrate was isolated from anaerobic bacteria in the intestine[159]. Butyrates, at high concentrations, inhibit the growth of various types of cancers such as colon, prostate and endometrial cancers[160,161]. Sodium butyrate (NaB) displays an effect on acetylation, phosphorylation and methylation of histones and other nuclear proteins[162].

1.5.2.7.5 Specific synthetic HDAC8 inhibitor

Inhibition of HDAC8 enzyme activity with the selective inhibitor, PCI-34051, induces apoptosis in T-cell lymphoma cell lines, however no such activity was observed in solid tumours and other haematological malignancies[91].

1.5.2.8 Cross resistance induced by HDAC inhibitors

Depsipeptide resistant KU812 cells displayed a cross resistance with several anticancer drugs like Vincristine, Etoposide and Doxorubicin by increasing the expression of P-glycoprotein (Pgp) in cancer cells. However, it does not exhibit cross resistance with Trichostatin A[163]. Studies also report that acquisition of SAHA resistance in tumour cells induces cross resistance to other HDAC inhibitors such Valproic acid, Trichostatin A, LBH589, JNJ26481585 through MDR independent mechanism but not Romidepsin and MGCD0103[164]. Fiskus and colleagues found that Dacinostat resistant cell lines (HL-60/LR) upregulate the expression of HDACs 1, 2, and 4 with hyperacetylation of non-histone protein Hsp90 but lack HDAC6 expression and are cross resistant to Vorinostat and Panobinostat[165].

1.5.2.9 Reversal of drug resistance to HDACi

Multidrug resistance can be overcome by co-administration of a Pgp inhibitor (Verapamil) with anticancer drugs. Verapamil blocks the expression of Pgp, thereby increasing intracellular drug accumulation leading to apoptosis. Because of serious cardiac adverse effects the combination has now been withdrawn[166]. HDACi treatment is also shown to be effective in

reversing drug resistance to conventional chemotherapy[167]. Sequential treatment with either 5-aza-2'-deoxycytidine (DAC) or SAHA can overcome the drug resistance by synergistic effects in Doxorubicin resistant cells. SAHA is less efficient than DAC to overcome such drug resistance[168]. Hydralazine is a DNA methylation inhibitor that overcomes MDR by inhibiting DNMT in MCF-7/Adr resistant cells[169].

1.6 Histone methylation

Protein methylation is a PTM that can occur on lysine and arginine residues on core histone and non-histone proteins. Unlike acetylation, histone methylation is linked to both transcriptional activation and repression depending upon the degree of methylation and the specific residue(s) that are methylated.

1.6.1 Lysine methylation

Lysine residues can either be mono-, di-, or trimethylated, with each methyl group replacing one of the hydrogen atoms in the NH_3^+ group of the side chain (**Figure 1.8**)[170]. Lysine methylation is "written" and "erased" by lysine methyltransferases (KMTs) and lysine demethylases (KDMs) respectively. The most studied lysine methylation PTMs are on

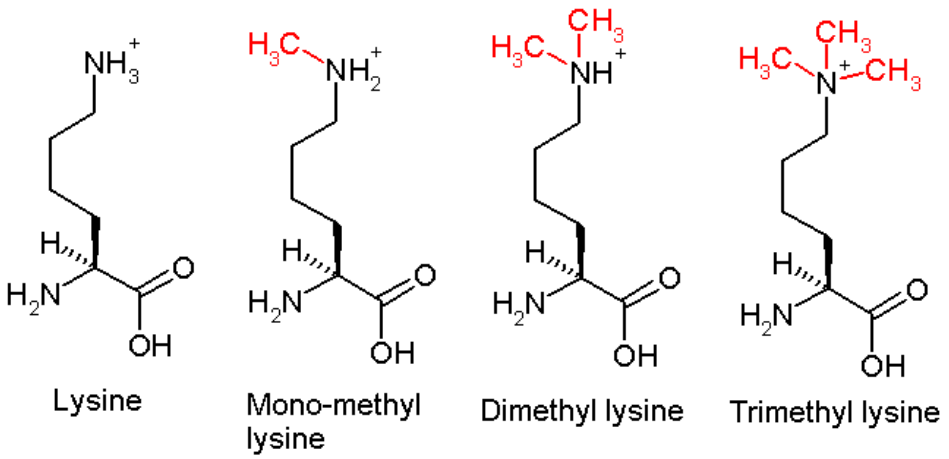

Figure 1.8 – Lysine methylation.

From left to right, the figure represents the four increasing degrees of methylation possible on a lysine residue (adapted from *Robert J. Klose et.al*)[170].

---

histone proteins at H3K4, H3K9, H3K27, H3K36, H3K79 and H4K20[171,172]. Methylation marks are more likely to be at a specific locations on a gene locus (for example, H3K4me3 is located at the TSS of an active gene, while H3K36me3 is mainly found along the body of actively transcribed genes[173]).

1.6.1.1 Lysine methyltransferases (KMTs)

KMTs catalyse the transfer of a methyl group from methyl donor S-adenosylmethionine to the ε-nitrogen of lysine. There are two major classes of KMTs that rely on the presence or

absence of the catalytic SET (for Su (var), Enhancer of Zeste and Trithorax) domain. The first identified KMT was SUV39H1 which facilitates trimethylation of H3K9 and contains a SET domain. A second group of enzymes which do not contain a SET domain can also act as KMTs by associating with the enzyme Dot1. Summary of the different KMTs, their substrates and associated mutation/overexpression in disease are shown in **Table 5**[174,175].

1.6.1.2 Lysine demethylases (KDMs)

Protein lysine methylation is removed by two classes of lysine-specific demethylases based upon their catalytic function. The first use a flavin adenine dinucleotide-dependent amine oxidase reaction (LSD domain-containing family), while the second utilise a Fe(II) and α-ketoglutarate-dependent dioxygenase reaction (JmJC domain-containing family). Due to the nature of the reaction, LSD containing enzymes can only demethylate di- and monomethylated lysines, while JmJC family members can demethylate tri, di- and monomethylated substrates. The KDM family of enzymes is summarised in **Table 6**[176-179].

Table 5 – KMTs, their substrates and links to cancer.

Protein family	Systematic name	Substrate specificity	Alteration in cancer	Associated cancer
	KMT1A	H3K9me3/2	Over expression	Breast
	KMT1B	H3K9me3/2		
SUV39	KMT1C	H3K9me2/1		
	KMT1D	H3K9me2/1		
	KMT1E	H3K9me3/2/1		
	KMT1F	H3K9me3		
EZH2	KMT8	H3K9me3/2		
	KMT6A	H3K27me3/2,	Mutations	DLBCL
SET2	KMT6B	H3K27me3/2/1	Mutations	MDS
	KMT2H	H3K9me3/2/1, H3K27me3/2/1		
	KMT3A	H3K36me3	Mutations	Renal and Breast
	KMT3B	H4K20me2/1	Mutations	AML
	KMT3G	H3K27me3/2/1, H4K20me2/1	Mutations	MM
	KMT3F	H3K9me3/2/1, H3K27me3/2/1	Mutations	AML
	KMT2A	H3K4me3	Mutations	ALL, AML
	KMT2B	H3K4me3	Mutations	DLBCL, FL
	KMT2C	H3K4me3	Mutations	Breast
SET1	KMT2D	H3K4me3		
	KMT2E			
	KMT2F	H3K4me3		
	KMT2G	H3K4me3		
	KMT2H	H3K36me2/1		
	KMT7	H3K4me1		
PRDM	KMT8A	H3K9me3/2		
	KMT8E	H3K9me1		
	KMT8D	H3K9me2/1		

Table 6 – KDMs,their substrates and links to cancer.

Protein family	Systematic name	Substrate specificity	Alteration in cancer	Associated cancer
LSD	KDM1A	H3K4me2/1, 3K9me2/1	over expressed	Prostate, breast, neuroblastoma
	KDM1B	H3K4me2/1		
JMJC	KDM2A	H3K36me2/1		
	KDM2B	H3K36me2/1, H3K4me3	Mutations	Lymphoma
	KDM3A	H3K9me2/1		
	KDM3B	H3K9me2/1		
	KDM4A	H3K9me3/2, H3K36me3/2		
	KDM4B	H3K9me3/2, H3K36me3/2		
	KDM4C	H3K9me3/2 H3K36me3/2	Over expressed	Prostate, carcinoma
	KDM4D	H3K9me3/2/1 H3K36me3/2		
	KDM4E	H3K9me3/2		
	KDM5A	H3K4me3/2	Over expressed	Gastric cancer
	KDM5B	H3K4me3/2	Over expressed	Breast, prostate, testis
	KDM5C	H3K4me3/2	Mutations	Multiple myeloma
	KDM5D	H3K4me3/2		
	KDM6A	H3K27me3/2		
	KDM6B	H3K27me3/2	Over expressed	Prostate
	KDM7	H3K9me3/2		
	KDM8	H3K36me2		

1.6.2 Arginine methylation

Arginines can be either mono- or dimethylated. Furthermore, dimethylation of arginine can be symmetric (with one methyl group added to each NH_2 group), or asymmetric when both methyl groups are placed onto the same nitrogen (**Figure 1.9**[170]). Protein arginine methyl transferases (PRMTs) catalyse the transfer of a methyl group to the guanidine nitrogen of arginine from S-adenosyl-L-methionine. PRMTs control transcription, RNA processing, cell signalling and DNA repair. There are 2 classes of PRMTs in humans. Type I (PRMT1, 2, 3, 4, 6 and 8) catalyse asymmetric demethylation of arginines, whereas type II (PRMT5 and 7) mediate symmetric dimethylation of target arginine residues. Both type I and II PRMTs can methylate to monomethyl-arginines[180].

Interestingly, the influence of therapies and resistance on arginine methylation is not well studied[181]. Previous studies have reported that the overexpression of PRMT1-8 is implicated in different types of malignancies such as breast, prostate, lung and colon cancers. High levels of PRMT1 and PRMT5 are not uncommon in leukaemia and lymphomas[182].

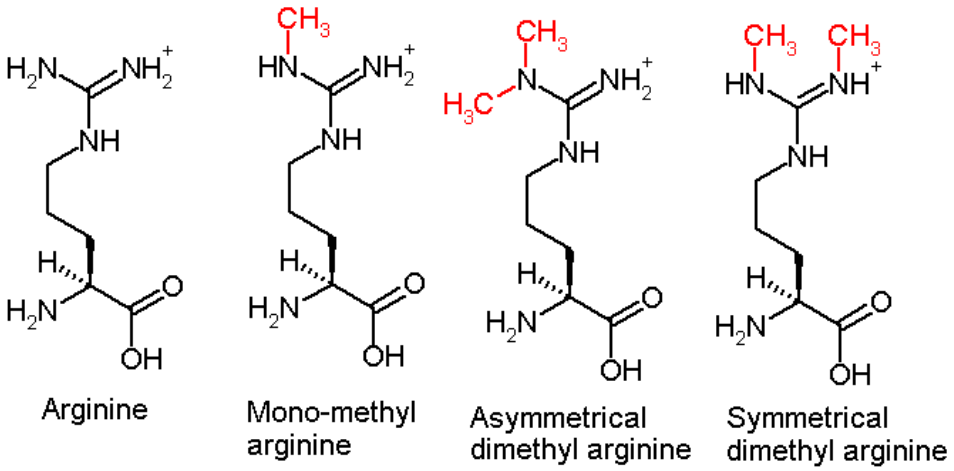

Figure 1.9 – Arginine methylation.

The figure represents the four states of arginine methylation that are possible. Please note the differences between symmetric and asymmetric dimethyl arginine (adapted *Robert J. Klose et.al.*)[170].

1.7 Chromatin PTM crosstalk

Histone PTMs are recognised or "read" by specific protein domains. For example, Bromodomains can bind to acetylated lysine residues, while Tudor domains recognise methylated lysines[183-185]. Because many epigenetic enzymes either possess 'reader' capabilities, or are associated with complexes that contain reader domains (e.g. SWI/SNF, COMPASS and PRC1/2), many histone modifications can "crosstalk" with one another[186-189].

Crosstalk is caused by regulation of epigenetic marks that are dependent on the reading and writing of other modifications. This is mainly achieved by steric hindrance of reader domains in binding to their targeted PTMs caused by modifications in adjacent amino acids. An example of this is histone H3R2 asymmetric dimethylation (H3R2me2a), a repressive mark that is catalysed by PRMT6, which antagonises the generation of histone H3K4 trimethylation. In contrast, PRMT5 and PRMT7 catalyse H3R2 symmetric dimethylation (H3R2me2s) which does not affect H3K4me3[190].

1.8 Cutaneous T-cell lymphoma

Cutaneous T-cell lymphomas (CTCL) describe a heterogeneous group of non-Hodgkin lymphomas characterized by malignant clonal transformation of post-thymic T-cells that infiltrate the skin. It comprises of both Mycosis fungoides (MF) and Sezary syndrome (SS)[191,192]. MF is the common type of primary CTCL, which is named from the mushroom-shaped tumor nodules resulting from the vertical proliferation of infiltrating cells. Sezary syndrome (SS) is a less frequent erythrodermic and leukaemic CTCL (L-CTCL). Both have a chronic, relapsing course, where patients frequently undergo multiple, consecutive therapies[193]. CTCLs represent about 80% of all

primary cutaneous lymphomas of which MF and SS comprise approximately 53%. Both anaplastic large cell lymphomas (CD30+) and CD30- peripheral T-cell lymphomas comprise another 35 percent. Survival rates have improved in CTCL which may be due to better treatments, insights into disease biology, or the inclusion of biologically benign disorders, such as lymphomatoid papulosis or large plaque parapsoriasis. CTCL comprise around 3.4% of non-Hodgkin's lymphoma (NHL) cases and are categorized into different stages based on lymph, skin, and blood involvement. Prognosis is based on the level of skin and blood involvement, and extracutaneous disease. The cause of CTCL is unknown. However, it is known that immune dysfunction may play critical role. Studies also report that epigenetic alterations play a crucial role in CTCL pathophysiology[194,195]. Recent reports suggest that characteristic chromosomal and mutational abnormalities are frequent in CTCL[196,197]. Studies have established that epidermotropic T cells from patients with MF and SS express high levels of telomerase[198].

1.8.1 Recent advances in the clinical management of CTCL

Pralatrexate is a folate antagonist that inhibits the dihydrofolate reductase enzyme and induces apoptosis of tumour cells by targeting DNA synthesis. It has greater affinity for reduced folate carrier-1 enzyme and an enhanced antineoplastic activity compared methotrexate in in vivo, in vitro and in clinical studies. In clinical studies, Pralatrexate showed a 41% overall response rate. Romidepsin is a recently approved drug for refractory CTCL patients who have received and failed at least one prior systemic therapy. In a trial in advanced CTCL, the objective response rate to Romidepsin was about 30-40%.

1.9 Mechanisms of drug resistance in cancer

Acquisition of drug resistance is a major problem in all cancer types. The pharmacological activity of several anticancer agents can be affected by drug deactivation, efflux mechanisms, drug target abundance, bypass/repair mechanisms (e.g. mutation of the target protein that causes the drug to lose efficacy) and alterations in apoptotic pathways all of which can lead to drug resistance[199].

Cells may become cross-resistant to other structurally unrelated drugs and this is termed multidrug resistance (MDR).

The majority of this resistance is mediated by the overexpression of ATP-binding cassette transporters such as P-glycoprotein 1 (Pgp)[200,201]. Pgp is a membrane bound transporter encoded by ABCB1 (MDR1) gene and has broad substrate specificity. Its normal function is to efflux harmful substances such as toxins or drugs. Increased expression of this transporter on the cell surface of tumour cells can lead to drug resistance in many cancers[200,202].

In the case of HDACis, reported drug resistance mechanisms include drug efflux (by Pgp upregulation), desensitization, target overexpression, and changes in anti-apoptotic or pro-survival mechanisms[199]. Romidepsin like other chemotherapeutic agents is a substrate for Pgp and multi-drug resistant protein1 (MRP1). Exposure of the cells to Romidepsin increases Pgp expression, which can be reversed by removal of drug[203]. However, previous studies suggest that the resistance to Romidepsin may be cell line-dependent[201]. Drug resistance in renal and colon cancer cell lines is mediated by the activation of breast cancer receptor protein (BCRP) upon continuous exposure to Romidepsin[204,205]. Recently, Arup and his colleagues have reported non-Pgp resistance mechanisms to HDACi treatment. By combining the use of the Pgp inhibitors Verapamil or valspodar with Romidepsin they have shown

resistance mechanisms that are dependent on induction of mitogen activated protein kinase (MAPK) kinase, MEK activation and low Bim expression[203].

Drug resistance to single and/or multiple HDACis as in other *in vitro* models makes combinational drug targets less effective in the treatment of haematological malignancies. Overexpression of Pgp is closely associated with various hematopoietic malignancies[206,207].

1.10 Aims and hypotheses of this study

Resistance to cancer therapies is a major problem in the clinical setting. Better understanding of the underlying mechanisms that mediate such resistance is required. The factors that promote a drug resistant phenotype are both cell intrinsic and extrinsic. Among cell intrinsic factors, mutations in drug targets and/or downstream mediators, modulation of efflux and influx pumps, and genome evolution are increasingly recognised as important for acquisition of resistance. The contribution of epigenetic reprogramming especially to epigenetic therapies is less clear. Such understanding may lead to the development of rational combinations and strategies to avoid and overcome resistance.

Therefore this study focussed on searching for general epigenetic resistance mechanisms and would not focus on Pgp-associated drug tolerance or genetic variation. There are 2 major aims of this thesis.

1. The first is to investigate the effects of HDACis on the epigenome of the target cells. More specifically, to investigate if increasing acetylation levels in a cell by HDAC inhibition can alter the overall epigenetic makeup of a cell, including other histone PTMs and the expression and function of genes that control specific epigenetic histone PTMs.
2. The second aim is to compare whether changes in the epigenome induced by HDACi are altered after development of HDACi resistance, and whether these alterations may be contributing towards this resistance.

Because treatment with HDACis can change gene expression it was hypothesised that these drugs also alter expression of genes that control the epigenome. Also, on changing acetylation status there may be reactive remodelling of the epigenome in the presence of HDAC inhibition. Additionally, epigenetic reprogramming may contribute to the development

of resistance to HDACi and may provide insights for future therapies to overcome resistance.

The following chapter (**Chapter 2**) describes all the materials and methods used in this thesis. There are then 4 experimental chapters followed sections that address overall conclusions and suggestions for future work.

Chapter 2

Material and Methods

Buffer recipes, reagents, antibodies, equipment and relevant software are detailed in the Appendix (**Table A1-A10**).

2.1 Tissue culture techniques

2.1.1 Background of human leukaemia and lymphoma cell lines.

HuT78 is a cutaneous T lymphocyte cell line derived from a 53-year-old male with sezary syndrome[208]. Daudi and Raji cell lines are both derived from Burkitt's lymphomas[209]. THP-1, a human monocytic leukaemia cell line was derived from 1- year-old male infant[210]. MCF7 is a human breast adenocarcinoma cell line established from a 69-year old adult female[211]. K562 is a chronic myelogenous leukaemic cell line established from 53-year old female[212]. These above cell lines were purchased from American type culture collection (ATCC) (LGC Standards, UK). MEC1 is a cell line derived from of a patient with B-chronic lymphocytic leukaemia[213] (CLL) in prolymphocytic transformation[214] and was obtained from Leibniz Institute

(DSMZ) German Collection of Microorganism and cell cultures (Braunschweig, Germany).

2.1.2 Resuscitation of frozen cells

To conduct functional experiments with cell lines, several controlling factors that affect their quality were taken into consideration, and include: thawing; culturing; passaging; and cryopreserving. Cryo-vials containing frozen cells were quickly thawed by transferring to a 37^{o}C water bath. Samples were warmed to the point just before the last piece of ice melted and then placed on wet ice.

2.1.3 Passaging of human B and T lymphocytic cell lines

HuT78 and K562 cells were cultured in complete Iscove's Modified Dulbecco's Medium (IMDM) (Sigma Aldrich) supplemented with 20% and 10% fetal calf serum (FCS) respectively; Daudi, Raji and THP-1 cells were cultured in complete RPMI-1640 medium supplemented with 10% FCS; MCF7 and MEC1 cells were maintained in complete Dulbecco's Modified Eagle's medium (DMEM) (Sigma Aldrich) supplemented with 10% FCS. All media were also supplemented with 100 units/mL penicillin and 100µg/mL streptomycin. Final cell cultures were maintained in vented

Nunc (T25) cultured flasks (Fisher Scientific, UK) and in a humidified incubator at 37°C under standard conditions of 5% carbon dioxide with 95% air. The cultured cell lines were tested regularly for mycoplasma infection using an established protocol (e-Myco™ Mycoplasma PCR Detection Kit; iNtRon).

HuT78, MEC1, Daudi, Raji and THP-1 cells are suspension cells and were regularly passaged to maintain optimal growth. Cells were kept at an optimum viable cell density by splitting twice weekly with fresh culture media into new T25 flasks until they were used in experiments or the total number of passages exceeded 10. Cell lines were not used beyond 10 passages. MCF-7 cells are adherent and require trypsinization for removal from the culture flask. Therefore, after removing the media, cells were washed with PBS and then incubated with 2-3mL of Trypsin/EDTA (Sigma) at 37°C for 2-3 mins to facilitate detachment from the flask. After complete detachment of cells, 10mL of growth media was added and cells were centrifuged at 200x*g* for 5 mins. Media was carefully removed and cell pellet resuspended with fresh media to carry out a cell count for viability or subculture.

2.1.4 Cryopreservation of cells

To minimize genetic and phenotypic changes of the cell lines, it was necessary to cryopreserve stock cell lines with minimal number of passages. HuT78, Daudi and MEC1 cells were grown and tested to be free of bacterial (mycoplasma), yeast, or fungal contamination under a microscope before experiments were initiated. The cells were confirmed to be healthy or viable and in exponential growth. Following harvest cells were subjected to centrifugation at 300×*g* for 5 mins and the cell pellet was re-suspended in room temperature growth media containing 10% FCS at a concentration of $1x10^7$cells/mL and then placed on ice. Once the cells were cooled, ice cold culture media with 20% DMSO was gradually added 1:1 in a drop wise fashion over the course of 30 mins. The cell suspension (1mL, $5×10^6$cells) was transferred to a cryovial and then gradually frozen at -80^{o}C freezer overnight by encasing in polystyrene. The following morning, the vials were placed in the liquid nitrogen freezer until further use.

2.1.5 Development of Romidepsin resistance clones (RHuT78 and RMEC1)

The class I HDAC inhibitor Romidepsin was used to generate resistant cell lines. HuT78 and MEC1 cells were made resistant

to their 48hrs IC_{50} values of 6nM and 9nM respectively. Resistance was promoted by exposing 20mLs of cells at $1x10^6$cells/mL to the appropriate drug concentration. Cell viability was assessed every 72hrs using DiOC6 and PI, and the drug-containing cell culture media refreshed. It is important to note that the culture volume was closely regulated to maintain an appropriate viable cell concentration for the cell line (e.g. HuT78 cells were kept at $3\text{-}4x10^5$ viable cells/mL; MEC1 at $5\text{-}6x10^5$ viable cell/mL). Upon continuous exposure to Romidepsin a resistant cell line with >80% viable cells developed after approximately 75 days. Resistant cell lines were split every 3-4 days with fresh culture media containing drug at the appropriate concentration. Parental and resistant cells were tested for cytogenetic phenotype by DNA purification using the Wizard Genomic DNA purification kit (Promega) and then analysed using the GenePrint 10 System (Promega). Parental and resistant HuT78 cells were cytogenetically identical at all-time points during this study as analysed using this technique (**Figure A2**).

2.2 Treatment of T and B lymphocyte cell lines with different HDACis and HATis

2.2.1 Determination of IC_{50} for Romidepsin, pan HDACis and HATis

The haematological cell lines HuT78, MEC1, Daudi and Raji were seeded at a density of 4×10^5 cells/mL and were incubated with Romidepsin (3-48nM; Celgene, USA), Vorinostat (20nM-48mM; Stratech scientific, UK), Sodium butyrate, Trichostatin-A (20nM-48mM; Sigma Aldrich, UK), Anacardic acid (6.25μM-100μM; Merck chemicals ltd, UK), C646 (HATi-II; 6.25μM-100μM; Merck chemicals ltd, UK) or an equivalent volume of DMSO. The cells were collected at the following time points: initial time (T0), 3, 6, 12, 24, 48 and 72hrs and cell death was evaluated using flow cytometry (see Section 2.7).

2.2.2 Treatment of HuT78 cells with DNMTi

HuT78 cell line were cultured at a cell density of 4×10^5cells/mL and were incubated with different concentrations of 5-Azacytidine (100nM-25μM), Decitabine (80nM-20μM) (kindly provided by Dr. Lakis Liloglou) or an equal volume of DMSO (as a control). The cells were cultured for 6 days and then cell death was measured by flow cytometry.

2.2.3 Inducing growth-arrest in HuT78 and MEC1 cells

HuT78 and MEC1 cells were first washed with phosphate buffer saline twice and were cultured in growth medium with or without 20% FBS. The viability and growth arrest was assessed by cell counting before and after 24hrs.

2.2.4 Cell counting and viability

Cell viability for HuT78, RHuT78, Daudi and MEC1 cell lines was determined by using the Trypan blue exclusion assay to distinguish live and dead cells. Non-viable or dead cells take up the dark blue dye and have a blue cytoplasm, while live cells appear bright and remain unstained. In order to calculate cell concentrations, cell suspensions were diluted to 1:2 with 0.1% Trypan blue dye solution, and the number of blue stained (dead) and unstained (live) cells were counted using a Haemocytometer and a light microscope. Results were recorded as percentage live cells within the total cell count. To determine the volume of cell suspension required to obtain desired cell density for experimental purpose the following equation was used.

$$V = CD_{des}/CD_{obt} \times n$$

Equation: where V=total volume of suspension

CD_{des} = desired cell density of suspension

CD_{obt} = obtained cell density of suspension and

n = number of treatments

2.3 Molecular Biology Techniques

2.3.1 Total RNA isolation from cultured cells

To study the gene expression levels of various epigenetic enzymes in different cell lines, total RNA was isolated from cells using the ZR RNA Midiprep™ kit (Zymo Research, UK) following the manufacturer's instructions. Initially, cells were centrifuged at 250x*g* at 4°C for 3mins. The media was removed and cells were lysed and harvested in a fresh microcentrifuge tube with 400µl of RNA lysis buffer and then centrifuged at 12,000×*g* for 1 min. The RNA lysis buffer breaks down all the compartments of the cell and dissolves lipids. The supernatant containing lysate was transferred to Zymo-Spin IIIC column, and centrifuged for 30s at 8000×*g.* 320µl of 95-100% ethanol was added to the flow-through, and transferred to a Zymo-Spin IIC

column and centrifuged at 12,000×*g* for 1 min. The column was then washed once with 400µl RNA prep buffer, once with 800µl and then with 400µl RNA wash buffer using 30s pulses of centrifugation at 12,000×*g.* The centrifugation was repeated again at 12,000×*g* for 2 min to clear residual wash buffer. Lastly, 30µl of elution buffer was added to the Zymo-Spin IIC column and centrifuged for 30s at 10000×*g* to elute the RNA. Surplus RNA remaining after isolation, purity check and reverse transcription was stored at -80^{o}C.

2.3.2 Assessment of RNA purity and quantity

The quality and quantity of isolated RNA was determined by a Nanodrop 2000 spectrophotometer (Thermo scientific, UK) by measuring the absorbance at a wavelength of 260nm and 280nm. The RNA absorbance ratio at 260nm and 280nm was used to assess the quality of RNA. A ratio of 1.6-2 was considered as pure RNA, a value below this indicates the presence of protein contamination. An additional ratio of light absorbance was taken (A_{260nm}/A_{230nm}) and values between 2 - 2.2 were taken as pure; values outside this range indicate possible peptide or other contamination.

Quantitation of RNA within the isolation preps was also performed with the Nanodrop 2000. To do this, the absorbance

value at 260nm was taken and divided by 0.025 (the extinction coefficient for single stranded RNA) to obtain the concentration in ng/µL.

2.3.3 Reverse transcription of complementary DNA (cDNA) from RNA

Single stranded cDNA was generated from purified isolated RNA by performing reverse transcription using oligo dT primers (a primer which adds Ts on to the poly A tail of mature mRNA). 1µg of total RNA in 12.5µL of water was mixed with 500ng of Oligo (dT) primer [500ng/µL (Promega, UK)], and was incubated for 5 mins at 70°C, and then kept on ice. In the meantime, reverse transcription master mix was prepared (per reaction 4µl 5×RT Buffer, 1µL (10,000U) Moloney murine leukaemia virus reverse transcriptase, 1µL (10mM) dNTP mix and 0.5µL (2,500U) RNase inhibitor plus (all from Promega, UK)). To start the cDNA synthesis 6.5µL of master mix was added to the 13.5µL of RNA/oligo dT mix. Synthesis was complete following incubation of the mixture at 42°C for 1hr. Synthesized cDNA was kept at -20°C until further use.

2.3.4 Polymerase chain reaction (PCR)

The PCR is a molecular technique that utilizes enzymatic reaction conducted by thermostable DNA polymerase to amplify a single copy or multiple copies of a DNA sequence of interest. Annealing temperatures of new primer sequences were optimised. Each PCR was verified to amplify a single product of the correct size by agarose gel electrophoresis. The complete thermal profile and reagents used for PCR reactions is presented in table below (**Table 7**).

2.3.5 Quantitative Real Time Polymerase Chain Reaction (qRT-PCR)

Quantitative, or real time, PCR (qRT-PCR) is a molecular technique that is widely used for quantifying mRNA of specific sequences. In order to measure the amplified sequences of cDNA in real time, the fluorescence signal that is released from a dye (such as EvaGreen) was used that binds to the minor groove of newly synthesised DNA double strands during the elongation phase of the PCR reaction. Relative quantification was performed using a reference gene, whereas absolute quantification was determined from a standard curve.

Table 7 – qRT-PCR cycles (A) and reaction mix (B) used for optimization of the new primers.

A

	Temp.	Time	Cycles
Initial denaturation	95°C	10 min	1
Denaturation	95°C	30 s	35
Annealing	56°C	30 s	
Extension	72°C	1 m	

B

Reagents	Volume	Concentration
HOT FIREPol®EvaGreen® qPCR Mix Plus	4µL	5X
Forward Primer	1µL	5pmol
Reverse Primer	1µL	5pmol
DNA template	0.5µL	From 20µL RT
Water	Made up to 20 µL	

Hot Fire pol EvaGreen master mix (Newmarket Scientific, UK) was used for qRT-PCR and performed according to the manufacturer's instructions. In all experiments RPL27 was used as a human endogenous reference gene for expression analysis of targeted genes in this study and all PCR reactions were performed in triplicate. It is reported that RPL27[215] expression is the most robust and constant reference gene within a comparison of all the classical reference genes (e.g. β-actin or glyceraldehyde 3-phosphate dehydrogenase) when measured in cells in different studies under diverse experimental conditions. The assays were performed with the Stratagene MX3000P PCR machine (Agilent Technologies, UK).

To normalise target gene expression to RPL27, the following equation was used:

$$\textbf{Target gene expression level} = 2^{(-\Delta Ct)}$$

Ct= cycle threshold

ΔCt= (Ct target gene-Ct reference gene)

Where Ct value represents the threshold number of cycles at which the machine can detect an exponential increase in fluorescence signal.

2.3.6 Agarose Gel Electrophoresis

Agarose gel electrophoresis is an easy, quick and widely used molecular technique for the separation, quantification and purification of nucleic acids and proteins based on their size of PCR product. Small DNA fragments are separated using high percentage agarose while for large DNA fragments low percentage agarose is used. The DNA fragments are placed in an electrical field and migrate toward the positive electrode. The size of the DNA fragment is determined by comparison to a DNA ladder which is composed of DNA fragments of known base pair length.

Agarose gels were prepared by weighing the desired amount of granular agarose (Web Scientific, UK) and adding 100mL of TBE (Tris-borate-Ethylenediaminetetraacetic acid (EDTA)) buffer (diluted from a 10× stock consisting of 0.445M Tris borate, 0.01M EDTA pH=8.2). The agarose was melted by heating in a microwave for 1 min, and then again in short bursts until all the agarose is melted and left for short time to cool but not solidify. To visualize the DNA under ultraviolet (UV) light Ethidium Bromide (0.2µg/mL) dye (Promega, UK) was added to slightly warm agarose solution and then the gel was gently poured it into the gel tray without formation of air bubbles and a well comb placed for sample introduction before allowing to solidify for at least 1hr.

The solidified agarose gel was placed in an electrophoresis tank filled with TBE buffer until the gel is covered completely and the well comb carefully removed before slowly pipetting DNA samples into the wells. Sample buffer 6×OrangeG (10mM Tris-HCl pH 8.0, 50mM EDTA, 15% Ficoll-400 and 0.5% OrangeG) was added to samples before loading DNA into the wells. The assembly was subjected to electrical current (100V constant voltage) for 1hr. DNA fragments were slowly separated during this period and observed as images under UV light (UVITEC, Alliance chroma system, UK).

2.3.7 Plasmid DNA extraction

A single bacterial glycerol stock or colony of bacteria containing the required plasmid was grown overnight on a constant shaker (180rpm) at 37°C in 50mL liquid broth containing the appropriate antibiotic selection. Bacterial culture was then centrifuged at a speed of 13,400rpm for 5 min, supernatant was discarded, and the pellet and was resuspend with 600µL of TE buffer. Plasmid was then extracted and purified using the Zyppy™ Plasmid Midiprep Kit (Zymo Research, UK).

2.4 Techniques for Loss of function studies

2.4.1 Overexpression of HDAC8-Flag

A FLAG tagged HDAC8 plasmid (Plasmid #13825; Addgene) was obtained, spread on an agar plate and a single colony cloned and midiprepped. HuT78 cells were passaged 24hrs prior to transfection. $2x10^6$ cells were then transfected with 2µg of the FLAG-HDAC8 plasmid or 2µg of a control pcDNA3.1 plasmid with no ORF insert using Nucleofector V kit and electroporation (Amaxa, Lonza group, Switzerland) following a protocol provided by the manufacturer. At the same time, a maxGFP plasmid (2µg) was also added to each plasmid transfection to assess transfection efficiency. One day after

transfection, HuT78 cells were analysed by flow cytometry for GFP expression. Cells were then split for downstream analysis.

2.4.2 Small hairpin RNA (shRNA) and transductions

Glycerol bacterial stocks containing shRNA lentivirus plasmids targeting HDAC8 or HDAC9 were obtained from the MISSION shRNA library (Sigma Aldrich, UK) available within the department of Haematology. Each was grown and extracted using the midiprep technique (Zymo Research, UK). Lentiviruses were generated in HEK293T cells and then used to transduce HuT78 cells. This procedure was done by Dr Mark Glenn within the department of Haematology.

2.5 Protein Electrophoresis and Blotting Analysis

2.5.1 Generation of cell lysate and protein determination

2.5.1.1 Preparation of cell lysate

Cells were harvested and pelleted by centrifugation at 1000×g for 5 mins at 4^{o}C and washed once with ice-cold 1×PBS. Samples were kept on ice at all times. Cells were lysed in 100µL/10^{6} cells in Sample Lysis buffer and were sonicated at 40% power for 30s to disrupt released DNA. Samples were heated at 95^{o}C for 10 mins before spinning down at 14,000rpm

for 10 mins to remove debris. Protein extracts could then be used directly or stored at -20°C.

2.5.1.2 Protein quantification using the Bradford method

The total protein concentration was determined by Bio-Rad DC protein assay kit (Bio-Rad laboratories Ltd, UK). 5µL of cell lysates or pre made dilutions of bovine serum albumin standards (0-2mg/mL) were added into 96 well plates in duplicate. 1mL of reagent A was mixed with 20µL of reagent S, and 25µL of this mixture was then added to each sample/standard on the 96-well plate. 200µL of reagent B was then added per well, and the plate was incubated at RT for 15 mins. Absorbance was then measured at 650nm using a spectrophotometer. The concentrations of protein samples were calculated by using protein standard values. The measurement was considered valid if there was a doubling of absorbance with each doubling of protein standard concentration, the correlation coefficient value for the standard curve was >0.99, and the variance between duplicates was <10%.

10µg of total protein was loaded for Western blotting. The volume of each sample loaded onto the gel was equalised with SDS lysis buffer, and then 5× loading sample buffer was added prior to gel loading.

2.5.2 SDS-PAGE and Western Blotting

2.5.2.1 Sodium Docecyl Sulphate Polyacrylamide Gel Electrophoresis (SDS-PAGE)

SDS-PAGE is a commonly used separation technique for the detection and analysis of specific proteins from a complex mixture based on size. In this technique, changes in the percentage of acrylamide can be used to determine the pore size within the gel, the larger the percentage of acrylamide the more cross-linking and the smaller the pore size. The cellular proteins migrate from negative (anode) end to positive (cathode) end in an electric field through the gel. Proteins are denatured in the presence of SDS which renders proteins highly electronegative so that their migration through the gel is independent of their isoelectric point, and is based upon the molecular weight of the protein. The target protein will be resolved from the other proteins and can be identified through Western blotting and immune-detection with a specific antibody.

SDS-PAGE gels were prepared using Bio-Rad minigel apparatus (Bio-Rad laboratories Ltd, UK): Stock solutions were mixed and 15µL tetramethylethylenediamine (TEMED) was added just before it was poured between the plates. This was then

carefully overlaid with water and allowed to set (~40min). Water was removed and the polyacrylamide stacking gel was prepared. 15 µL TEMED was added just before pouring and a 10 or 15 well comb was used to create sample wells in the stacking gel. The gels were then used immediately upon polymerisation.

Protein samples (prepared in Section 2.5.1.2) were loaded into the sample wells of the gel with the Precision Plus Protein™ Kaleidoscope™ Prestained Protein Standards. Gel electrophoresis apparatus was assembled and 1× running buffer was poured into the central reservoir. Protein separation was achieved with the application of a constant 30mA per gel for 60 min.

2.5.2.2 Western blotting

Proteins separated by SDS-PAGE were transferred to polyvinylidine difluoride (PVDF) membranes using a Western blotting technique. PVDF membranes (0.45mm pore size, Roche Diagnostic Limited, UK) were cut into a 6×9cm size, permeabilised in methanol for 30s and then washed and kept in transfer buffer until the transfer. Similarly, the sponges and Whattman filter papers were soaked in transfer buffer and then the 'sandwich' of sponge: blotting paper: gel: membrane:

blotting paper: sponge, was prepared and clamped together, making sure no air bubbles are trapped between the layers. The sandwich was placed in the correct orientation (gel closest to cathode) into the transfer tank along with ice cold transfer buffer and an ice pack. Finally, a constant electrical current of 400mA was applied for 1hr.

2.5.2.3 Membrane probing and incubation with antibodies

After Western blotting transfer the membrane was incubated at RT in blocking buffer to prevent non-specific interactions and background binding of the primary and/or secondary antibody to the membrane. The membrane was then incubated overnight at 4^{o}C or at RT for 1hr (depending upon the antibody) with the primary antibody diluted in blocking buffer under gentle agitation. After washing the membrane 4 times, for 5 min each, in fresh TBST buffer, HRP conjugated secondary antibody diluted in blocking buffer was added to the membrane for 1hr at RT. After this step the membrane was again washed using the same protocol and then visualised.

2.5.2.4 Detection of protein

Bound secondary antibody (and hopefully the protein of interest) was detected using either WESTAR® Supernova enhanced chemiluminescent (ECL) substrate reagent (Geneflow, UK) or Immobilon™ Western Chemiluminescent HRP substrates (Merck Millipore, UK) and imaged using an LAS-1000 (Fujifilm, Japan). Densitometry was performed using AIDA image analyser software (v4.27.039) or Image J software.

2.6 Cell proliferation and cell cycle

2.6.1 Proliferation by BrdU ELISA assay

5-bromo-2'-deoxyuridine (BrdU) is a thymidine analog used to measure the quantity of DNA produced by cells transiting the S-phase of the cell cycle during the incubation period with the compound. It is incorporated directly into DNA of newly synthesized cells and can be detected by anti-BrdU antibody.

Experiments were performed using the BrdU ELISA kit (Roche, UK). Cells were incubated with 3µg/mL of BrdU reagent for 4hrs at 37^{o}C. 5x10^{3} cells were then transferred to a 96-well plate to perform the ELISA. Cells were centrifuged at 300rpm for 10 mins in the 96-well plate and the culture media was removed. Centrifuged cells were then fixed to the plate and

denatured with 100µL of FixDenat solution for 30 mins at RT. Solution was removed and wells washed with kit wash buffer and 100µL of BrdU mouse monoclonal antibody was added and incubated for 1hr at RT. The Microplates were then washed 3 times with wash buffer and 100µL of Anti-BrdU-POD secondary antibody for detection of bound primary antibody was added. After further washing HRP substrate was added and incubated for 30 mins at RT to develop a colour. Finally, absorbance was measured at 450nm by using an ELISA plate reader.

2.6.2 PI analysis of cell cycle status

$1x10^6$ cells were collected, washed with PBS and then fixed with -20^oC methanol (95%) for 15mins. Cells were then centrifuged at 250x*g* and methanol discarded. Cell pellet was then resuspended in PBS and 50ug/mL RNase A was added. Samples were then incubated at room temperature for 45mins. During this incubation, cells were gently passed twice through a 29G needle. PI was then added at 10ug/mL and acquired on FACS Calibur at low speed (100-500 events/sec).

2.7 Apoptosis by FACS

The induction of apoptosis was quantified effectively by 3, 3'-dihexyloxacarbocyanine iodide (DiOC6) and propidium iodide

(PI) using Flow cytometry. DiOC6, is a fluorescent dye which measures mitochondrial membrane potential and PI stains nucleic acids thereby differentiate apoptotic and necrotic cells. Fluorescence intensity was measured using Flow cytometry and percentage live and dead cells were calculated. (PI^-DioC6^+ = Alive, PI^+DioC6^- = dead, PI^-DioC6^- = apoptotic).

2.8 Statistical Analysis

The data in this thesis were analysed for statistical significance using either Student's t-test for paired data, or Mann-Whitney U-test and Graphpad prism (version 6). The software used for these calculations was either Microsoft Excel™ or IBM-SPSS (v22). Compusyn software was used for Chou-Talalay analysis for drug combination studies and Genex software was used to generate heatmaps for gene expression changes.

Chapter 3

Characterisation of HDAC inhibitors and establishment of Romidepsin resistant cell lines

3.1 Introduction

Drugs that specifically target epigenetic pathways have relatively recently found importance for clinical use. In particularly, drugs that modulate the post-translational modification of histone acetylation have been of keen interest due to their potency for inducing cell cycle arrest and apoptosis, especially in haematological malignancies. Despite promising initial clinical applications for HDACi, development of drug resistance seems inevitable. There are multiple studies describing mechanisms of resistance towards HDACi which include loss of the pro-apoptotic protein BIM through MAPK activation and increased efflux of the drug by overexpression of the MDR1 protein pump[203].

Despite these insights into the resistance mechanisms, little is known about how these epigenetic drugs alter the epigenome

as a whole and in particular the enzymes that directly regulate this process. Also, whether these effects on the epigenome alter with, and contribute towards, the development of resistance is unclear.

This study therefore required the development of representative haematological cell lines that are resistant to Romidepsin to facilitate further downstream studies. We chose the cell lines HuT78 and MEC1 because HDACis are used in the clinical treatment of relapsed CTCL and the specific interest of the department in the B-cell malignancy CLL respectively.

3.2 Results

To facilitate the studies of epigenetic drugs and their effects on the epigenome, various cell lines were initially screened for their apoptotic sensitivity to various HDACis and HATis.

3.2.1 Apoptosis of haematological cell lines after treatment with Romidepsin

The haematological cell lines HuT78, MEC1, Daudi and Raji (see methodology for cell of origin of these cell lines) were initially screened for their sensitivity to the HDACi Romidepsin. Cells were treated with a range of physiologically achievable concentrations (3-48nM) for up to 72hrs and then apoptosis was measured by staining with DiOC6 and PI followed by measurements using flow cytometry. The percentage viable cells that were $DiOC6^{+}PI^{-}$ were calculated relative to the cells treated with the vehicle control and plotted on a line graph (**Figure 3.1**).

Figure 3.1 shows that all the cell lines studied have apoptotic sensitivity to Romidepsin treatment. The percentage of apoptotic cells increased in a time dependant manner for all cell lines. HuT78 cells (**Figure 3.1A**) were the most sensitive (48hrs IC_{50} of 6nM) while Daudi cells (**Figure 3.1C**) required

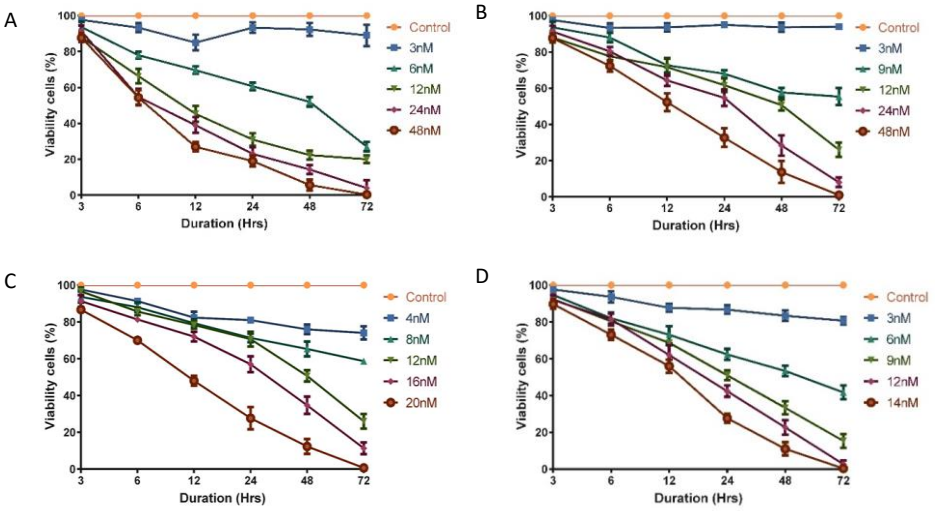

Figure 3.1 - Apoptosis of haematological cell lines after treatment with Romidepsin for up to 72hrs.

Cell lines were passaged and cultured for 24hrs, followed by treatment with either the DMSO vehicle control (Control) or Romidepsin at the described concentration for up to 72hrs. Apoptosis was measured at 3, 6, 12, 24, 48 and 72hrs after treatment by the relative staining of DiOC6 and PI using flow cytometry. Data is illustrated as percentage viability compared to the Control sample. Cell lines treated were: **A.** HuT78; **B.** MEC1; **C.** Daudi; **D.** Raji. n=3 for each time point and concentration.

higher concentrations (48hrs IC_{50} of 12nM); refer to **Table 8** for all 48hrs IC_{50} values.

3.2.2 Apoptosis of HuT78 and MEC1 cells after treatment with the pan HDACis vorinostat, Sodium butyrate, or Trichostatin A

Given that both HuT78 and MEC1 cells were sensitive to Romidepsin at low nM concentrations, these cell lines were further analysed for their apoptotic sensitivity to other HDACis. Similar to the experiments with Romidepsin above, we treated the cell lines with varying concentrations of each HDACi and checked apoptosis using PI and DiOC6 with flow cytometry at multiple time points over a 72hrs period. The drugs used were Vorinostat, Sodium butyrate and Trichostatin A, which target Class I/II HDACs. Drug concentration ranges were chosen according to past studies that show induction of apoptosis in HuT78 and other cell lines[216-219].

Figure 3.2 shows that all three HDACis induce apoptosis in both HuT78 and MEC1 cells in a dose and time dependant manner. HuT78 cells were more sensitive to Sodium butyrate than MEC1 cells (48hrs IC_{50} of 12mM vs 17mM respectively; 48hrs, $p = 0.05$), while Vorinostat was more potent at inducing

Table 8 - Determination of IC_{50} value of Romidepsin in different cell lines using Graphpad prism v6.

Drug	Cell Type	48hr IC_{50}
Romidepsin	HuT78	6nM
	MEC1	9nM
	Daudi	12nM
	Raji	10nM

Data are presented as mean of three independent experiments. For each cell line, data were analysed using 2way ANOVA complemented with Dunnett's multiple comparisons test. Each cell line was statistically significant. IC_{50} values were rounded up or down to the closest nM integer.

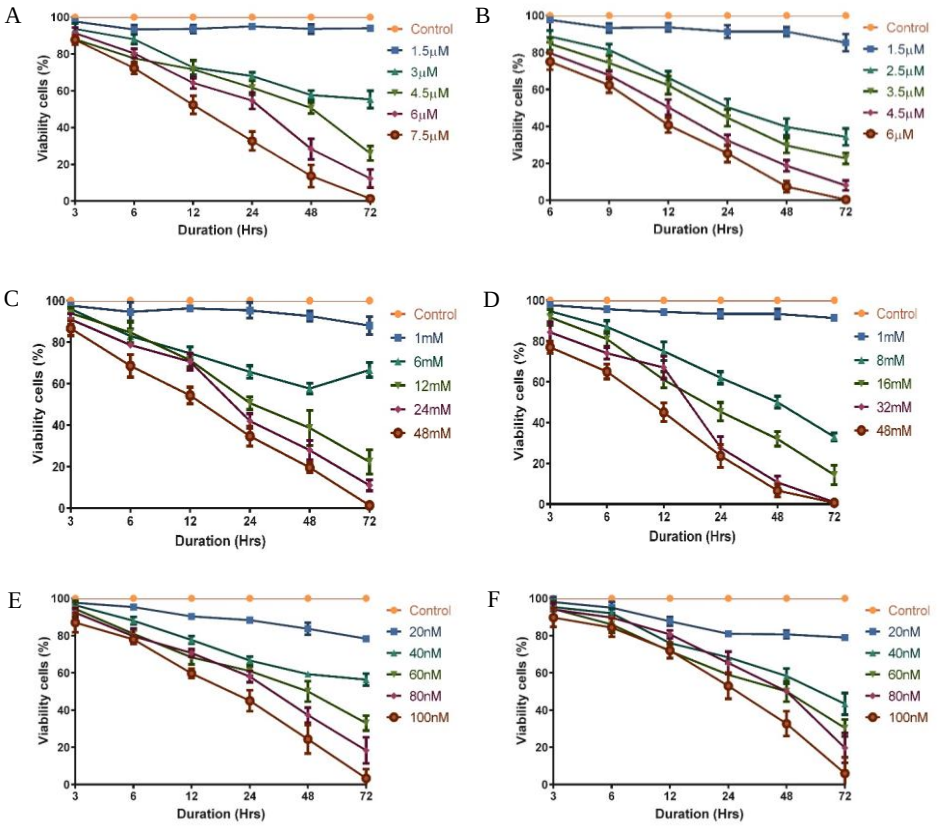

Figure 3.2 - Apoptosis in either HuT78 or MEC1 cells upon treatment over 72hrs with various concentrations of pan HDACis.

Cell culture and treatment was performed as in **Figure 3.1**. HuT78 (**A**, **C** and **E**) and MEC1 (**B**, **D** and **F**) cells were harvested at specific timepoints after culturing with vorinostat (**A** and **B**), sodium butyrate (**C** and **D**) and trichostatin A (**E** and **F**) and apoptosis was quantified by staining with DioC6 and PI and measurement using flow cytometry. n=3 for each time point and concentration.

apoptosis in MEC1 cells than HuT78 (48hrs IC_{50} of 4μM vs 5μM respectively; 48hrs difference, p = 0.01). Trichostatin A induced death in both cell lines with equal efficacy (48hrs IC_{50} of 64nM; 48hrs, p = 0.05. Please refer to **Table 9**.

3.2.3 Effects of HATis on cell death in HuT78 and MEC1 cells.

Having established the apoptosis-inducing efficacy of various HDACis on HuT78 and MEC1 cells, these cell lines were next used to test HATis in a similar fashion. Anacardic acid was chosen as it is a well characterised HAT inhibitor[220-222]; in addition, we also chose a novel inhibitor, called HAT inhibitor II (HATi-II), whose apoptotic efficacy had not previously been described prior to this work. In preliminary experiments, cells were treated with a broad range of HATi concentrations (25nM to 100μM) so a narrower range of drug concentrations could be derived and administered that would produce apoptosis. **Figure 3.3** shows the final drug concentrations used (6.25μM to 100μM) and the apoptosis induced at the multiple time points. Similar levels of apoptosis for each drug were observed in both HuT78 and MEC1 cells. HATi-II has a 48hrs IC_{50} of 26μM and 21μM for HuT78 and MEC1 respectively, while Anacardic acid is 24μM and 21μM.

Table 9 - Determination of IC_{50} value of various HDACis in HuT78 and MEC1 cell lines using Graphpad prism v6.

Drug	Cell Type	48hr IC_{50}
Sodium Butyrate	HuT78	12mM
	MEC1	17mM
Vorinostat	HuT78	5μM
	MEC1	4μM
Trichostatin A	HuT78	65nM
	MEC1	64nM

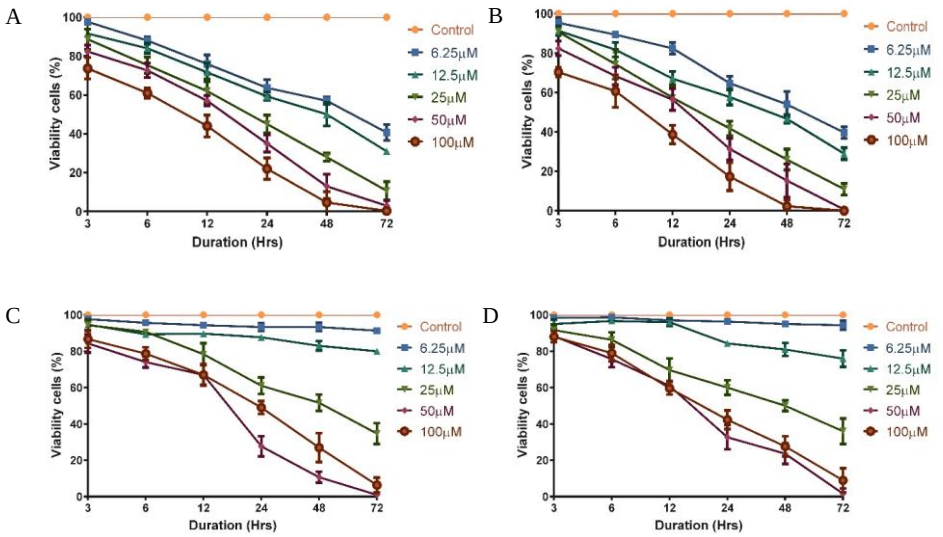

Figure 3.3 - Apoptosis induced in HuT78 and MEC1 cells after treatment with Anacardic acid or HATi-II over a 72hrs period.

Sample culturing and treatment was performed as in **Figure 3.1**. HuT78 (**A** and **C**) and MEC1 (**B** and **D**) cells were treated with the vehicle control (Control) or with either HATi-II (**A** and **B**) or anacardic acid (**C** and **D**) at the described drug concentration. All cell lines were harvested and stained with DioC6 and PI for the measurement of cell viability and analysed by flow cytometry. n=3 for each time point and concentration.

Recently published work on HATi-II showed that this inhibitor requires serum-free media to induce apoptosis in K562 cells (a chronic myeloid leukemia cell line). However, no difference in apoptosis was observed between serum free and complete media conditions upon treatment of HuT78 or MEC1 with this HATi (**Figure 3.4**).

3.2.4 Development of resistant cell lines.

Having established the IC_{50} values for each epigenetic drug, the next aim was to develop resistant cell line counterparts. HuT78 and MEC1 cells were exposed to Romidepsin at their appropriate 48hrs IC_{50} value of 6nM and 9nM respectively. For detailed methodology into the development of resistant cell lines please refer to material and methods section 2.1.5. **Figure 3.5** shows the viability of HuT78 cells during the development of the first RHuT78 cell line. The HuT78 cell-line culture regained viability to >80% after ~75days of culture with 6nM Romidepsin and were deemed RHuT78 cells after this time. This was repeated a further 2 times for both HuT78 and MEC1 to obtain a total of 3 RHuT78 and 3 RMEC1 cell lines.

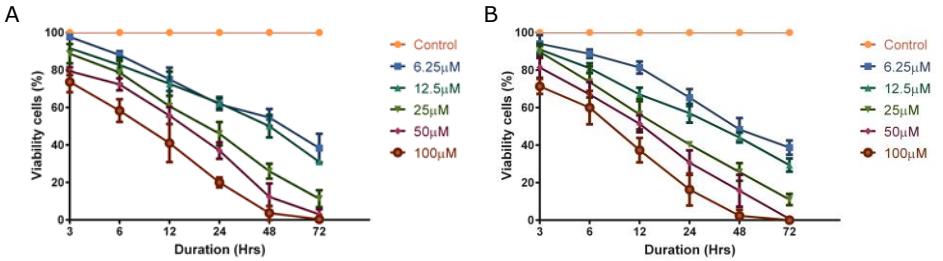

Figure 3.4 - Apoptosis induced in HuT78 and MEC1 cells upon treatment with HATi-II in serum-free conditions.

Cell lines were left for 24hrs (MEC1) or 36hrs (HuT78) without fetal calf serum to cause cell cycle arrest and then were treated with appropriate concentrations with HATi-II. Cells were shown not be undergoing mitosis due to absolute cell numbers did not increase over the culture period. Part **A** and **B** shows HuT78 and MEC1 respectively.

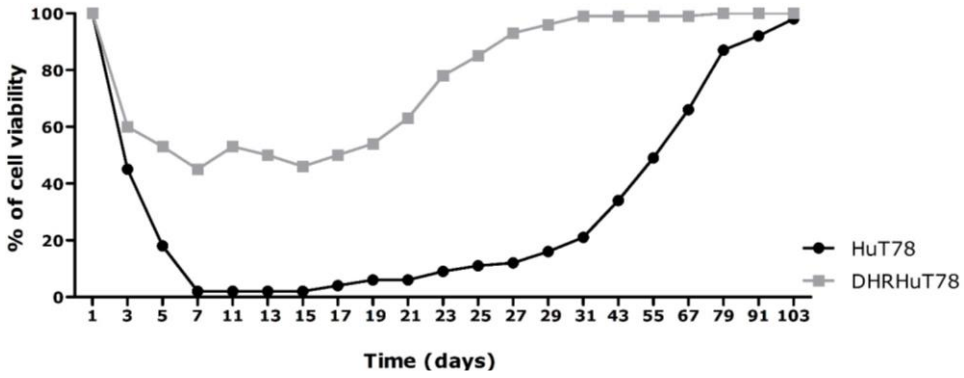

Figure 3.5 – Viability of cells during RHuT78 cell line development from HuT78 or from DHRHuT78.

$1x10^7$ HuT78 or DHRHuT78 cells were continually treated with 6nM Romidepsin and percent of viable cells was measured at the indicated time points during culture by measuring PI+DiOC6 staining using flow cytometry. Viability was checked every 2 days up to 31days followed by every 12days after this. Upon generation of a cell line that was >80% viable, these cells were then considered RHuT78. Please refer to the materials and methods section for detailed explanation of RHuT78 cell line development.

3.2.5 Development of a drug holiday RHuT78 cell line

Upon establishing the RHuT78 cell lines, some of the resistant cells were continually cultured in the absence of Romidepsin which we termed drug holiday RHuT78 (DHRHuT78). These were produced to provide a comparison with HuT78 and RHuT78 for future studies, and to establish if any changes seen in RHuT78 were permanent or reversible. DHRHuT78 regained sensitivity to Romidepsin equivalent to HuT78 cell, 8-12weeks after removal of HDACi from the RHuT78 cells. Interestingly, it was observed that these 8-12week "old" DHRHuT78 cells had a larger percentage of initial drug resistant cells and therefore could generate >80% viable RHuT78 cultures much faster than HuT78 cells do after addition of Romidepsin.

3.2.6 Observation of cell morphology and proliferative changes in RHuT78 cells

After the development of the RHuT78 cell lines, and upon continued culture in the presence of the drug, it became evident after ~2 months that the cells from all 3 RHuT78 cultures showed alterations in size (smaller) and shape (more elongated). This difference in morphology could be clearly observed both under the microscope (not shown) and by reduced forward and side light scatter properties during flow

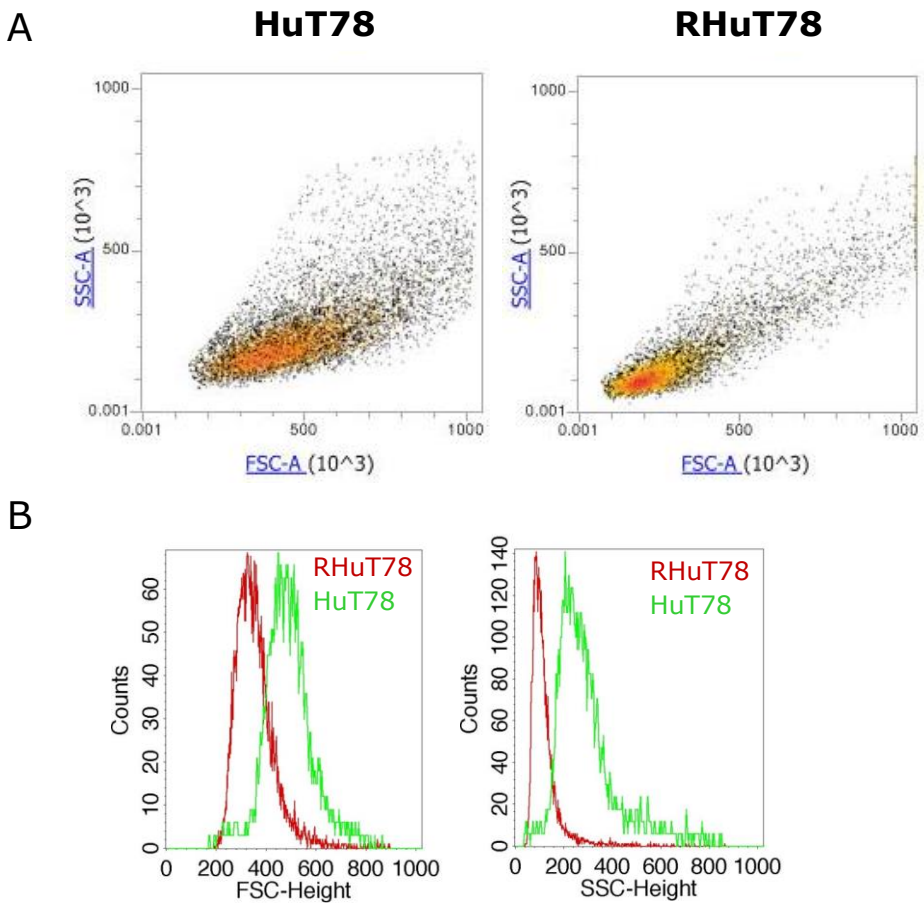

Figure 3.6 – Cell morphology changes of RHuT78 cells compared to their parental cell line HuT78.

A) Scatter blot showing differences in forward (FSC) and side (SSC) scatter of live cells by flow cytometry. An increase in cell size causes an increase in FSC, while an increase in SSC is proportional to cell size and cellular granularity. **B)** Histograms showing FSC (right) and SSC (left) properties of RHuT78 and parental HuT78 cells.

cytometry (**Figure 3.6A and B**). No obvious morphological changes were observed in RMEC1 cells, however, they did alter cell growth patterns in terms of their normal clumping behaviour changing to that of a unicellular culture (not shown).

In addition to changes in morphological characteristics, both the RHuT78 cell lines proliferated faster than the parental cultures and drug holiday counterpart. Cell doubling time was reduced from 36hrs in HuT78 and DHRHuT78 to 31hrs in RHuT78 (**Figure 3.7**). The proliferative increase in these resistant cell lines is discussed further in **Chapter 5**.

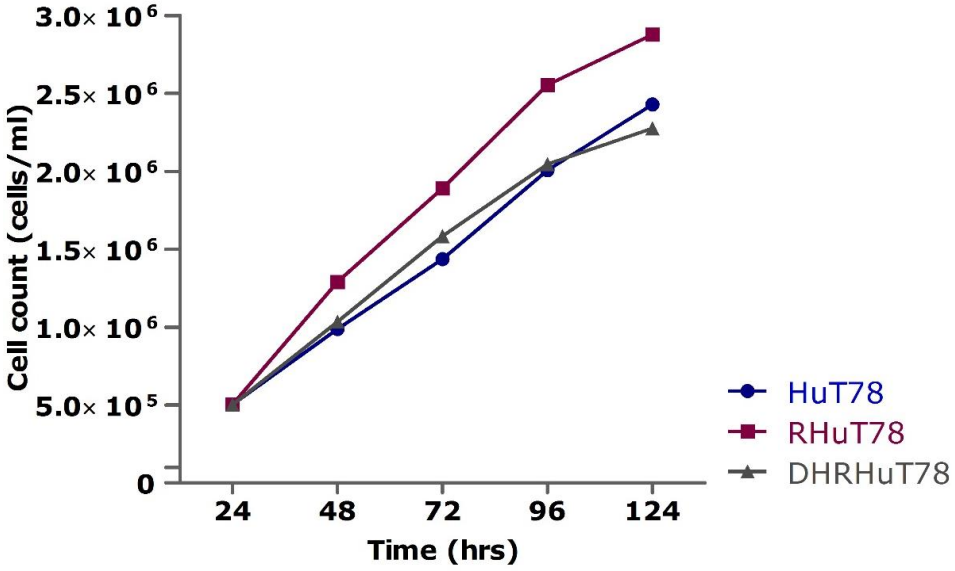

Figure 3.7 – Graph showing cell culture growth rates of HuT78, RHuT78 and DHRHuT78.

Cells were passaged to $5x10^5$ cells/mL and cultured for 4 days. Cell numbers were counted every 24hrs and plotted on a line graph. Doubling time of HuT78 and DHRHuT78 were 44hrs, while RHuT78 were 38hrs.

3.3 Discussion

The two major aims of this chapter were to establish the apoptotic-inducing efficacy of various HDACis and HATis on the cell lines HuT78, MEC1, Daudi and Raji, followed by the development of HuT78 and MEC1 cell lines that are resistant to their 48hrs IC_{50} concentration of Romidepsin (6nM and 9nM respectively).

Treatment of the 4 cell lines with Romidepsin induced apoptosis in the low nM concentration range. The CTCL cell line HuT78 of T cell origin showed the highest sensitivity at 6nM, while the other 3 B-cell derived cell lines were slightly less sensitive at 9-12nM. These concentrations are similar to those presented by other groups in previous publications on Romidespin treatment of HuT78[135,140,195,223-227]. The other HDACis tested were Vorinostat, Sodium butyrate and Trichostatin A. Each of these drugs induced apoptosis in the 4 cell lines in a time and concentration dependant manner. Again, the concentrations required to induce cell death matched those already presented in the field[145,156,157,217,228].

HATis are relatively novel agents compared to HDACis, and little is known about their effects on apoptosis in lymphoid cell lines. Treatment of HuT78 cells and MEC1 cells caused an

increase in cell death equally in both cell lines that was both time and concentration dependant. The compound HATi-II had slightly higher efficacy than Anarcardic acid, with apoptotic effects seen at 6μM and 25μM respectively.

During this chapter, HuT78 and MEC1 cells lines were developed that are resistant to Romidepsin. After treatment with Romidepsin a large percentage of cells in the original cultures died, and regrowth of the remaining cells took more than 2 months. Interestingly, after establishment of each resistant cell line and continued culture with Romidepsin for several months, morphological and proliferative changes were observed. These changes were unlikely due to outgrowth of a randomly mutated clone as similar phenomenon was seen in all resistant cell lines that were developed separately. Also, removal of the drug and creation of DHRHuT78 cells caused the proliferation rate to revert back to the original parental line HuT78. Instead, we hypothesise that continued exposure to Romidepsin produced a structured change in the epigenome and transcriptome that could be replicated in all 3 RHuT78 cell lines generated. Also, the delay in these observations suggests either that the culture as a whole gradually altered in morphology and proliferation over the extended time period; Alternatively, a small subclone of faster proliferating cells were

likely present from the beginning with a smaller elongated morphology and overtime these cells proliferated to become the dominant clone within the culture. Either way, the continual culturing of these cell lines with Romidepsin clearly selects for a more aggressively proliferating cell and this knowledge could have implications for continual clinical administration of Romidepsin. Because of the interesting nature in this observation, this phenomenon is studied further in **Chapter 5**.

Chapter 4

Investigation into the effects of Romidepsin on the epigenome

4.1 Introduction

HDACis show promising clinical application for cancer treatment, but their effects on complex biological systems remains incomplete. In particular, little is known about how the epigenome of a cell is remodelled after the addition of HDACis. Studies have shown that histone PTMs other than acetylation can alter upon the addition of HDACis. This change is brought about through 3 distinct mechanisms which are: competition for a particular histone tail residue by different PTM inducing enzymes (e.g. increased acetylation of H3K9 leads to lower methylation of this residue); changes in expression levels of epigenetic enzymes that regulate PTMs other than acetylation[229]; and/or alterations in recruitment or activation of epigenetic complexes facilitated by the acetylation mark[230,231]. Also, it is not clear whether development of resistance to HDACi further alters the way in which the cell remodels its epigenome in response to the drug.

In the last chapter, both HuT78 and MEC1 cell lines were developed that are resistant to Romidepsin (6nM and 9nM respectively - termed RHuT78 and RMEC1 respectively). Utilising these cell lines, remodelling of the epigenome upon treatment with the HDACi Romidepsin could be investigated under the two different cellular responses of sensitivity and resistance. Previous studies in HeLa and HL60 cell lines show that upon HDACi treatment, an increase in total histone acetylation is accompanied by a rise in H3K4me3 levels[230,231], a mark associated with transcriptional activation. Therefore, this study was initiated by analysing the changes in H3 acetylation (H3Ac – the antibody used detects both H3K9/K14 acetylation) and comparing these with that of H3K4me3 in HuT78 and RHuT78 cells. Also, changes in H3K27me3 (associated with gene repression), another well characterised histone H3 PTM, was also studied for comparison.

4.2 Results

4.2.1 Effects of Romidepsin on H3 acetylation, H3K4me3 and H3K27me3 in HuT78 and RHuT78 cells.

Histone PTMs were investigated using Western blotting to see if global changes could be observed upon treatment with and without 6nM Romidepsin, and whether any difference in responses was evident between HuT78 and RHuT78 cells. Cultures were passaged and then either left untreated or treated immediately with 6nM Romidepsin. Cells were harvested at multiple time points for up to 48hrs after treatment. Lysates were immunoblotted and probed for H3Ac (antibody detects H3K9/14 acetylation), H3K4me3 and H3K27me3 (**Figure 4.1**; representative of n=3 blots). Blots were also probed for total histone H3 as a loading control. HuT78 and RHuT78 samples at time zero (T_0) are present on both gels so densitometry values could be normalised between blots and therefore compared with one another (**Figure 4.1** and **Figure 4.2**).

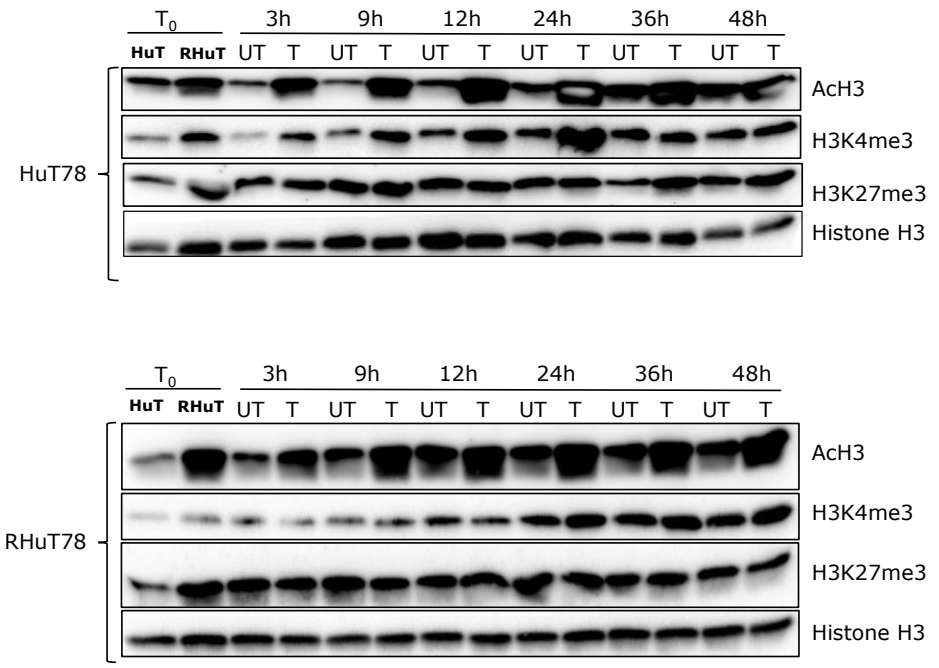

Figure 4.1 - Difference in histone H3 PTMs after treatment with and without Romidepsin between HUT78 and RHuT78 cells.

Western blot of HuT78 and RHuT78 lysates after being left untreated (UT) or treated with 6nM Romidepsin (T) for up to 48hrs. Western blot membranes were probed for H3Ac, H3K4me3 and H3K27me3. Total histone H3 was used as a loading control. The same lysates of time zero (T_0) HuT78 and RHuT78 cells were loaded on both blots so results could be compared.

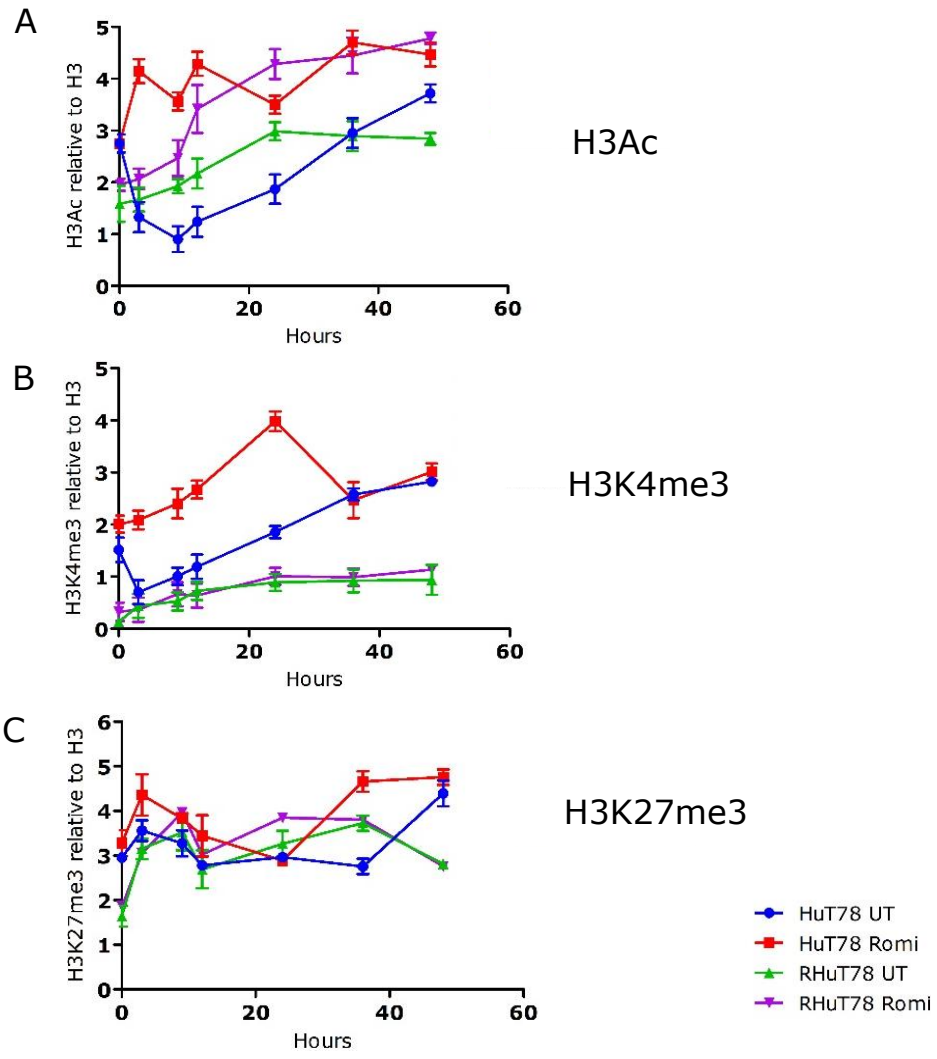

Figure 4.2 - Densitometry analysis of Western blots shown in Figure 4.1.

Values are calculated relative to total histone H3 and then the RHuT78 blot is analysed relative to the HuT78 blot using the repeated sample of T_0 HuT78 (HuT). (n=3) No statistical analysis was performed.

As expected, treatment with Romidepsin increased H3Ac in HuT78 cells, with levels peaking at around 24hrs after treatment. H3Ac also increased spontaneously after 48hrs of culture, although levels did not reach those achieved after treatment with Romidepsin.

Like H3Ac, levels of H3K4me3 in HuT78 also increased spontaneously in culture after passage of the cells. As observed in other studies[230,231], treatment with Romidepsin increased these levels even further; with quantities of the H3K4me3 mimicking that of H3Ac levels and peaking at 24hrs. However, unlike H3Ac, the quantity of H3K4me3 dropped back to untreated levels between 36-48hrs. In contrast to H3K4me3, the PTM H3K27me3 did not alter significantly with or without treatment during the first 24hrs of culture. After this time, H3K27me3 did increase at later time points but did so in both treated and untreated samples.

Having established the normal HuT78 response to Romidepsin in terms of the three studied H3 PTMs, the results were compared to that observed in RHuT78. Quantities of H3Ac and H3K4me3 were higher in RHuT78 cells at T_0. Upon removal of the drug and the culturing of the RHuT78 cells in drug-free media, levels of H3Ac reduced within 3hrs back to those seen in

normal HuT78 cells. Continued culture of untreated RHuT78 cells was accompanied by a spontaneous increase in H3Ac, similar to that observed in HuT78 cells. Also, similar to normal HuT78 cells, levels of H3K4me3 in untreated RHuT78 cells mimicked H3Ac and increased spontaneously. H3K27me3 stayed similar throughout the culture.

H3Ac and H3K4me3 did increase significantly in RHuT78 cells after exposure to the HDACi. However, levels of these two PTMs did not reach quantities achieved by HuT78 cells, particularly at the 24hrs time point. Also, despite H3K4me3 increasing in treated RHuT78 cells, levels did not greatly exceed those seen in untreated cells.

These results show that changes in H3Ac, H3K4me3 and H3K27me3 are similar in untreated HuT78 and RHuT78. It also highlights that resistant cells still have significant intracellular concentrations of Romidepsin to influence histone PTMs, although the effects of the drug are not quite as pronounced as HuT78 cells. In particular, changes in levels of H3K4me3 between treated and untreated HuT78 cells were much greater than the difference between that of RHuT78 cells.

4.2.2 Differences in H3R2 methylation in HuT78 compared to RHuT78

Because of the observed difference in H3K4me3 in HuT78 and RHuT78 after treatment with Romidepsin, lysates were next probed for the symmetric and asymmetric variants of H3R2me2 (H3R2me2s and H3R2me2a respectively). H3R2me2a has been shown to be mutually exclusive with H3K4me3 and blocks H3K4 methyltransferase activity[181,232]. It was therefore hypothesised that the difference in H3K4me3 changes between HuT78 and RHuT78 cells upon treatment with Romidepsin may be influenced by alterations in the H3R2me2 mark.

As shown in **Figure 4.3** and **Figure 4.4** levels of the symmetric PTM fluctuated in both HuT78 and RHuT78 cells. Increased quantities of this mark were first observed at 12hrs in HuT78 cells, but only much later at 36hrs in RHuT78 cells. Also, these increases in H3R2me2s were seen ~12hrs earlier in Romidepsin treated samples than untreated samples. However quantities of this symmetric H3R2me2 PTM were similar in untreated and treated samples for both sensitive and resistant cells.

Regarding the asymmetric mark, treatment of HuT78 cells with Romidepsin caused levels of H3R2me2a to remain relatively

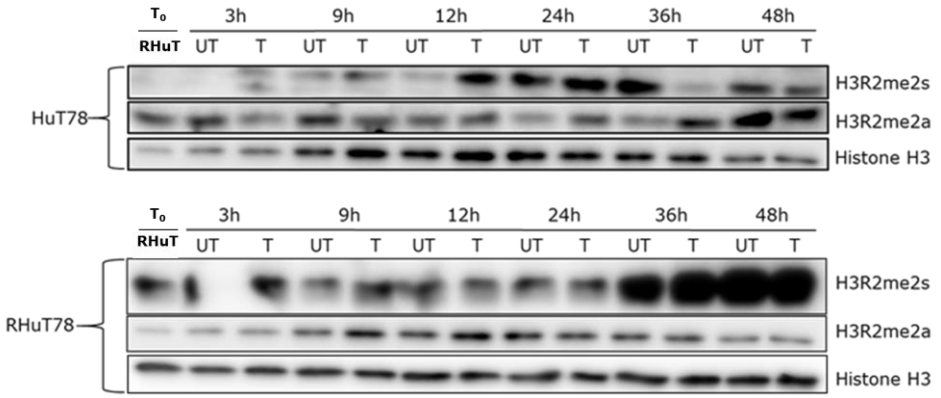

Figure 4.3 - Western blot showing H3R2 symmetric and asymmetric dimethylation in HuT78 and RHuT78 cells.

Western blots were performed as in **Figure 4.1** and probed for H3R2me2s and H3R2me2a. Histone H3 was again used a loading control.

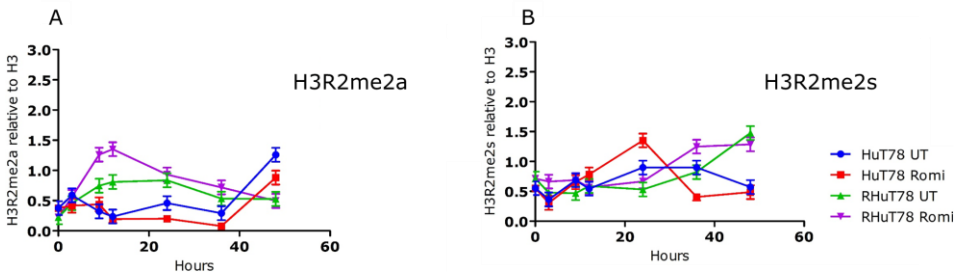

Figure 4.4 - Densitometry analysis of Western blots shown in Figure 4.3.

Values are calculated relative to total histone H3 and then the RHuT78 blot is made relative to the HuT78 blot using the repeated sample of T_0 RHuT. (n=3) No statistical analysis was performed.

constant throughout the 48hrs of culture. In contrast, untreated HuT78 cells fluctuated in the levels of this asymmetric mark, peaking in expression at 9hrs and then again at 48hrs. In contrast, levels of H3R2me2a in RHuT78 cells fluctuated in both treated and untreated samples, with the highest expression being both at ~12hrs. Also, levels of the asymmetric mark in RHuT78 cells reached higher levels in treated samples than untreated samples.

It was therefore concluded that H3R2me2 marks alter spontaneously and in response to treatment with Romidepsin. The symmetric mark changed the most during culture, but it seemed unlikely to be influencing resistance to Romidepsin due to the finding of similar levels in both HuT78 and RHuT78 cells with and without treatment. The differences seen in the asymmetric mark between HuT78 cells and RHuT78 cells were also interesting but did not explain the differences seen in the levels of the H3K4me3 marks as previously hypothesised (i.e. there was no observed inverse relationship using western blotting). We therefore decided that the study should focus on to looking at expression levels of enzymes that regulate these epigenetic marks, starting with those of the KDM family.

4.2.3 Protein expression changes of lysine demethylase enzymes in RHuT78 with and without treatment with Romidepsin

Having initially examined changes in histone methylation we next investigated whether treatment of RHuT78 and RMEC1 cells could alter expression levels of epigenetic enzymes. We initially started this work by looking at protein expression levels by Western blot using an antibody sample kit that was already available within the department. This sample kit included antibodies for KDM3B, KDM4A, KDM5A, KDM5C and PHF (the other antibodies included in the kit were tried but no specific protein bands were detected by Western blot).

Figure 4.5 and **Figure 4.6** show the expression of these epigenetic enzymes in RHuT78 cells with and without treatment with Romidepsin. Levels of KDM3B (H3K9 demethylase), KDM4A (H3K9/K36 demethylase), KDM5A and KDM5C (H3K4me2/3 demethylases) showed no consistent change between treated and untreated samples over the 24hr period. In contrast, PHF2 (an H3K9 demethylase) was induced upon treatment with Romidepsin; expression levels increased by 9hrs and was even higher by 12hrs, but then went back to untreated levels by 24hrs.

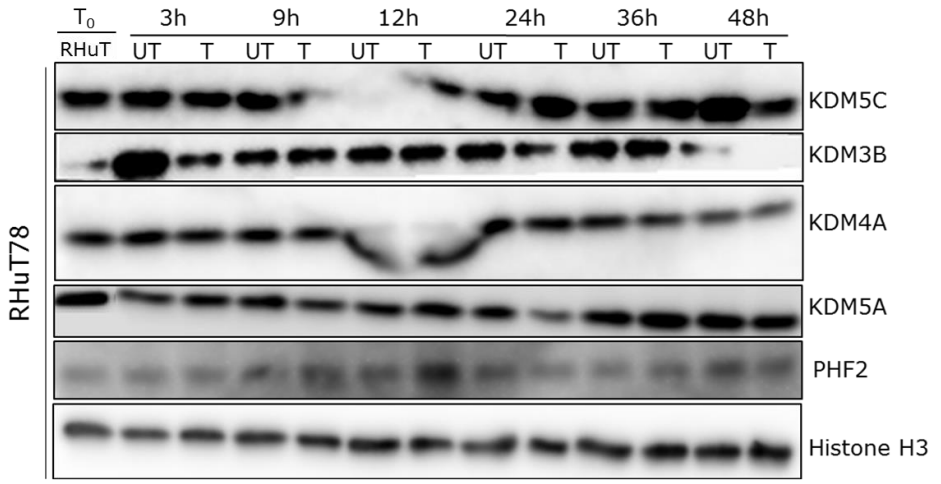

Figure 4.5 - Expression of epigenetic enzymes in RHuT78 cells with and without treatment with Romidepsin.

RHuT78 cells were passaged and then either lysed (T_0 RHuT), left untreated (UT) or treated immediately with Romidepsin (T). Samples were taken and lysed at the indicated time points. Protein lysates were then separated on an SDS-PAGE gel, Western blotted and probed for KDM3B, KDM4A, KDM5A, KDM5C or PHF2. Histone H3 was used as a loading control.

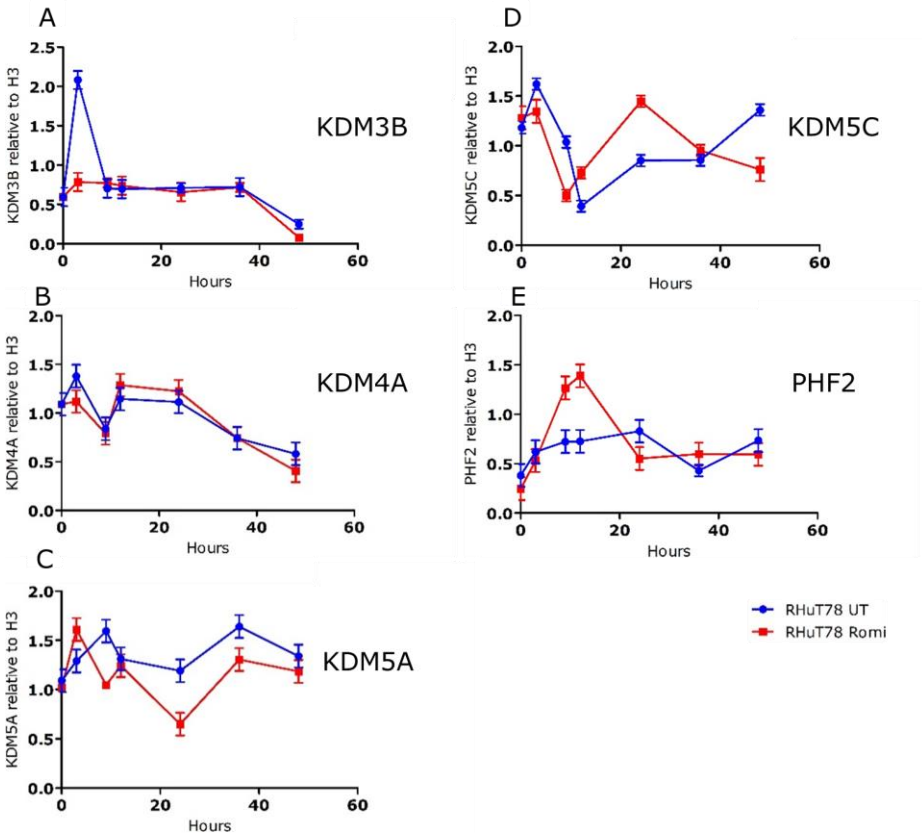

Figure 4.6 – Densitometry analysis of Western blot results shown in Figure 4.5.

Values are made relative to total histone H3. (n=3) No statistical analysis was performed.

It was therefore concluded that the expression levels of 4 of the epigenetic enzymes studied did not change upon treatment. These included 2 H3K4me2/3 demethylases, KDM5A and KDM5C, suggesting that alterations in H3K4me3 levels seen upon treatment with Romidepsin were not due to changes in expression of these enzymes. Interestingly, PHF2 expression did transiently increase upon treatment with Romidepsin. However, because increased expression levels of this enzyme would most likely lead to lower abundance of H3K9me2/3 and therefore potentially increase the quantity of H3K9Ac, it was hypothesised that this change was unlikely to counteract HDACis and contribute towards resistance.

It remained a possibility that even though levels of protein did not change in resistant cells upon treatment, levels of certain epigenetic enzymes were constantly higher in RHuT78 than they were in the HuT78 parental cell line. Therefore, HuT78, RHuT78 and DHRHuT78 cells were taken after serial passages and examined by western blotting to study changes in KDM expression. Because we were particularly interested in the alterations in H3K4me3 seen in **Figure 4.1**, we probed the blot for KDM5A expression. As shown in **Figure 4.7** levels of KDM5A protein expression are clearly higher in RHuT78 cells than both the HuT78 and DHRHuT78 cells. This result indicates

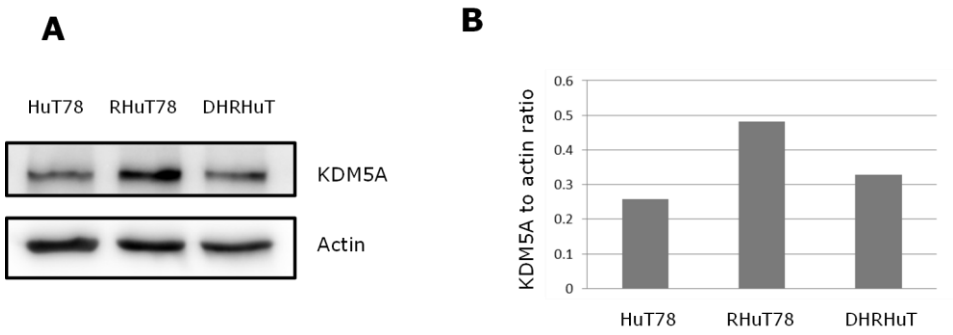

Figure 4.7 – Levels of KDM5A protein expression in HuT78, RHuT78 and DHRHuT78.

A) Western blot of HuT78, RHuT78 and DHRHuT78 cell lysates probed for KDM5A. **B)** Densitometry values of KDM5A relative to actin of Western blot shown in Figure 4.7A (n=1).

that lower levels of H3K4me3 may be caused by a higher level of KDM5A protein in RHuT78.

Having examined a select number of epigenetic enzymes by immunoblotting, the study was expanded to a much wider range of enzymes using quantitative PCR analysis.

4.2.4 PCR array analysis of epigenetic gene expression changes in RHuT78 cells upon treatment with Romidepsin.

Using a predesigned gene profiling PCR array from Qiagen, we initially compared expression of 84 epigenetic genes in RHuT78 cells treated with and without Romidepsin. Cells were passaged, cultured for 24hrs without the drug, and then treated with 6nM Romidepsin for 24hrs before harvesting for mRNA extraction.

Figure 4.8 (**Table A8** and **Figure A1** in Appendix) shows the results of the PCR array that illustrates expression fold differences of epigenetic genes between Romidepsin treated and untreated samples of RHuT78 cells. 17 epigenetic genes altered their expression more than 1.5 fold, 6 were down-regulated and 11 were up-regulated. The 3 highest up-regulated genes were HDAC9 (3.06 fold), HDAC5, (2.86 fold) and MLL3 (2.47 fold). In contrast, AURKC (2.47 fold), SETD7

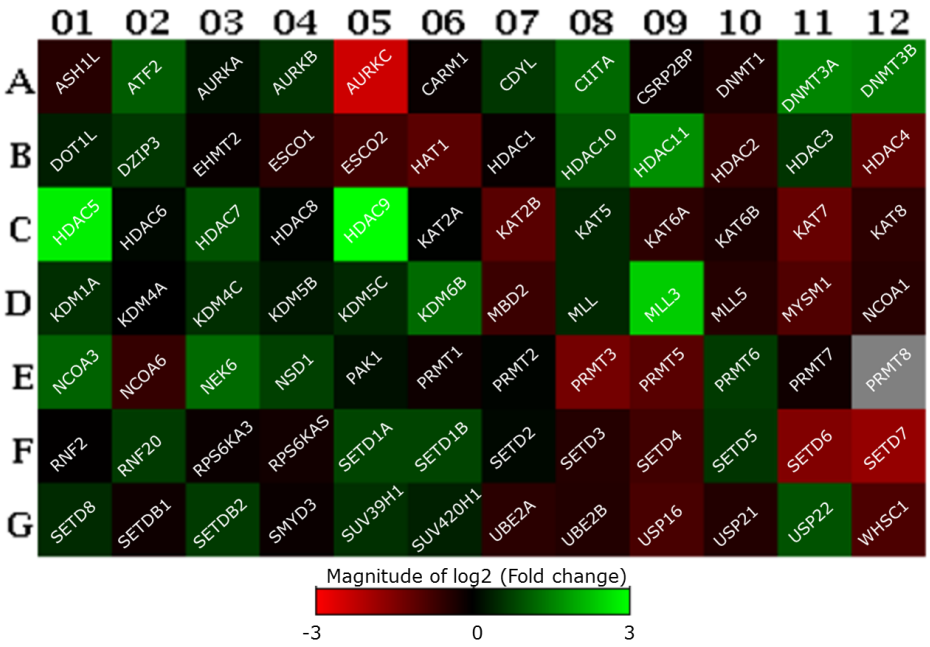

Figure 4.8 – Epigenetic gene expression in RHuT78 cells with and without treatment with Romidepsin.

Heat map depicting fold change in epigenetic gene expression generated from the human epigenetic chromatin modification PCR array plate between untreated and 6nM Romidepsin treated RHuT78. Cells were passaged, left untreated for 24hrs and then either treated with or without Romidepsin for a further 24hrs before RNA was purified. PRMT8 has a grey box as it had a high Ct threshold due to low expression and was excluded from the analysis.

(1.94 fold) and SETD6 (1.77 fold) were the 3 most down-regulated genes.

4.2.5 Comparison of epigenetic gene changes between RHuT78 and HuT78 cells

To validate these results and to compare gene expression changes of RHuT78 to that seen in HuT78 cells after treatment with Romidepsin, new primer pairs for qRT-PCR analysis were created for each of the 17 epigenetic genes that were altered upon treatment. In addition, 7 new primer pairs were created for genes that have been shown to be altered in leukemia and lymphoma but were either not included on the array (KDM2B, KDM5A, KDM6A) or shown not to be changed >1.5 fold in expression (HDAC8, KDM1A, KDM4C and PRMT2). From these 24 primer pairs, 22 showed specific amplification and were analysed further (PRMT3 and SETD7 failed to amplify specifically - **Figure 4.9**). From the 19 genes that were analysed by qRT-PCR and which were originally on the array plate, 14 showed similar changes in expression while 5 genes altered the way in which responded to Romidepsin (AURKC, HDAC8, KDM2B, PRMT2 and SETD6). These alterations in response may be due to biological variation between the different experiments (qRT-PCR experiments were performed

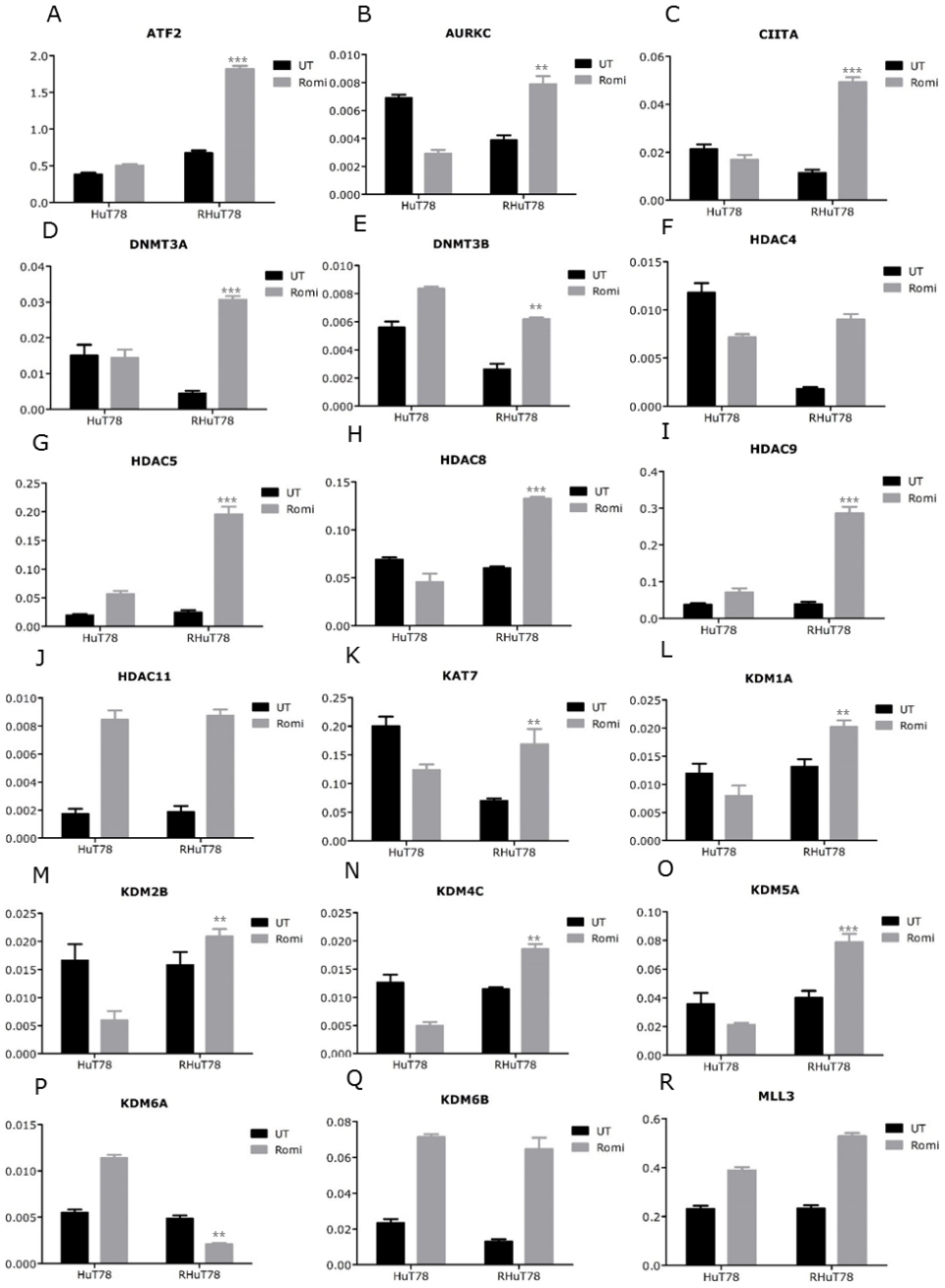
A
ATF2
B
AURKC
C
CIITA
D
DNMT3A
E
DNMT3B
F
HDAC4
G
HDAC5
H
HDAC8
I
HDAC9
J
HDAC11
K
KAT7
L
KDM1A
M
KDM2B
N
KDM4C
O
KDM5A
P
KDM6A
Q
KDM6B
R
MLL3
UT
Romi
HuT78
RHuT78

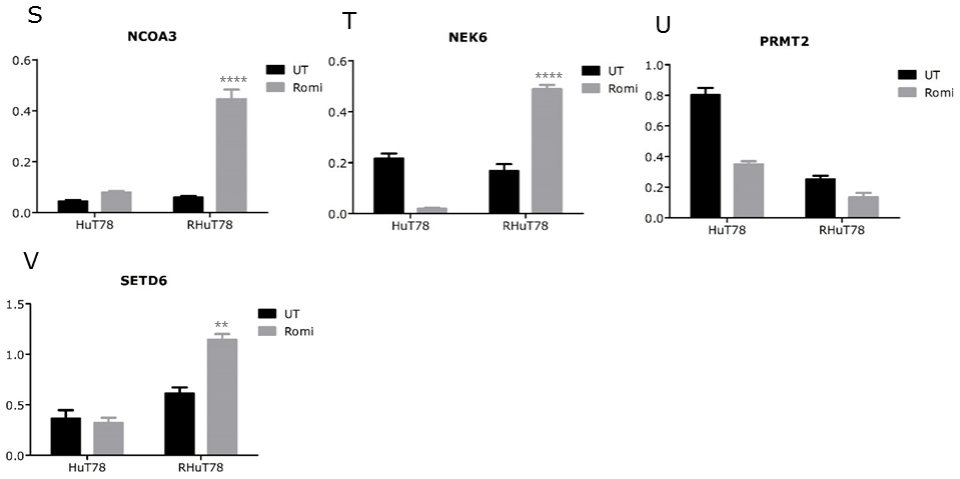

Figure 4.9 - Comparison of expression changes in selected epigenetic genes between HuT78 and RHuT78 cells with and without treatment using Romidepsin.

cDNA was prepared as in **Figure 4.8**. Expression levels of 22 epigenetic genes were analysed by RT-qPCR. The relative expression level of each gene was normalized to that of RPL27, which remained consistent between cell types and treatments. Genes are organised in alphabetical order. Error bars are standard error of the mean between n=3 PCR experiments. Δ fold changes were statistically tested using two-way ANOVA. ****, P<0.0001; ***, P<0.001; **, P<0.01; *, P<0.05.

on 3 biological replicates analysed 3 times [n=9] while the array plate was from a single experiment) or because the primers used in the array plate differed from those used in the subsequent qRT-PCR experiments.

From the 22 genes quantified for expression by qRT-PCR, 5 showed little or no difference in fold change of expression between HuT78 and RHuT78 cells with and without treatment (Δ fold change <2; DNMT3B, HDAC11, KDM6B, MLL3 and PRMT2 - **Figure 4.12**). Out of the remaining 17 genes that had differing responses between HuT78 and RHuT78 cells (Δ fold change >2), 4 showed exaggerated responses in RHuT78 cells (ATF2, HDAC5, HDAC9, and NCOA3) while the remaining 13 had opposite responses in the two cell types: 12 genes remained the same or decreased in HuT78 cells while increasing in RHuT78 (including DNMT3A, HDAC8 and NEK6), while KDM6A was the only epigenetic gene that increased in HuT78 but decreased in RHuT78. Interestingly, HDAC8 failed to increase on the PCR array but had strong up-regulation using different primers that amplified over different exon-exon boundaries. This could indicate that specific splice variants of HDAC8 may be increased upon Romidepsin treatment.

Having studied these selected genes in HuT78 and RHuT78, it now seemed important to establish if changes in gene expression were consistent between cell types and also between different models of resistance to Romidepsin. By comparing these models of Romidepsin resistance we could establish epigenetic genes that were consistently altered after treatment. Also, comparing expression changes between resistant and parental cell lines may provide evidence that alterations in specific epigenetic gene responses is contributing towards a general insensitivity towards Romidepsin.

4.2.6 Epigenetic gene changes in MEC1/RMEC1 and R_{50}HuT78 cells after treatment with Romidepsin

Having already developed a Romidepsin resistant MEC1 cell line in the previous chapter we next evaluated epigenetic gene changes upon treatment with Romidepsin in this model of resistance. Alongside this, we also performed the same experiment on a HuT78 cell line which is resistant to 50nM of Romidepsin in the presence of the P-glycoprotein efflux pump inhibitor Verapamil (termed R_{50}HuT78; acquired from Susan E Bates NIH, USA[203]). **Figure 4.10 and Figure 4.11** show the results of MEC1/RMEC1 and R_{50}HuT78 respectively. Despite performing this experiment on the R_{50}HuT78 cells, it was

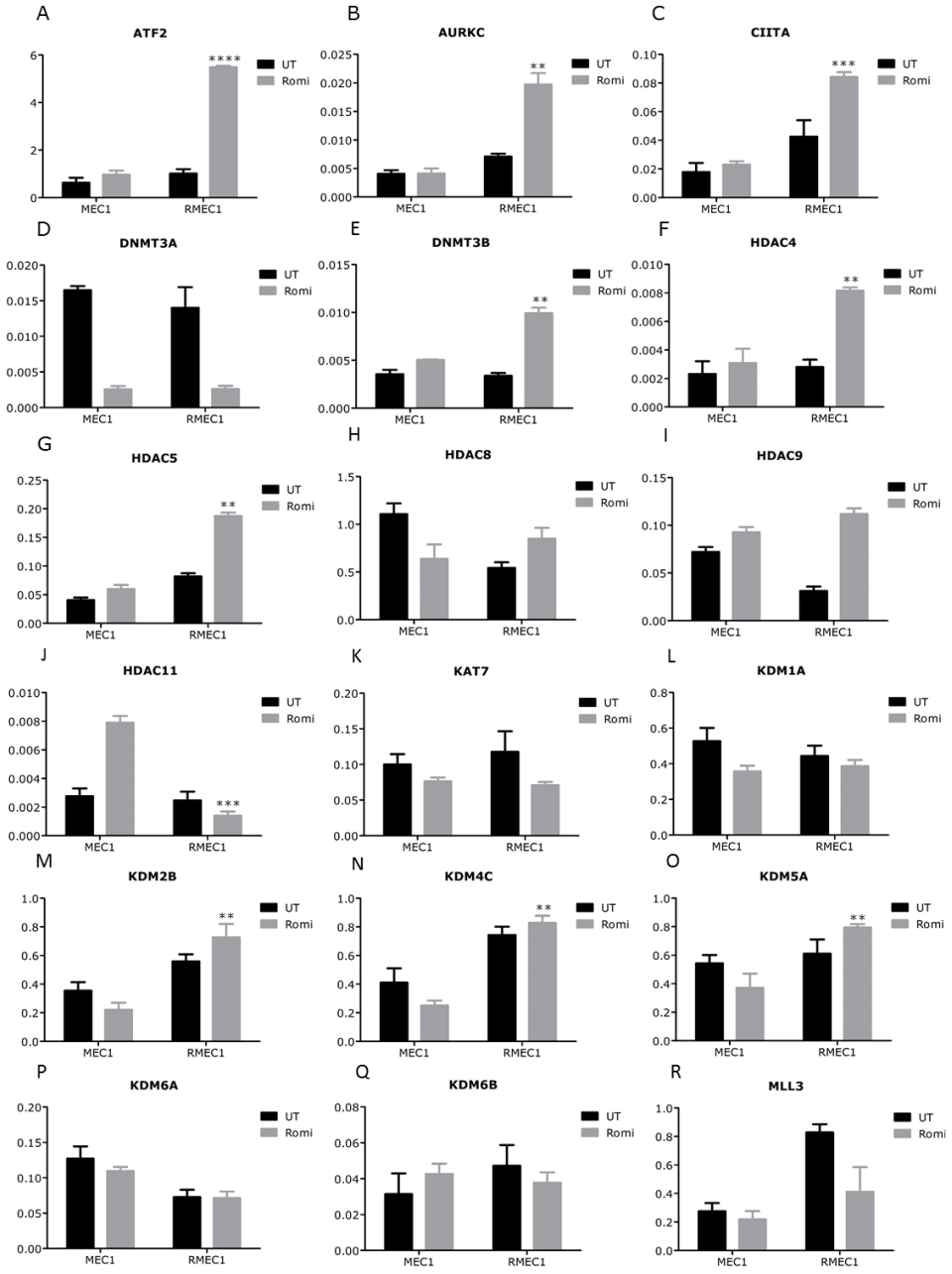
A
ATF2
B
AURKC
C
CIITA
D
DNMT3A
E
DNMT3B
F
HDAC4
G
HDAC5
H
HDAC8
I
HDAC9
J
HDAC11
K
KAT7
L
KDM1A
M
KDM2B
N
KDM4C
O
KDM5A
P
KDM6A
Q
KDM6B
R
MLL3
UT
Romi
MEC1
RMEC1

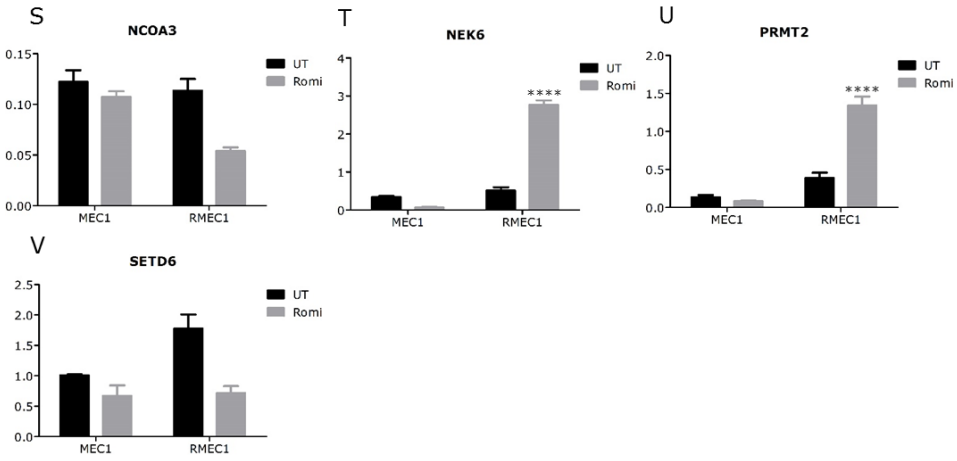

Figure 4.10 – Comparison of changes in selected epigenetic gene expression between MEC1 and RMEC1.

Experiment and statistical analysis was performed as in Figure 4.9. Again, RPL27 was equally expressed and did not change upon treatment in the two groups of MEC1 and RMEC1. Error bars indicate standard error of the mean of n=3 independent experiments. Δ fold changes were statistically tested using two-way ANOVA. ****, $P<0.0001$; ***, $P<0.001$; **, $P<0.01$; *, $P<0.05$.

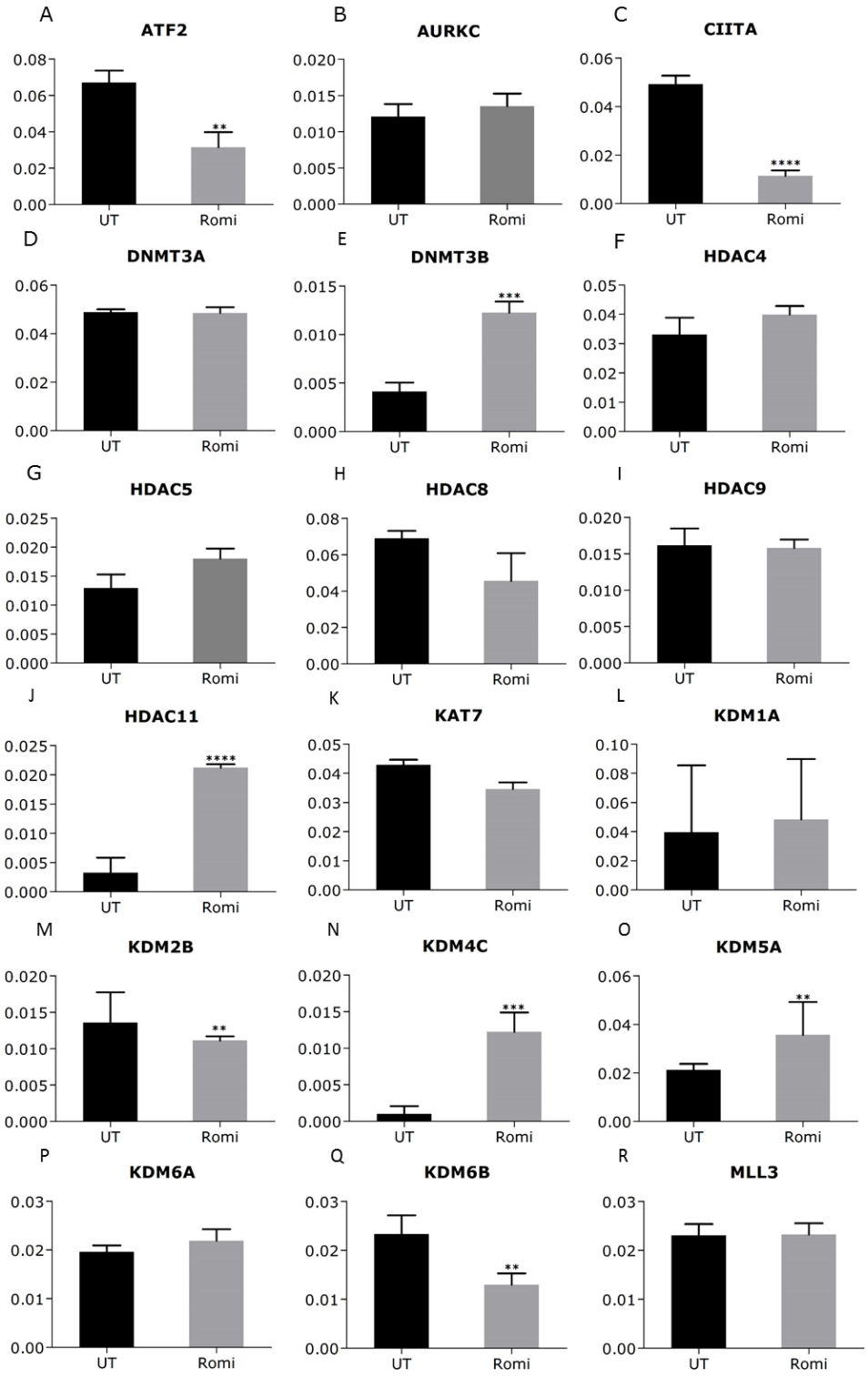
A
ATF2
0.08
0.06
0.04
0.02
0.00
**
UT
Romi
B
AURKC
0.020
0.015
0.010
0.005
0.000
UT
Romi
C
CIITA
0.06
0.04
0.02
0.00
****
UT
Romi
D
DNMT3A
0.06
0.04
0.02
0.00
UT
Romi
E
DNMT3B
0.015
0.010
0.005
0.000
***
UT
Romi
F
HDAC4
0.05
0.04
0.03
0.02
0.01
0.00
UT
Romi
G
HDAC5
0.025
0.020
0.015
0.010
0.005
0.000
UT
Romi
H
HDAC8
0.08
0.06
0.04
0.02
0.00
UT
Romi
I
HDAC9
0.020
0.015
0.010
0.005
0.000
UT
Romi
J
HDAC11
0.025
0.020
0.015
0.010
0.005
0.000
****
UT
Romi
K
KAT7
0.05
0.04
0.03
0.02
0.01
0.00
UT
Romi
L
KDM1A
0.10
0.08
0.06
0.04
0.02
0.00
UT
Romi
M
KDM2B
0.020
0.015
0.010
0.005
0.000
**
UT
Romi
N
KDM4C
0.020
0.015
0.010
0.005
0.000
***
UT
Romi
O
KDM5A
0.06
0.04
0.02
0.00
**
UT
Romi
P
KDM6A
0.03
0.02
0.01
0.00
UT
Romi
Q
KDM6B
0.03
0.02
0.01
0.00
**
UT
Romi
R
MLL3
0.03
0.02
0.01
0.00
UT
Romi

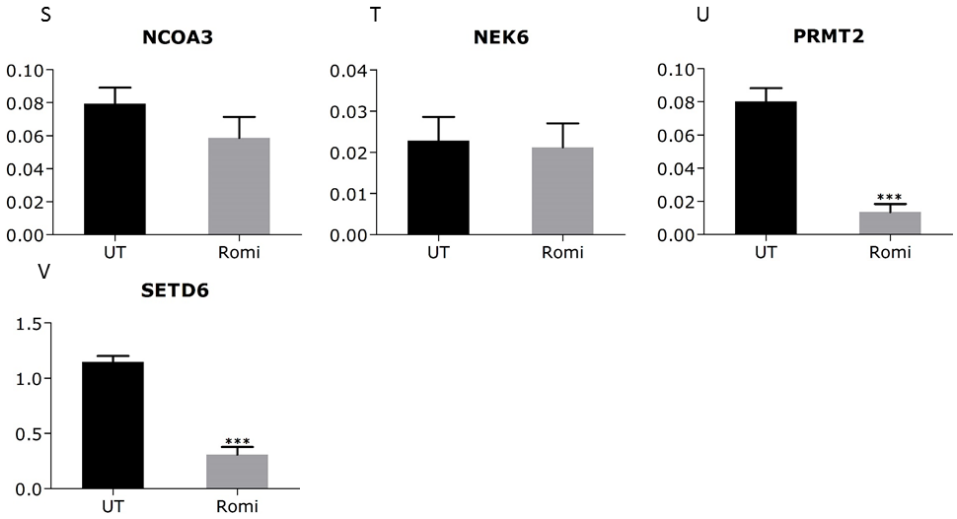

Figure 4.11 - Changes in selected epigenetic gene expression in untreated and Romidepsin treated R_{50}HuT78.

Experiment and statistical analysis performed as in **Figure 4.9**. All gene expression was made relative to the reference gene RPL27. UT, untreated; Romi, 50nM Romidepsin. (N.B. The R_{50}HuT78 was not fully resistant to Romidepsin at the time of performing these experiments). Error bars are standard error of the mean between n=3 PCR experiments. Δ fold changes were statistically tested using two-way ANOVA. ****, P<0.0001; ***, P<0.001; **, P<0.01; *, P<0.05.

quickly realised that this cell line was not fully resistant in our hands to 50nM Romidepsin in the presence of Verapamil. Therefore, the results for this cell line were not used for direct comparison against that of RHuT78 and RMEC1. Interestingly, the majority of genes that had altered expression changes after Romidepsin in R_{50}HuT78 were more similar to that of normal HuT78 cells (15/22) than RHuT78 (5/22).

In MEC1 cells, out of the 22 genes studied 13 showed little or no difference in change of expression between MEC1 and RMEC1 cells with and without treatment (Δ fold change <2 - **Figure 4.12**). The remaining 9 genes showed changes in gene expression (Δ fold change >2); 3 of these 9 genes (ATF2, DNMT3B and HDAC9) showed exaggerated increase or decrease in expression in RMEC1; while 6 had opposite changes in expression (5 out of these 6 decreased or stayed unchanged in MEC1 upon Romidepsin treatment while increasing in RMEC1 – AURKC, HDAC8, KDM2B, NEK6 and PRMT2; HDAC11 was the only gene to increase in MEC1 but decrease in RMEC1).

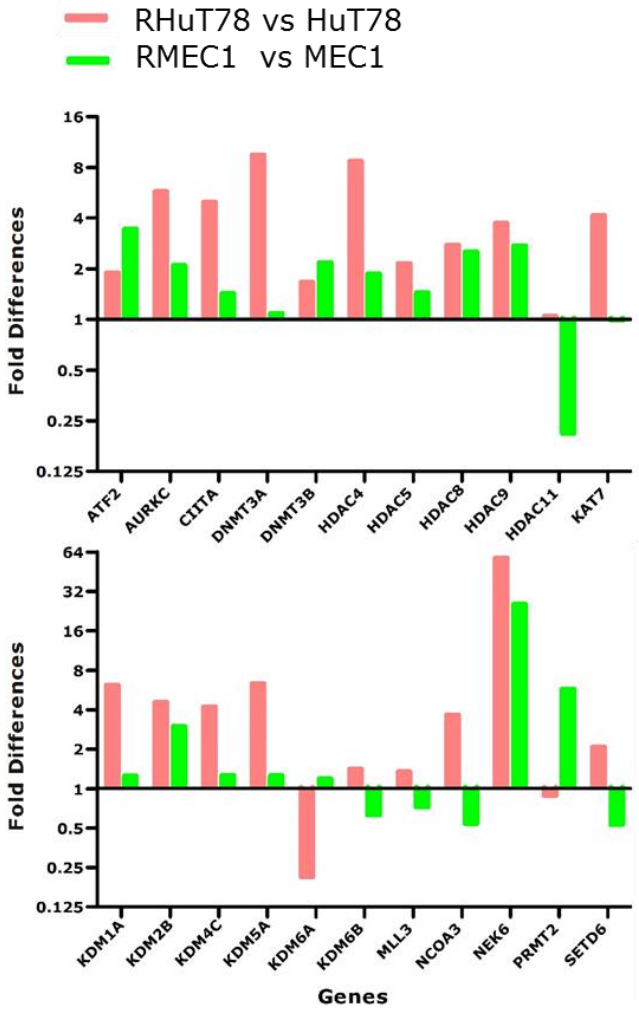

Figure 4.12 – Comparison of Δ fold changes in epigenetic gene expression in RHuT78 vs HuT78 and RMEC1 vs MEC1 after treatment with Romidepsin.

Δ fold changes in expression after treatment with Romidepsin were taken for each corresponding resistant and non-resistant cell line from **Figure 4.9** (red bars) and **Figure 4.10** (green bars) and plotted on a bar chart. Y axis is plotted as log base 2.

4.2.7 Comparison of epigenetic gene expression changes upon treatment with Romidepsin in different cell types.

To establish if changes in epigenetic gene expression were consistent between cell types and between resistant models upon treatment with Romidespin, we compared expression changes of the 22 evaluated genes shown in **Figure 4.9** and **Figure 4.10**.

Using principal component analysis (PCA) on the 22 epigenetic genes analysed, the HuT78, RHuT78, MEC1 and RMEC1 cell lines were compared with and without treatment with Romidepsin. As can be seen from **Figure 4.13**, cell type can clearly be seen to be split according to PC2, while Romidepsin treatment segregates them according to PC3. Despite cell type segregation by PC2, Romidepsin treated RHuT78 and RMEC1 cell lines both segregate very closely together. This observation shows that the change of response to Romidepsin in resistant cell lines is similar and independent of the cell of origin. Interestingly, untreated RHuT78 and RMEC1 are both closer in gene expression to their untreated/treated parental cell line counterparts.

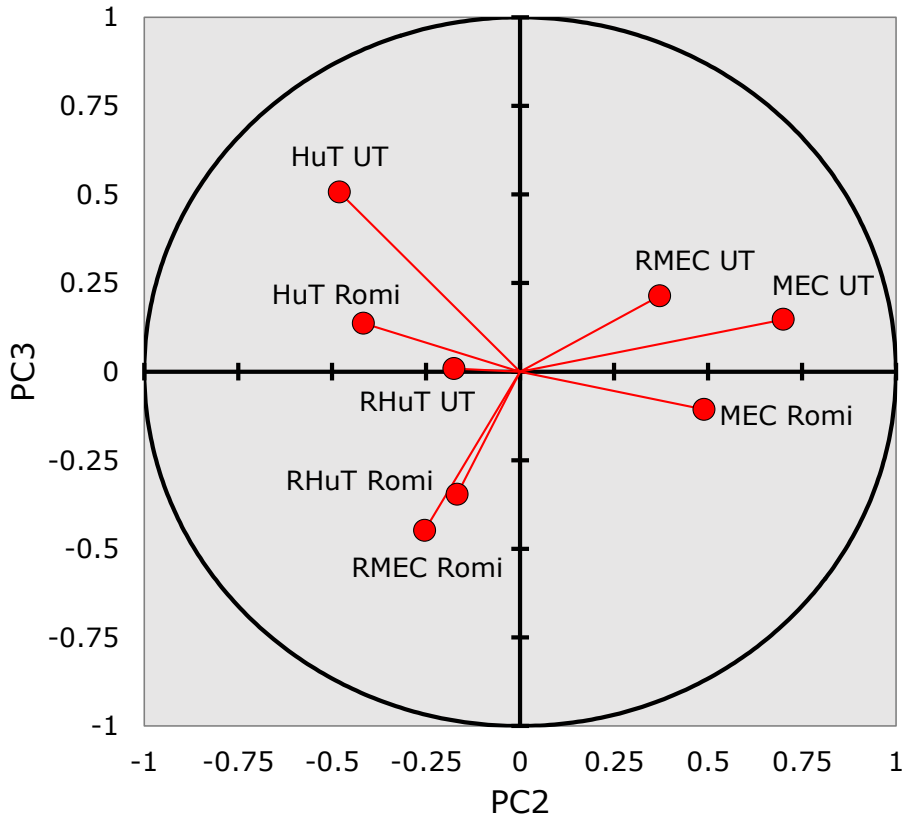

Figure 4.13 – PCA based upon expression of 22 epigenetic genes in HuT78, RHuT78, MEC1 and RMEC1 with and without Romidepsin treatment.

Analysis was performed using the XLSTAT software Version 2016.01.26745. UT, 24hrs untreated; Romi, 24hrs Romidepsin treatment.

To evaluate which genes had comparable changes in their response following development of resistance in both HuT78 and MEC1 we compared the Δ fold change in both cell types. As can be seen from **Figure 4.12**, 14/22 genes had similar alterations in response to Romidepsin between parental and resistant cell types. The genes that altered similarly and most significantly in both instances (Δ fold change in both cell types >2) were ATF2, AURKC, HDAC8, HDAC9, KDM2B and NEK6.

4.3 Discussion

The main aims of this chapter were to establish whether HDACi Romidepsin causes changes in histone PTMs other than acetylation and also if the drug alters expression of epigenetic genes that modulate histone PTMs. Results for parental cell lines of HuT78 and MEC1 were compared with their drug resistant counterparts.

Treatment with Romidepsin increased acetylation in both HuT78 and RHuT78 cells. This shows that despite the RHuT78 cells being resistant to 6nM Romidepsin, the drug can still enter the cell and inhibit HDAC activity. Interestingly, despite an increase in H3Ac levels in both cell types, H3K4me3 levels were not altered in RHuT78 cells upon treatment with Romidepsin. In contrast, treatment of HuT78 cells caused a dramatic fold increase in global levels of H3K4me3 over the first 24hrs of culture.

Because of this difference, we examined KDM5A (a H3K4me3 demethylase) expression in these cells. Levels of KDM5A did not change in RHuT78 cells after treatment with Romidepsin. However, the level of this demethylase was basally higher in resistant cells when compared to HuT78 and DHRHuT78. This is interesting because KDM5A expression levels are believed to

decrease upon treatment with HDACi[233], and this can clearly be seen when we look at mRNA expression changes in both HuT78 and MEC1. However, the level of KDM5A mRNA increases in resistant cell lines upon treatment with Romidepsin, and the protein levels of KDM5A also remain high. An increase in KDM5A expression and reduced H3K4me3 levels are also observed in other drug tolerant cell lines[234] and therefore may be a feature of resistance in general.

Using an epigenetic PCR array, levels of epigenetic gene expression was examined in RHuT78 cells with and without treatment with Romidepsin. A total of 17/84 genes had a log2 fold change of >2 upon treatment. These genes included a number of HDAC class II family members (HDAC4, 5 and 9) and the DNA methyltransferases DNMT3A and 3B. Using the results from this PCR, a smaller group of 22 genes were selected that showed either a log fold difference of >2 upon treatment in the array or which had been proven to be important in leukemia and lymphoma development. Using these 22 genes, Romidepsin treated and untreated HuT78, RHuT78, RMEC1 and MEC1 samples were all compared. PCA illustrated that the two resistant cell lines alter their gene expression very similarly independent of the cell of origin. Genes that altered the most in both RHuT78 vs HuT78 and

RMEC1 vs MEC1 cells were ATF2, AURKC, HDAC8, HDAC9, KDM2B and NEK6. Interestingly, NEK6 is required for progression through the M phase (specifically the metaphase) of the cell cycle. It is reduced in both HuT78 and MEC1 cells after treatment with Romidepsin, but increases in both RHuT78 and RMEC1 after treatment. Romidepsin normally inhibits the cell cycle but this HDACi seems to enhance proliferation in resistant cell lines (see next chapter). It was therefore hypothesised that changes in the expression of the NEK6 gene may be linked to changes in cell cycle status of these cells.

Consistent alteration of HDAC8 and HDAC9 expression changes between resistant and non-resistant cells upon treatment with Romidepsin suggested potential shared response mechanisms that develop upon resistance. These acetyltransferases and the potential importance of changes in DNMT expression are investigated in more detail during **Chapter 6**.

Chapter 5

Studies into the altered proliferative rates of Romidepsin resistant cell lines

5.1 Introduction

During the development of RHuT78 cells and continued passages in the presence of Romidepsin, it was noticed that these resistant cells were consistently at much higher density after 3 days of growth than their parental cell counterparts (**Figure 3.7**). Previous studies have shown an inhibition of the cell cycle upon treatment with Romidepsin through up regulation of the CDK inhibitor protein $p21^{WAF1/CIP1}$. Therefore, it was intriguing how resistant cells not only were resistant to Romidepsin in terms of apoptosis, but also seemed to gain a proliferative advantage. This work would have particular relevance to clinical administration of Romidepsin to patients with resistance that is not yet apparent clinically, as continued use of the drug would potentially be disadvantageous and harmful.

This work therefore started by investigating whether the RHuT78 cells selected by Romidepsin inherently proliferated

faster or and whether this increased growth rate was also drug induced. In addition, whether this phenomenon was also true for other Romidepsin resistant cell lines such as RMEC1 was also investigated.

5.2 Results

5.2.1 Measurement of Romidepsin-induced proliferation in HuT78 and MEC1 resistant and non-resistant cell lines by BrdU assay

HuT78, RHuT78 and DHRHuT78 or MEC1, RMEC1 and DHRMEC1 were passaged, left untreated for 24hrs and then treated for 48hrs with and without 6nM and 9nM of Romidepsin respectively. Proliferation rates were then measured by a BrdU incorporation assay. BrdU is incorporated into newly synthesised DNA during the S phase of the cell cycle. Cells were cultured for 4hrs with BrdU, and therefore the quantity of new DNA synthesis between 48-52hrs was measured in the cells (**Figure 5.1**). This experiment shows that HuT78 and DHRHUT78 cells react very similarly and both decrease proliferation upon treatment with Romidepsin. In contrast, despite proliferative rates being similar when the cells were left untreated, treatment of RHuT78 cells with 6nM Romidepsin caused an increase in proliferation. These results show that the enhanced proliferation observed in **Chapter 3** in RHuT78 is also true for RMEC1 cells.

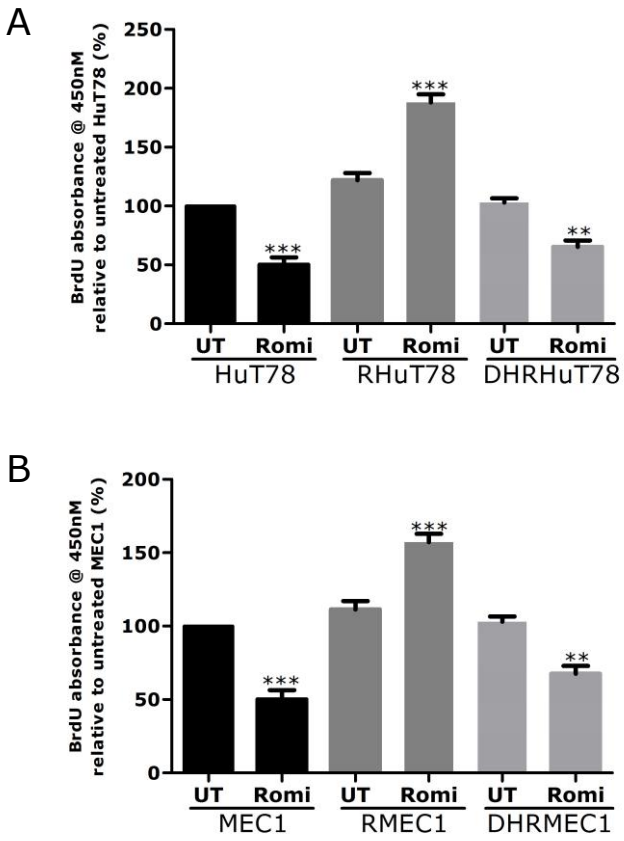

Figure 5.1 – Proliferation effects of Romidepsin on HuT78 and MEC1 parental, drug resistant and drug holiday cell lines.

Cells were passaged, cultured for 24hrs and then treated with (Romi) and without (UT) 6nM Romidepsin. After 48hrs cells were exposed to BrdU and left for a further 4hrs after which the BrdU ELISA was performed. Absorbance at 450nm was measured and all results were made relative to the respective untreated parental cell line. **A)** Results for HuT78, RHuT78 and DHRHuT78. **B)** Results for MEC1, RMEC1 and DHRMEC1. Error bars are standard error of the mean between n=3 BrdU experiments. Values were statistically tested using two-way ANOVA. ***, $P<0.01$; **, $P<0.05$.

Surprisingly, the proliferation increase seen in both resistant cell lines is not inherent but is dependent upon the presence of Romidepsin; removal of the drug causes proliferation to reduce to similar levels as the parental cell lines.

5.2.2 Effects of increasing concentration of Romidepsin on proliferation in resistant cell lines

HuT78 and RHuT78 were processed the same as in section 5.2.1 but this time with increasing concentrations of Romidepsin (0.5-10nM for HuT78 and 0-12nM for MEC1). Proliferation rate was then measured at 24 and 48hrs later by a 4hrs incubation with BrdU (**Figure 5.2**).

As can be seen in **Figure 5.2**, addition of increasing concentrations of Romidepsin to HuT78 and MEC1 cells induced dose dependent decrease in proliferation. However, upon the addition of the HDACi to RHuT78 or RMEC1 cells there was a dose dependent increase in proliferation up to the drug concentration used to develop the resistance (6nM and 9nM respectively). Above these concentrations both RHuT78 and RMEC1 had reduced proliferation.

These result show that proliferation increases in a dose dependent manner, peaking at the concentration at which the

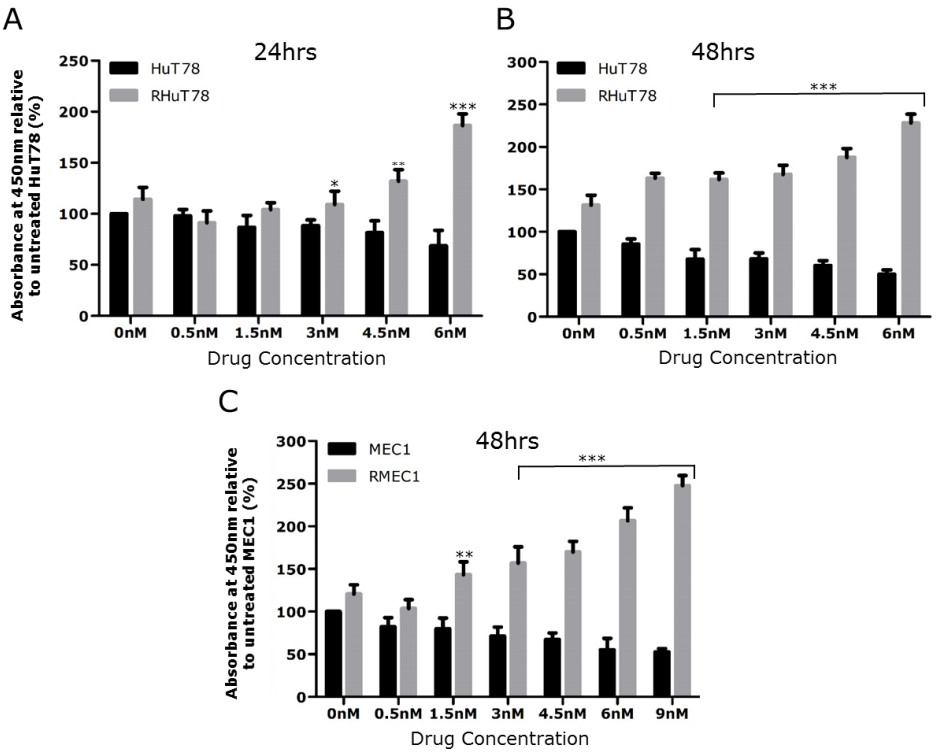

Figure 5.2 – Incorporation of BrdU in HuT78/RHuT78 and MEC1/RMEC1 after treatment with varying concentrations of Romidepsin.

Cells were passaged, cultured for 24hrs and then treated with the indicated concentration of Romidepsin. 24 or 48hrs later, BrdU was added to the cells for 4hrs and then the cells were taken for the BrdU ELISA experiment. All absorbance values from the ELISA are made relative to the untreated parental cell line. **A)** 24hrs HuT78/RHuT78. **B)** 48hrs HuT78/RHuT78. **C)** 48hrs MEC1/RMEC1. Error bars are standard error of the mean between n=3 BrdU experiments. Values were statistically tested using two-way ANOVA. ***, $P<0.002$; **, $P<0.01$; *, $P<0.05$.

resistance cells were developed. Above this concentration of Romidepsin, the cells start to undergo cell cycle arrest, similar to effects seen in the parental cell line cultured with lower quantities of the drug.

5.2.3 Effects of alternative HDACis on proliferation in Romidepsin resistant cell lines

Having established that Romidepsin induces enhanced proliferation in resistant cells, it next seemed important to establish whether other HDACis could have similar effects. Therefore HuT78, RHuT78, MEC1 and RMEC1 cells were left untreated or treated with the IC_{50} concentrations of the HDACis NaB, SAHA or TSA (established in **Chapter 3**), and proliferative responses induced by these drugs were compared to Romidepsin. As shown in **Figure 5.3**, all three alternative HDACis caused cell cycle arrest in both HuT78 and MEC1 cells as expected. **Figure 5.4** illustrates that all these drugs also up regulated $p21^{WAF1/CIP1}$ in HuT78 cells. In contrast, both RHuT78 and RMEC1 cells increased proliferation when these drugs were present in the media (**Figure 5.4**). Only the NaB concentration had to be reduced below the IC_{50} in order to get this effect, although at this concentration the proliferation was still inhibited in the parental cell lines. Therefore, it was concluded

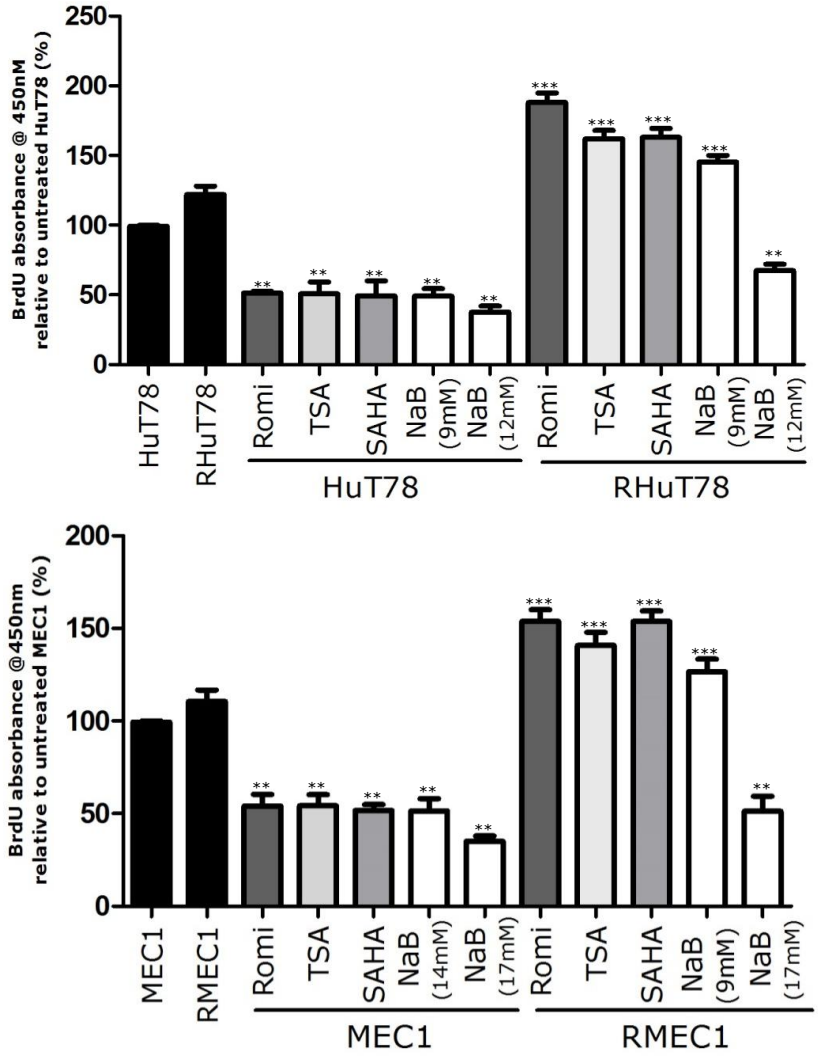

Figure 5.3 – HDACi effects on proliferation in HuT78 and RHuT78.

Experiment was performed the same as **Figure 5.1**, but cells this time were treated with the cell-type specific IC_{50} of each HDACi (see **Chapter 3**). Absorbance @450nm is made relative to the parental cell line and displayed as a percentage. Error bars show SEM of n=3 experiments, *** indicates $p<0.001$ **, $P<0.01$.

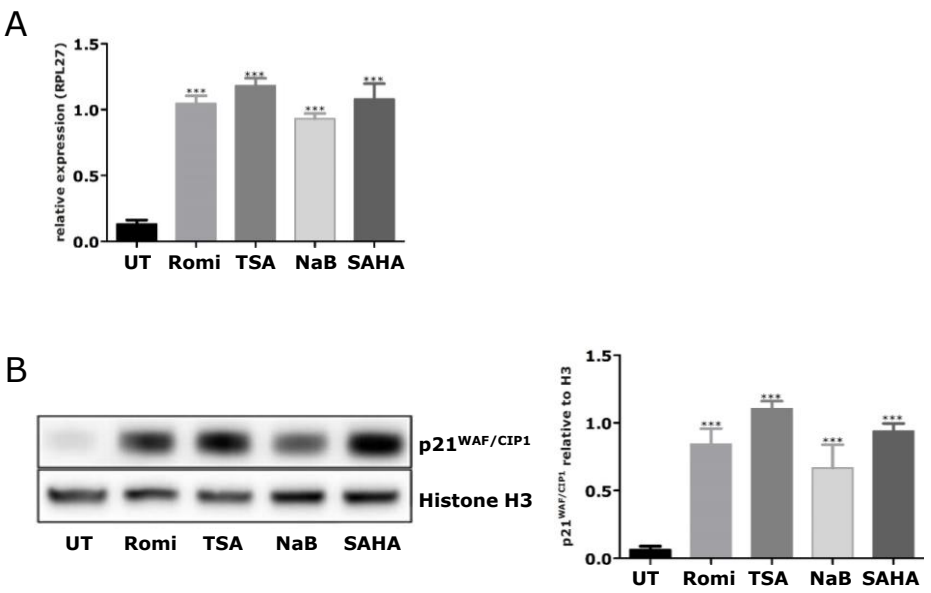

Figure 5.4 – Changes in p21$^{WAF1/CIP1}$ mRNA and protein expression in HuT78 cells upon treatment with Various HDACi.

HuT78 cells were left untreated (UT) or treated with Romidepsin (Romi), TSA, NaB or SAHA. **A)** 24hrs after treatment mRNA was measured for p21$^{WAF1/CIP1}$ and made relative to the house keeping gene RPL27. **B)** 48hrs after treatment, lysates of these cells were ran on a Western blot and probed for p21$^{WAF1/CIP1}$ protein (left) and then analysed by densitometry (right). Error bars show SEM of n=3 experiments, *** indicates $p<0.001$.

that RHuT78 cells were prone to proliferate not only in response to Romidepsin, but also upon exposure to a wide range of HDACis suggesting an adaptive response to the changes in the acetylation status in the epigenome.

5.2.4 Levels of Cyclin protein expression in Romidepsin treated HuT78 and RHuT78 cells.

Increased proliferation caused by HDACis may be explained by changes in expression of proteins that directly control the cell cycle. Therefore, resistant and non-resistant cells were treated with different concentrations of Romidepsin and Cyclin A, B1 and E levels were evaluated by Western blot. As can be seen from **Figure 5.5** and **Figure 5.6**, levels of Cyclin A and E were very similar and remained constant in untreated HuT78 and RHuT78 cells at both 24 and 48hrs. Cyclin B1 was much higher in HuT78 at 24hrs, but these levels decreased to those seen in RHuT78 cells by 48hrs.

Levels of Cyclins altered in HuT78 cells upon increasing concentrations of Romidepsin, with the most obvious changes being observed at 48hrs after treatment. Levels of Cyclin A and B1 both decreased upon treatment with >1.5nM Romidepsin in a dose dependant manner while Cyclin E increased with increasing concentrations of the HDACi. In RHuT78 cells, levels

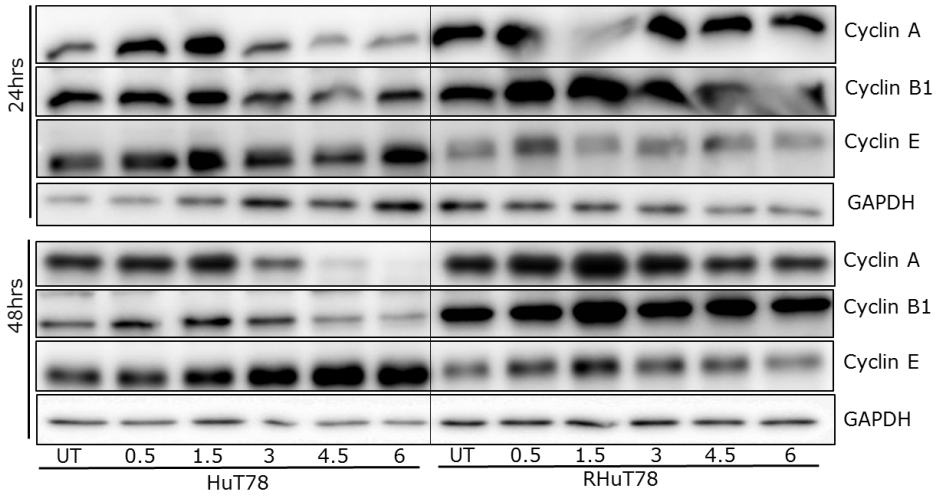

Figure 5.5 - Western blot analysis of cyclin expression in HuT78 and RHuT78 after treatment with increasing concentrations of Romidepsin.

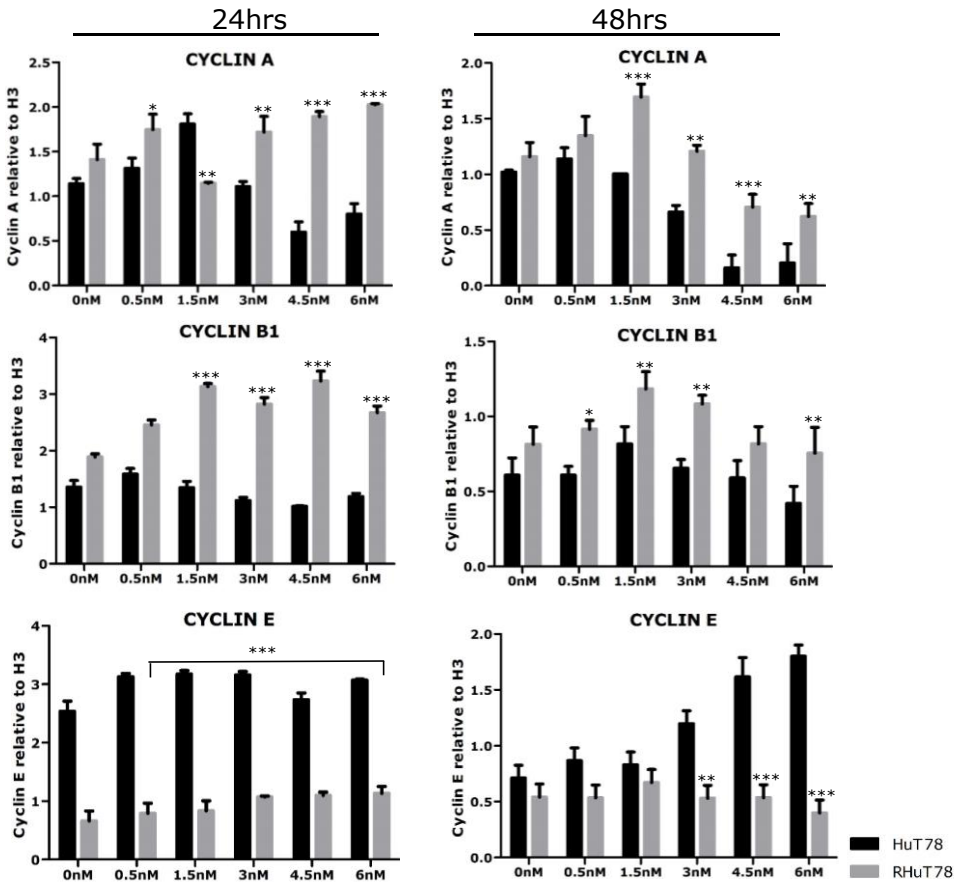

Figure 5.6 – Densitometry analysis of Figure 5.5. Error bars indicate standard error of the mean of n=3 independent experiments. Values were statistically tested using two-way ANOVA. ***, P<0.001; **, P<0.01; *, P<0.05.

of Cyclin A remained at high levels compared to HuT78 cells despite increasing concentrations of Romidepsin. Also, levels of Cyclin B1 increased in a dose dependent manner and this was particularly observed at 24hrs for Cyclin E which remained low in the RHuT78 culture.

These results indicate clear differences in cyclin expression between HuT78 cells and RHuT78 cells after treatment with increasing concentrations of Romidepsin. Interestingly, levels of cyclins were similar in untreated cells, and is in keeping with the equivalent rates of proliferation seen in **Figure 5.2**. After treatment with Romidepsin, HuT78 cells increase their levels of Cyclin E while decreasing Cyclin A, and to a lesser extent Cyclin B1. This indicates that HuT78 cells are halted in cell cycle at the G1 to S phase transition. In contrast, consistently low levels of Cyclin E while increasing levels of Cyclin B1 upon treatment with Romidepsin in RHuT78 cells suggests that Romidepsin treatment promotes entry of these cells into the G2/M phase of the cell cycle.

5.2.5 Cell cycle analysis of HuT78 and RHuT78

To evaluate further the cell cycle changes in RHuT78 cells compared to HuT78, we analysed cell cycle status using a PI staining method. As shown in **Figure 5.7**, PI staining of

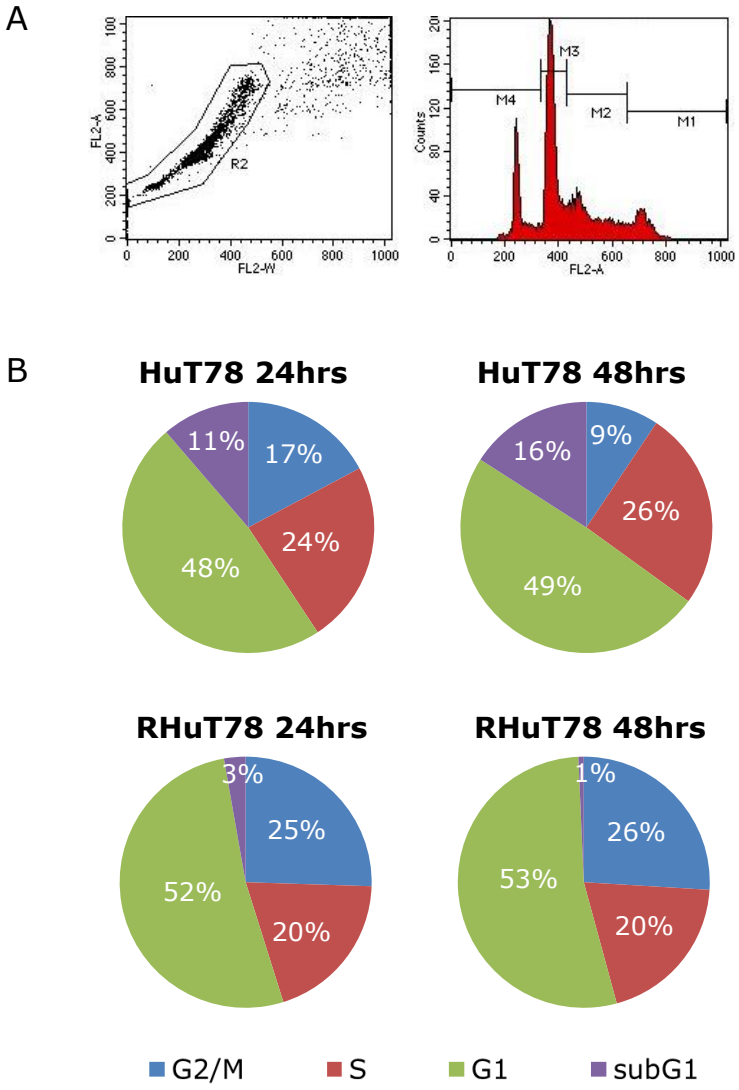

Figure 5.7 – Cell cycle analysis of HuT78 and RHuT78 using PI.

A) Representative flow cytometry analysis of PI stained cells. Singlet cells were selected in the scatter diagram on the left (R2 gate) and these events were plotted on the histogram on the right. M1 = G2/M, M2 = S, M3 = G1 and M4=subG1. **B)** Pie charts of data collected in (A), showing data for RHuT and HuT78 at 24 and 48hrs after passage

methanol fixed cells clearly distinguished between G1, S, G2/M and subG1 (G0) stages of the cell cycle. Also, percentage of cells in the G2/M phase of the cell cycle was greatly increased in RHuT78 cells in the presence of 6nM Romidepsin compared to HuT78. These results are consistent with the cyclin levels (particularly the increase in cyclin B1) and suggest more cells are progressing through the S phase of the cell cycle and are therefore situated in the G2/M phase. Interestingly, the number of cells in the subG1 (G0) phase of the cell cycle was also reduced in the RHuT78 cells compared to the parental HuT78.

5.2.6 The effects of HATi-II on proliferation and Romidepsin-induced proliferation in RHuT78 cells

Having established that HDACis drive proliferation of the resistant RHuT78 cells, we next examined the effects of HATi on this process. RHuT78 cells were untreated or treated with either 6nM Romidepsin or the IC_{50} concentration of HATi-II (26μM) for 24hrs. Cells that progressed through the S phase of the cell cycle over the next 4hrs were then measured by a BrdU assay. **Figure 5.8A** shows that Romidepsin increases BrdU incorporation as expected. Treatment with HATi-II caused a decrease in proliferation of RHuT78 cells. Importantly, when Romidepsin and HATi-II were added at the same, the HATi

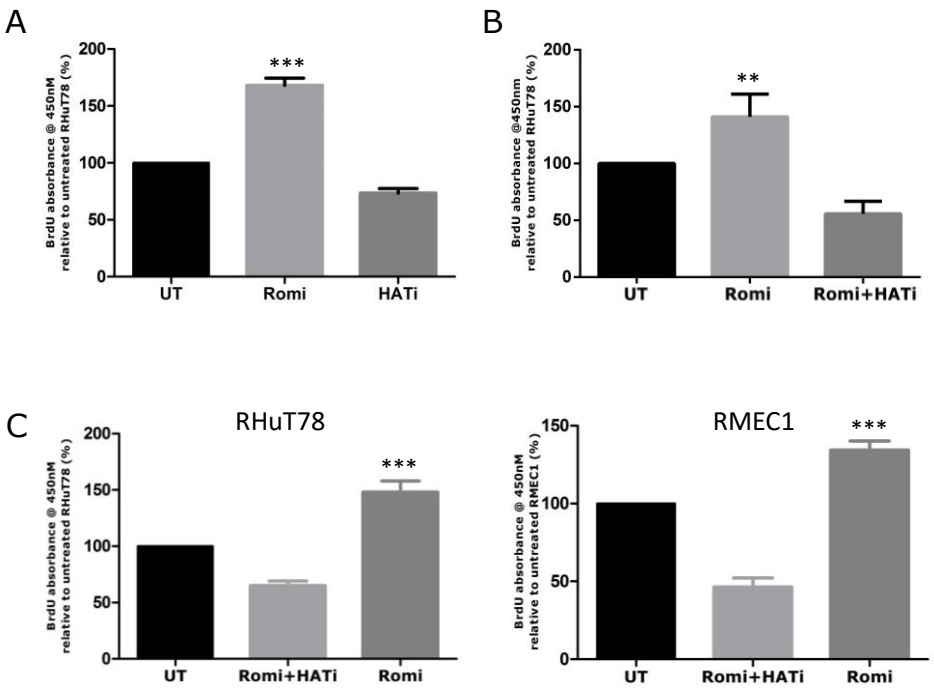

Figure 5.8 – Effects of HATi-II on proliferation of RHuT78 cells.

Bar charts showing BrdU incorporation by ELISA. **A)** RHuT78 cells were passaged, left untreated for 48hrs (UT), or left untreated 24hrs following by 24hrs treatment with either 6nM Romidepsin (Romi) or 26μM HATi-II (HATi). **B)** Cells were treated as in (A) but this time Romi and HATi were added together at the same time. **C)** Cells (RHuT78 on left and RMEC1 on right) were passaged, and either treated with and without 6nM Romidepsin. After 24hrs, Romidepsin treated samples were left for a further 24hrs either with just Romidepsin or Romidepsin+HATi-II. N=3 for each sample. ***, $p<0.002$, ANOVA test.

blocked the proliferative burst caused by Romidepsin and reduced proliferation to that seen upon treatment with HATi-II alone (**Figure 5.8B**). This repression of proliferation by HATi-II was also observed when RHuT78 cells were treated first for 24hrs with 6nM Romidepsin (allowing the proliferative burst to initiate) and then the HATi was added alongside Romidepsin for the following 24hrs (**Figure 5.8C**).

5.2.7 Proliferation effects in other models of drug resistance

Having shown that Romidepsin induces proliferation in RHuT78 cells, it was next investigated whether this phenomenon was also true for other models of drug resistance. We investigated the breast cancer cell line MCF-7 and its resistant cell line TamR (resistant to 100nM Tamoxifen), as well as the acute myeloid leukaemia cell line THP-1 and its associated resistant cell line CTHP-1 (resistant to 10μM Cytarabine). Other cells lines models of drug resistance were also used but the cell viability for these was not optimal (data not shown). Again, we passaged the cells and cultured them untreated for 24hrs before treating each cell line with and without their respective drug for a further 24hrs. Incubation for 4hrs with BrdU was used to measure proliferation.

Figure 5.9 shows the result of this BrdU assay with values normalised to that of the untreated parental cell line. These experiments show that treatment with the drug reduces proliferation of the non-resistant parental cell lines. Proliferation of the untreated TamR resistant cell line was similar to the untreated parental MCF-7 cell line. Upon treatment with Tamoxifen, the resistant cell line slightly increased proliferation by 24hrs, although this was not statistically significant. Regarding CTHP-1 cells, proliferation was reduced in untreated cells and this was increased upon addition of Cytarabine, although the induced level of proliferation did not exceed that observed in the untreated resistant cell line.

These results indicate that, unlike HDACi treatment of RHuT78 cells, proliferation in other models of resistant cell lines is not significantly enhanced above that of the parental cells in the presence of their respective drug.

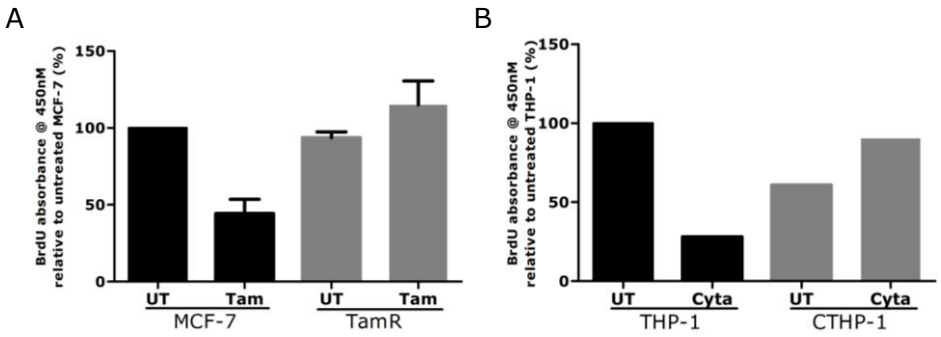

Figure 5.9- Effects of proliferation in Tamoxifen and Cytarabine resistant cell lines.

A) Cells were passaged, plated at 25% confluency, and left untreated for 24hrs. Cells were then treated with (Tam) and without (UT) 100nM Tamoxifen for 24hrs. BrdU was added for the next 4hrs and proliferation was measured using a BrdU ELISA (error bars are from assay performed once in triplicate).

B) Cells were passaged, plated at $4x10^5$/mL, and left untreated for 24hrs. Cells were then treated with (Cyta) and without (UT) 10μM Cytarabine for 24hrs. BrdU was added for the next 4hrs and proliferation was measured using a BrdU ELISA (n=1).

Also, unlike HDACi, some drugs make the resistant cells reliant upon the presence of the compound to maintain normal (similar to parental cell line) proliferative rates (and possibly viability). Therefore addition of the drug increases proliferation but these levels do not exceed that of the untreated parental cell line.

5.2.8 Effects of low doses of Romidepsin on proliferation of HuT78 cells

It remained possible, because of increased action of efflux mechanisms on Romidepsin (e.g. MDR1), that a reduced HDACi concentration inside the RHuT78 cells was facilitating proliferative responses. This hypothesis was supported by the observation that increasing the concentration of Romidepsin past the optimal 6nM quickly altered the proliferative advantage gained by HDAC inhibition in these cells. We therefore tried to reproduce this phenomenon in parental HuT78 by culturing these cells with low concentration of Romidepsin, ranging from 0.1-0.5nM. This was compared with proliferation seen in RHuT78 cells treated under the same range of conditions using a BrdU assay as before.

As can be seen from **Figure 5.10**, parental HuT78 cells showed ~15% increase of BrdU incorporation at low concentrations of 0.25nM-0.3nM Romidepsin ($p=0.001$). At these same

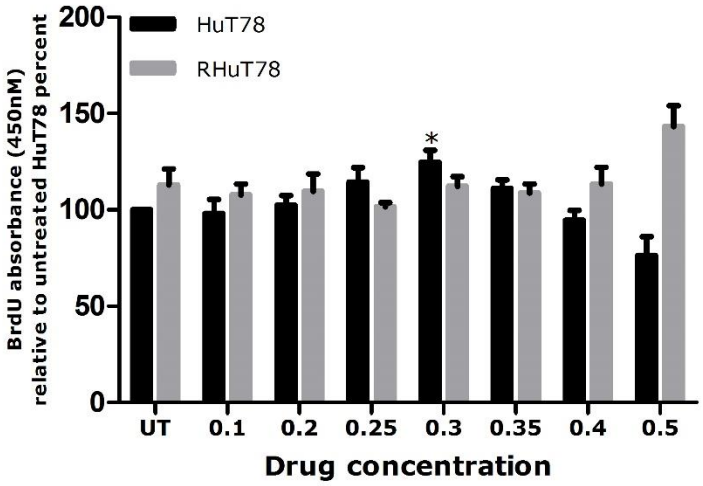

Figure 5.10 – Proliferation of parental HuT78 cells at low concentrations of Romidepsin.

HuT78 and RHuT78 cells were cultured the same as in Figure 5.1, but a low range of 0.1-0.5nM Romidepsin was used. n=5; *, p=0.001 by using non parametric student T test.

concentrations of Romidepsin, enhanced proliferation was not seen in the RHuT78 cells. These results show that low levels of Romidepsin does not induce cell cycle arrest but can enhance proliferation in parental HuT78 cells.

5.3 Discussion

In this chapter we have investigated the effects of HDAC inhibitors on proliferation in parental and resistant cell lines. The initial observations that triggered this study are described in **Chapter 3**, with absolute cell numbers increasing in cultures of RHuT78 cells much faster than their parental cell line or drug holiday counterparts. We therefore started by investigating whether the increased proliferative rate was inherent in Romidepsin resistant cells or whether it was Romidepsin induced. Therefore we treated parental, resistant and drug holiday HuT78 and MEC1 cells with and without Romidepsin and showed that the increased proliferation was reliant upon the presence of the drug in the culture. This phenomenon was dose dependent and proliferation rates peaked at the concentration of Romidepsin at which the resistant cell line had been developed (6nM for HuT78 and 9nM for RMEC1). Interestingly, proliferation quickly dropped to that seen in treated parental cells when the concentration of Romidepsin exceeded these optimal quantities of the drug.

Having established that Romidepsin increased proliferation in the resistant cell lines, other HDACi were investigated to see if they had similar effects on the cell cycle. Treatment of HuT78 and MEC1, parental and resistant cell lines with the IC_{50}

concentration of 3 different HDACis (established in **Chapter 3**) caused very similar results to that observed upon Romidepsin treatment. Proliferation decreased in parental cell lines (and was associated with an increase in p21 expression) while increasing in resistant cultures. NaB did decrease the proliferation in resistant cells at its respective IC_{50} concentration, but decreasing this concentration by only ~25% caused a proliferative burst in resistant cells while still strongly inhibiting cell cycle progression in parental cultures. These results indicate that quantitative or qualitative acetylation changes (causing alteration in gene activation and/or expression changes) caused by increasing HDACi concentrations drives these resistant cells from a state of proliferation into one of apoptosis.

The above hypotheses could also be supported by the treatment with HATi-II, which caused decreased proliferation of RHuT78 cells even in the presence of Romidepsin. However, these results could be interpreted in one of two different ways: either that the unhindered activity of HATs (caused during the repression of HDACs) is driving the proliferation and that by repressing HAT activity at the same time as HDAC activity, the RHuT78 cells no longer gain a proliferative advantage; or HATi-II is causing the RHuT78 cells to undergo cell cycle arrest

through an alternative mechanism which overrides the proliferative advantage gained by HDAC inhibition. Either way, combinational treatment with HDACi and HATi, though counterintuitive, may have therapeutic potential.

Cell cycle analysis using PI suggested that more cells in the Romidepsin treated resistant cells were present in the G2/M phase of the cell cycle. As the cells proliferate faster than the normal counterparts, this could suggest that the checkpoint for progression through the G1/S phase of the cell cycle is overcome faster in the resistant cells. This hypothesis is also supported by the observation that resistant cells have lower overall levels of Cyclin A in the culture, suggesting fewer cells are at the G1/S checkpoint at any particular point in time.

Upon treatment of HuT78 cells with low doses of Romidepsin, we were able to show a low but reproducible increase in proliferation at a very narrow range of drug concentration. This result shows that slowly increasing the quantity of Romidepsin that is inside the cell alters the cellular response from having no effect at very low concentration (<0.2nM), to proliferation (0.25-0.35nM) and ultimately to cell cycle arrest and apoptosis (>0.35nM). These results strongly suggest that the enhanced proliferation in RHuT78 cells is caused by low levels of

Romidepsin in the resistant cells facilitated by efflux mechanisms (such as MDR1). This subject is discussed in more detail in **Chapter 7**: Discussion and future work.

Regarding proliferation in other models of drug resistance, it still remains possible that resistant cell lines enhance proliferation in response to the relevant drugs. This is because the failure to see proliferation greater than that seen in the parental cell line may be a consequence of initially culturing the resistant cells for 24hrs without the presence of the drug. Thus, unlike RHuT78 cells which in the absence of HDACi maintain proliferation similar to the parental cell line, the other resistant cell lines showed reduced proliferation and viability upon absence of their drug. Therefore, the protocol to measure the comparative proliferation between parental and resistant cell lines should be done on resistant cells that have not initially been exposed to conditions without the drug that induce a reduction in proliferation.

Chapter 6

Studies investigating epigenetic mechanisms of resistance to Romidepsin.

6.1 Introduction

HDACi have great potential for therapeutic use in the clinic, but development of resistance to this class of drugs remains a problem. Alterations in protein expression and signalling pathway activation after HDACi treatment highlight potential avenues for synergistic drug treatment that could enhance efficacy of HDACis and also greatly decrease the risk of development of resistance.

In **Chapter 4** it was shown that epigenetic genes change expression upon treatment with Romidepsin, and many of these alterations differ between resistant and parental cells. To extrapolate these results we performed this experiment again but this time using alternative HDAC and HAT inhibitors. From the previous chapter (**Chapter 5**), it was shown that RHuT78 cells remain resistant to alternative HDACis, while HATis induce apoptosis of these cells.

Out of the genes that showed disparity in expression between RHuT78 and HuT78 cells after treatment with Romidepsin, the deacetylase proteins HDAC8 and HDAC9 seemed of particular interest. They showed higher mRNA expression after treatment with Romidepsin in resistant compared to non-resistant cells. It was hypothesised that HDAC8 and HDAC9 overexpression may contribute towards the resistant phenotype as they are only weakly inhibited by Romidepsin (relative to HDAC1 and HDAC2)[235-238]. Also, HDAC8 and HDAC9 overexpression are both implicated in enhancing proliferation and cell survival[239,240]. Furthermore, HDAC9 has been linked to increased survival after treatment with HDACis in other cell lines[241]. The expression of these proteins was therefore manipulated in HuT78 and RHuT78 cells to establish if they were likely to be contributing towards resistance and/or enhanced proliferation in resistant cells.

Other genes that were consistently up regulated in our Romidepsin-resistant cell line models were the DNA methyltransferases, particularly DNMT3A and DNMT3B. These enzymes control *de novo* methylation of DNA and suggest that altered DNA methylation may provide insensitivity to Romidepsin. Small molecule inhibitors are available for this family of enzymes and were used in this chapter to explore

synergistic effects of DNMTi with Romidepsin and their effects on RHuT78 cells.

6.2 Results

6.2.1 Gene expression changes upon treatment with HATis or alternative HDACis in parental, resistant and drug holiday cell lines

During the studies described in **Chapter 5** it was established that the RHuT78 cell line responds similarly to alternative HDACis as it does to Romidepsin (i.e. maintains resistance and increases proliferation). In contrast, HATis induced apoptosis and cell cycle arrest in these Romidepsin-resistant cells similar to that seen in the parental cell line HuT78.

We therefore postulated that changes in epigenetic gene expression upon treatment with Romidepsin would be similar to that elicited by alternative HDACis and may give clues to which epigenetic genes contribute towards general resistance and proliferation on exposure to HDACis. Also, comparing these responses with that induced by HATis (to which the cells were not resistant) would provide further insights into gene expression changes that are specifically altered in RHuT78 cells in response to HDAC inhibition.

Therefore, we treated RHuT78 and RMEC1 cells with either one of three HDACis or one of two HATis (IC_{50} drug concentrations were used for each cell line) and compared altered epigenetic

gene expression profiles to their respective parental and drug holiday counterparts. **Figure 6.1** shows the differences in mRNA expression of 41 epigenetic genes in cell lines after treatment; the data is represented as a heat map for each drug and cell line comparison (**Figure 6.1** - RHuT78 vs HuT78, RHuT78 vs DHRHuT78, RMEC1 vs MEC1, RMEC1 vs DHRMEC1).

ATF2 and KDM5A increased in RHuT78 cells as seen previously (**Figure 4.7** and **Figure 4.9**). However, increased expression of these 2 genes were observed in response to all 5 stimuli (both HDACi and HATi) suggesting that enhanced induction was not specific to either HDAC inhibition or whether the cells are resistant to the drug. In contrast, HDAC8, HDAC9 and NEK6 increased in RHuT78 upon treatment with all 3 HDACis, but decreased or reduced upon treatment with HATis (**Figure 6.1** and **Figure 6.2**). These genes also seemed promising candidates as they had already been shown to induce cell survival and proliferation in other cell types[242-245].

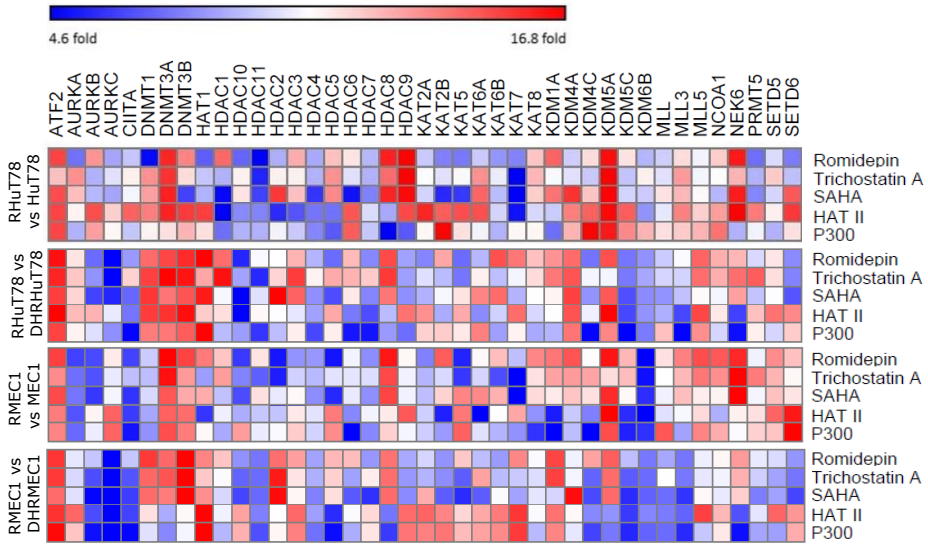

Figure 6.1 – Comparison of epigenetic gene expression changes between HuT78 and MEC1 parental, resistant and drug-holiday counterparts after treatment with a range of HDAC and HAT inhibitors.

Heat map showing changes in epigenetic gene mRNA expression between cell lines as measured by qRT-PCR. Changes of gene expression upon treatment with the indicated stimuli (IC_{50} concentration; right-hand side) were made relative to the untreated control for each cell line and then fold differences for each gene (top) between the indicated cell lines (left-hand side) were plotted. All gene expression values were initially normalised against the housekeeping gene RPL27.

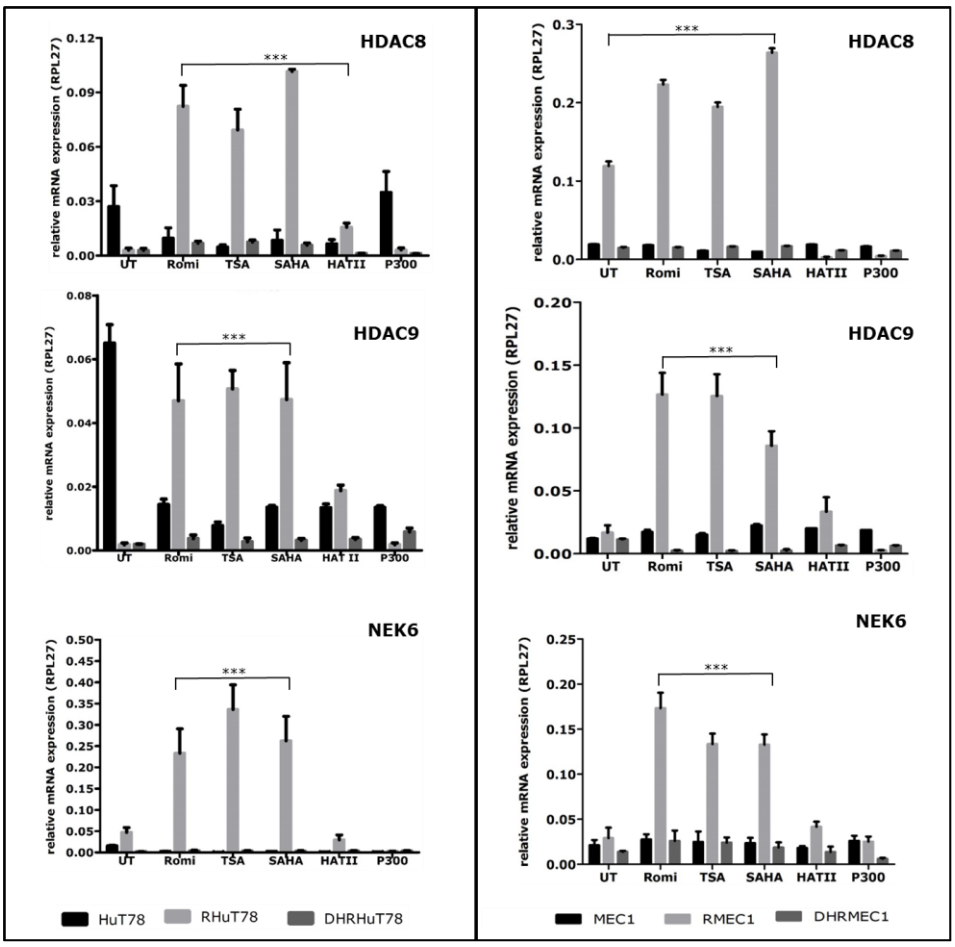

Figure 6.2 – mRNA levels of HDAC8, HDAC9 and NEK6 in parental, resistant and drug holiday HuT78 and MEC1 cells upon treatment with HDAC and HAT inhibitors.

Cells (HuT78 derived on left and MEC1 derived on right) were passaged, left for 24hrs untreated and then left untreated (UT) or treated with the IC_{50} value (see **Chapter 3**) of each indicated drug for 24hrs. Cells were then harvested and analysed using qRT-PCR for mRNA expression of each gene. Error bars are standard error of the mean between n=3 PCR experiments. Δ fold changes were statistically tested using two-way ANOVA. ***, P<0.001.

6.2.2 Effects of HDAC8 and HDAC9 knockdown

To establish whether HDAC8 and/or HDAC9 were required for resistance and/or proliferation in response to Romidepsin, we performed knockdown experiments using short hairpin RNA (shRNA) in RHuT78 and RMEC1 cells. 5 shRNAs targeting each gene were transduced separately using a lentivirus based stable transduction method (followed by selection using puromycin). Targeted knockdown was compared to a non-targeted control shRNA (scr-shRNA).

Compared to the scr-shRNA or the HDAC9-targeting shRNA, knockdown of HDAC8 caused cell viability and proliferation to drop considerably in both RHuT78 and RMEC1 cells. Upon continued culturing, these cells failed to regain viability and cultures could not be maintained (data not shown). In contrast, HDAC9 was efficiently knockdown to undetectable levels in both cell lines by two shRNA's (**Figure 6.3**). Despite these efficient knockdowns, cells continued to remain viable and proliferate in the presence of Romidepsin (data not shown). We therefore concluded that HDAC9 was unlikely to be the cause of Romidepsin resistance or proliferation in resistant cell lines and

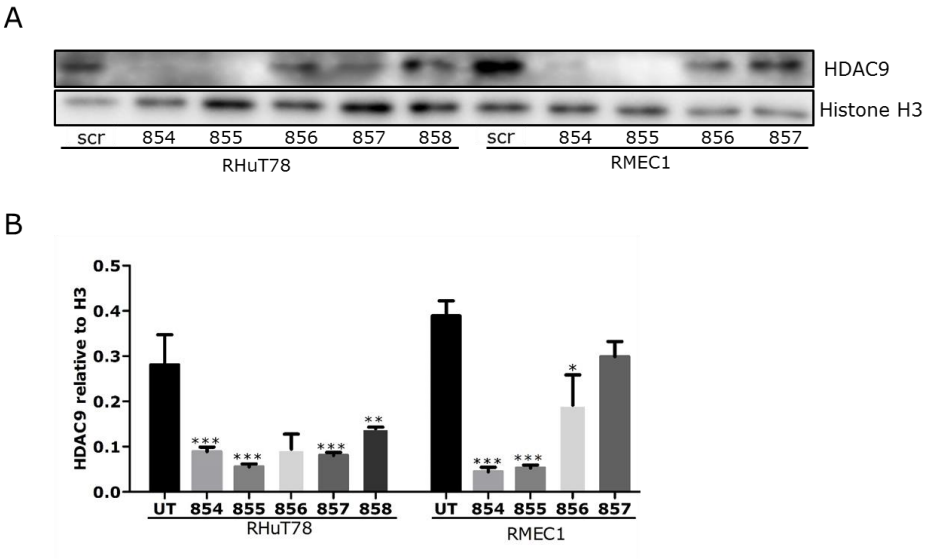

Figure 6.3 – HDAC9 knockdown in RHuT78 and RMEC1 cells.

RHuT78 or RMEC1 cells were transduced using lentivirus with either shRNA targeting HDAC9 or with a scrambled none targeting control shRNA (scr). After transduction cells were selected using puromycin for 14 days and then analysed by Western blot for HDAC9 protein expression. **A)** Western blot probed with anti-HDAC9 antibody. Anti-histone H3 was used as a loading control. **B)** Densitometry analysis of the Western blot in part A). Error bars indicate standard error of the mean of n=3 independent experiments. Values were statistically tested using two-way ANOVA. ***, P<0.001; **, P<0.01; *, P<0.05.

was not to be studied further. As resistant cells could not maintain viability without HDAC8, it remained possible that this deacetylase could be contributing towards tolerance to HDACis.

6.2.3 Effects of HATi on Romidepsin-induced HDAC8 and NEK6 expression.

In **Chapter 5** it was shown that treatment with HATi reduced proliferation even in the presence of Romidepsin (**Figure 5.8**). Therefore we wanted to establish whether or not changes in proliferation induced by HATi could also be linked with alterations in HDAC8 and NEK6 expression induced by Romidepsin. Therefore we left RHuT78 cells untreated or, treated these cells with Romidepsin, HATi or a combination of both for 24hrs and checked expression of HDAC8 and NEK6 mRNA. As can be seen from **Figure 6.4**, levels of HDAC8 and NEK6 both increased upon treatment with Romidepsin as expected. Treatment with HATi reduced expression of these genes and could also abolish HDAC8 and NEK6 gene upregulation in response to Romidepsin. These results corroborate with findings in **Chapter 5**, and show that expression of HDAC8 and NEK6 are both closely associated with proliferation of the cells in the context of acetylation. Also, the

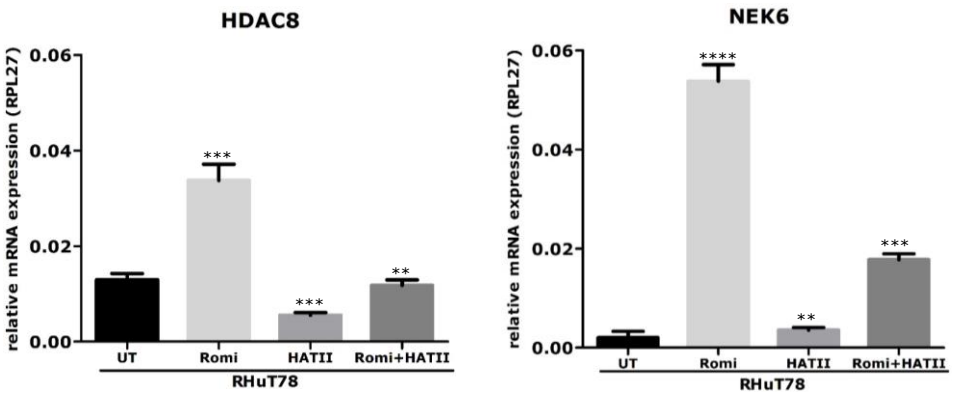

Figure 6.4 – Effect of HATi on Romidepsin-induced expression of HDAC8 and NEK6.

RHuT78 cells were treated and analysed as in **Figure 6.2** but this time with the additional co-treatment using the IC_{50} concentrations of Romidepsin and HATi-II (Romi+HATII). Error bars are standard error of the mean between n=3 PCR experiments. Δ fold changes were statistically tested using two-way ANOVA. ****, P<0.0001; ***, P<0.001; **, P<0.01.

---

result suggests that HAT activity is required to drive expression of HDAC8 and NEK6 in RHuT78 cells.

6.2.4 HDAC8 and NEK6 induction in cell cycle arrested parental, resistant and drug holiday HuT78 and MEC1 cells upon treatment with and without Romidepsin

It remained possible that induction of HDAC8 or NEK6 was caused by increased cell cycle progression rather than the other

way around. Therefore, we caused cell cycle arrest in parental, resistant and drug holiday HuT78 and MEC1 cells by reducing serum levels. Cell cycle arrest was observed by cell density not changing over a 48hrs time period (data not shown). We then treated these cells with and without various HDACis or HATis and observed changes in mRNA for HDAC8 and NEK6 after 24hrs. As can be seen in **Figure 6.5**, expression of HDAC8 was still induced in cell cycle arrested RHuT78 and RMEC1 cells in response to all HDACis, but did not do so in response to HATis. Parental or DHRHuT78 of both HuT78 and MEC1 had HDAC8 expression that remained low in response to all stimuli. Regarding NEK6, expression changed similar to HDAC8 in RHuT78 cells, but different responses were seen in RMEC1 cells. In this B cell line, expression was relatively high without treatment compared to parental and drug holiday cells, and did not increase further upon addition of HDACi. Inhibition of HATs either caused NEK6 expression in RMEC1 cells to stay the same or decrease. It was concluded that HDAC8, but not NEK6, showed expression changes in both cell types that matched proliferation and resistant phenotypes and could be induced independently of cell cycle progression.

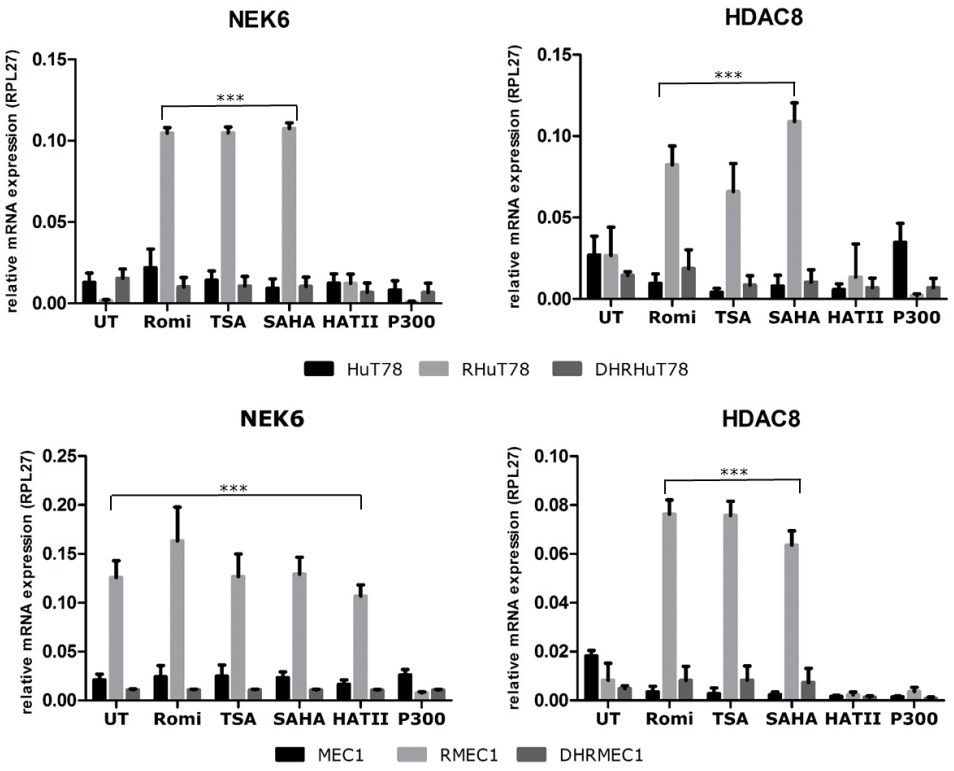

Figure 6.5 – Expression of HDAC8 and NEK6 in cell-cycle arrested cells with and without treatment with HDACi's and HATi's.

Cells were cell cycle arrested using serum starvation (5% FBS used) and this was confirmed using cell counting. After arresting the cells, cells were treated with the IC_{50} of the indicated drug and analysed for RNA expression as in **Figure 6.2.** Error bars are standard error of the mean between n=3 PCR experiments. Δ fold changes were statistically tested using two-way ANOVA. ***, P<0.001.

6.2.5 HDAC8 protein is expressed at higher levels in RHuT78 cells upon treatment with Romidepsin

To confirm that an increase in HDAC8 mRNA levels upon treatment with Romidepsin led to an increase in HDAC8 protein we treated RHuT78 cells with and without 6nM Romidepsin for 48hrs and compared them to HuT78 cells treated in the same way. As can be seen from **Figure 6.6**, levels of HDAC8 protein were similar in UT HuT78 and RHuT78 cells. However, after treatment with Romidepsin for 48hrs, HDAC8 protein expression increased by 33% in RHuT78 cells while it decreased in HuT78 cells by 22%. It was concluded that Romidepsin does drive an increase in HDAC8 protein expression specifically in the resistant cell line and hypothesised that this could potentially be contributing to resistance and enhanced proliferation.

6.2.6 Overexpression of HDAC8 in HuT78 cells

As HDAC8 looked a likely candidate for potentially driving resistance and/or proliferation, further studies investigating HDAC8 were warranted. Therefore, overexpression of HDAC8 in HuT78 cells was performed and cells were measured for their proliferation and resistance to Romidepsin.

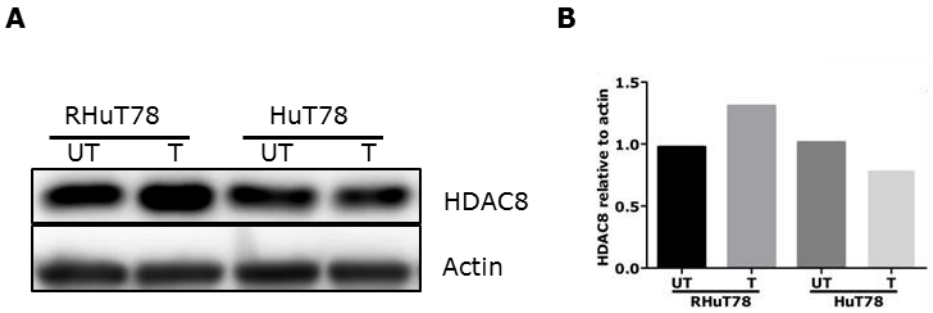

Figure 6.6 – Levels of HDAC8 protein in lysates of RHuT78 and HuT78 cells treated with and without Romidepsin.

A) 10ug of protein from each cell lysate were separated by SDS-PAGE and levels of HDAC8 were measured by Western blotting and probed with an anti-HDAC8 antibody. Equal loading was measured using an anti-Actin antibody. UT, untreated; T, treated with 6nM Romidepsin. **B)** Bar chart illustrating the densitometry analysis of part A. (n=1).

HDAC8-Flag protein was overexpressed in HuT78 cells by transfecting these cells with a pcDNA3.1-HDAC8-Flag (pcHDAC8) plasmid. The pmaxGFP plasmid was also co-transfected with pcHDAC8 and used as a surrogate marker of transfection efficiency after electroporation. Transfection of an empty pcDNA3.1 plasmid instead of pcHDAC8 was used as a negative control.

Figure 6.7A shows flow cytometry analysis of GFP expression induced by the pmaxGFP plasmid in combination with either pcDNA3.1 or pcHDAC8. Approximately 63% of cells expressed the GFP protein after 24hrs. In concordance with this, **Figure 6.7B** illustrates that 48hrs after transfection with pcHDAC8 (but not pcDNA3.1), increased expression of HDAC8 is detectable by Western blot, and this is also associated with appearance of the flag epitope in these lysates at the correct molecular weight for HDAC8-Flag. These results show that overexpression of HDAC8-Flag protein is causing a 32% increase in total expression of HDAC8 similar to levels seen in RHuT78 cells treated with Romidepsin (33% increase, **Figure 6.6**).

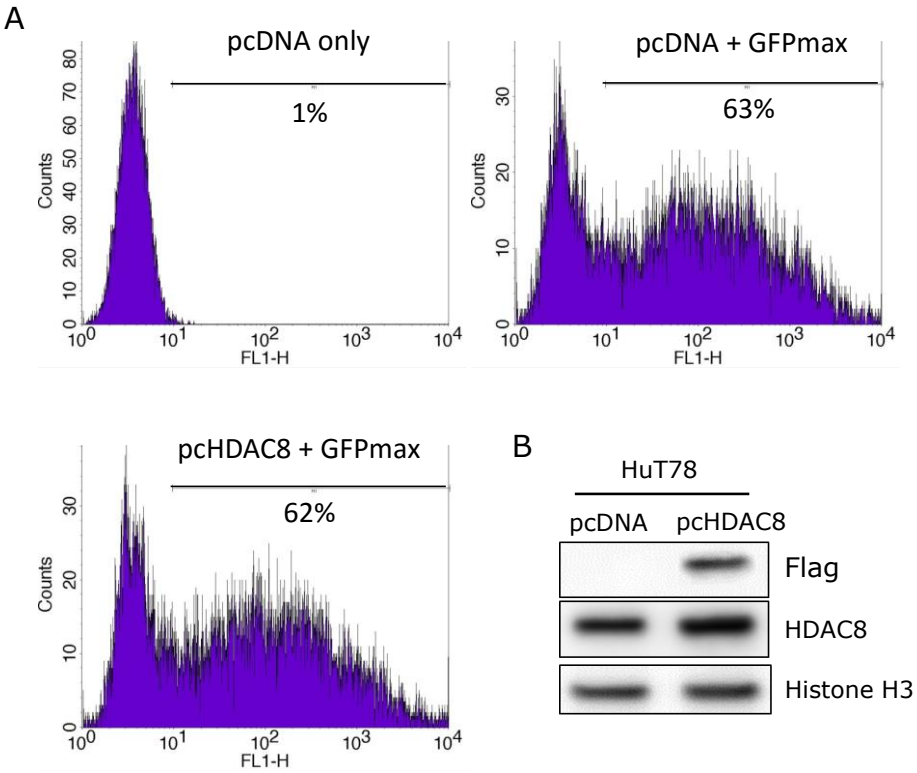

Figure 6.7 – Overexpression of HDAC8 in HuT78 cells.

Cells were transfected using electroporation with pcDNA3.1 plasmid (pcDNA) only or, either with pcDNA + GFPmax plasmid or pcDNA3.1-HDAC8-Flag (pcHDAC8) plasmid + GFPmax plasmid. **A)** Flow cytometry analysis of GFP expression in each sample 24hrs after electroporation **B)** Western blot of cell lysates 48hrs after transfection probed with either anti-Flag or anti-HDAC8. Total histone H3 was used as a loading control and relative HDAC8 densitometry values are shown underneath. (n=1).

6.2.7 Effects of HDAC8 overexpression on proliferation and Romidepsin resistance

Having established that HDAC8 was being over-expressed in at least a proportion of HuT78 cells due to the forced expression of HDAC8-Flag protein, cell cultures were analysed for their proliferative potential and resistance to apoptosis by Romidepsin. Cells analysed in **Figure 6.7A** were further cultured either with BrdU for 4hrs and used for a proliferation assay, or with 0, 3, 6 or 9nM Romidepsin for 48hrs and analysed for apoptosis by analysing PI and DioC6 staining using flow cytometry. **Figure 6.8A and B** show the results for these proliferation and apoptosis experiments respectively. Proliferation rate of the pcHDAC8 increased compared to the empty pcDNA3.1 control vector. Furthermore, addition of a specific HDAC8 inhibitor (PCI-34051) could abolish the increased proliferation in pcHDAC8 cells. This result shows that increased HDAC8 expression can drive proliferation in HuT78 cells. This is also strong evidence that high expression of HDAC8 protein in Romidepsin treated RHuT78 cells is the major cause of increased proliferation in these cells.

A

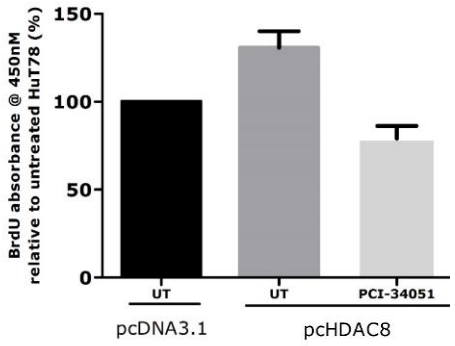

B

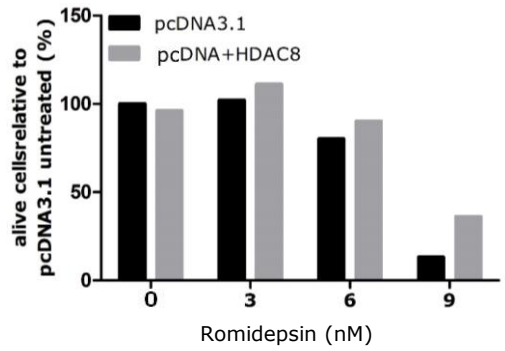

Figure 6.8 – The effects of overexpressed HDAC8 on proliferation and resistance to Romidepsin in HuT78 cells.

A) Cells from **Figure 6.6A** were cultured for a further 24hrs either untreated (UT) or with HDAC8 inhibitor PCI-34051 as shown. Cells were then analysed for proliferation by exposure to BrdU for 4hrs followed by an ELISA. Absorbance was made relative to the untreated pcDNA3.1 only cell line (error bars are from assay performed once in triplicate). **B)** Same as in A) but this time cells were treated with the indicated concentration of Romidepsin for 48hrs and then analysed using flow cytometry for apoptosis by staining with PI+DioC6 (n=1).

Regarding apoptosis, the number of live cells was higher in the pcHDAC8 transfected cells after treatment with Romidepsin than that present in pcDNA3.1 control cells. This was particularly noticeable at the higher concentration of 9nM Romidepsin. These results suggest that increases in HDAC8 expression can both drive proliferation of HuT78 cells and provide resistance to apoptosis induced by Romidepsin.

6.2.8 Effects of DNMT inhibition on Romidepsin induced apoptosis of HuT78 cells

During treatment with multiple HDACis it was noticed that resistant cells consistently upregulated expression of one or both DNMT3A or 3B genes, and this was more so than parental and drug holiday counterparts. Furthermore, it is known that DNA methylation inhibitors can synergise with HDAC inhibitors and increase HDACi-induced apoptosis. We therefore examined whether treatment with DNMTi could synergise with Romidepsin and whether this was sufficient to overcome resistance to HDACis in RHuT78 cells.

Parental HuT78 cells were treated with a range of Romidepsin concentrations (0-9nM) either alone or in combination with a concentration range of the DNMTis, 5-Azacytidine (0-13μM) or Decitabine (0-13μM). Also, three parallel experiments were

performed that differed in terms of when each drug was added to the culture (illustrated in **Figure 6.9A**) to address the importance of drug scheduling. Apoptosis was then analysed by PI and DioC6 staining and measured by flow cytometry (**Figure 6.9B**). These results were analysed using Compusyn software and Chou-Talalay analysis to see if Romidepsin is synergistic with DNMTis. The software was able to calculate the concentrations that showed the greatest level of synergy (**Table 10**), and these values would be used in future experiments.

6.2.9 Time course study showing cell-cycle arrest and apoptosis induced by Romidepsin and DNMTis in RHuT78 cells

Having established the concentrations of DNMTis and Romidepsin that showed the most synergistic effect in HuT78 cells, RHuT78 cells were next treated with these concentrations and cell-cycle arrest plus apoptosis was measured over a 6 days period (**Figure 6.10**).

Level of cell-cycle arrest and apoptosis induced with either DNMTi alone was low (<25%) during the 6 days of culture. Combination of DNMTis with Romidepsin caused levels of cell-cycle arrest and apoptosis to greatly increase in RHuT78 with

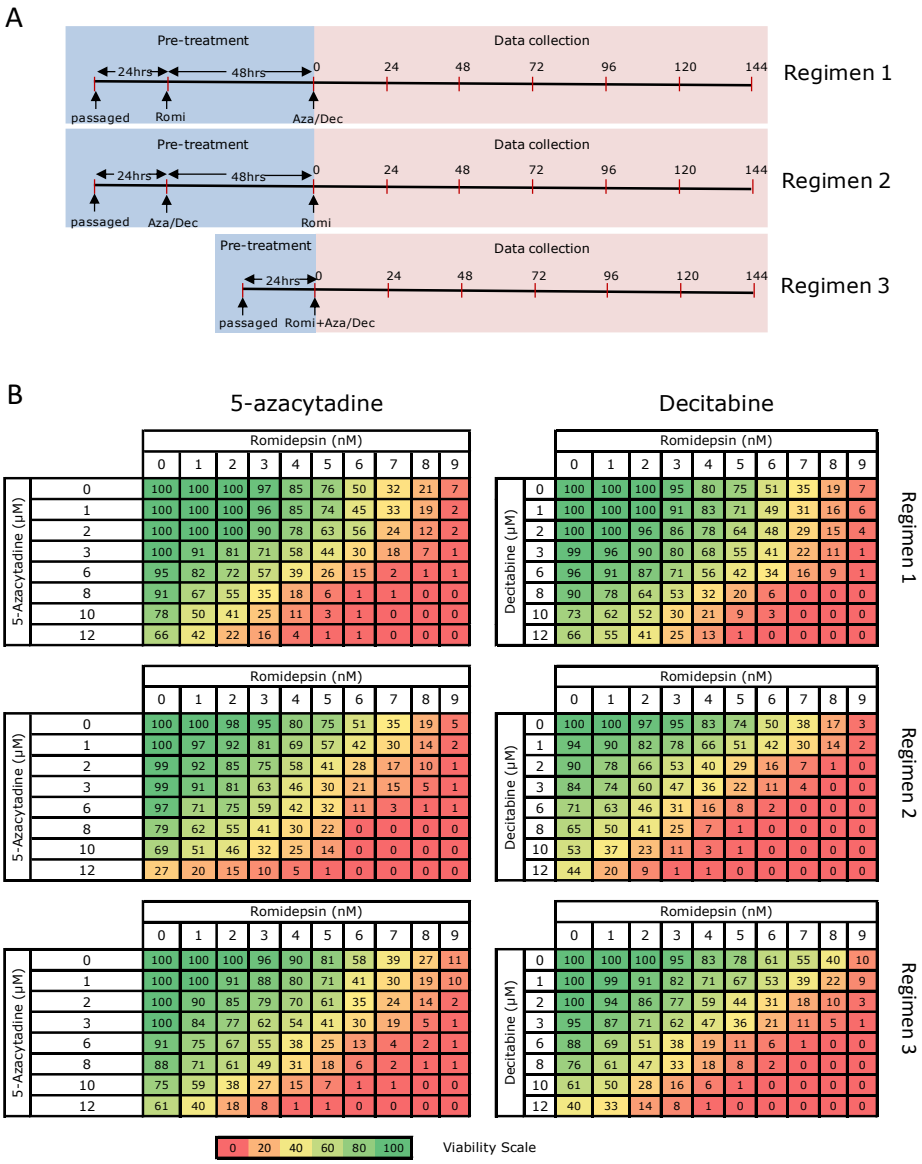

Figure 6.9 – Apoptosis induced in HuT78 cells by Romidepsin in combination with the DNMTi's 5-Azacytidine and Decitabine.

Legend for Figure 6.9

A) Diagram illustrating the three regimens of Romidepsin (Romi) and DNMTi (Aza, 5-Azacytadine; deci, Decitabine) treatments and subsequent data collection.

B) Heatmaps illustrating the percentage alive HuT78 cells after treatment for 48hrs with increasing concentrations of Romidepsin or DNMTi either alone or in combination with each other. Apoptosis was measured by flow cytometry after staining with PI+DioC6. Values are made relative to the untreated sample (i.e. 0nM Romipdesin and 0μM DNMTi).

---

synergistic induction of apoptosis being apparent as early as 24hrs.

Decitabine was more potent at inducing cell cycle arrest and apoptosis than 5-Azacytadine. Furthermore, pre-treatment with the DNMTi for 48hrs prior to exposure to Romidepsin caused apoptosis to occur quicker than if the drug regimen was reversed or each drug was added at the same time. These results show that Romidepsin drug resistance and proliferation can be overcome in RHuT78 cells using DNMTi, and that pre-treating cells with DNMTi before addition of Romidepsin had the greatest synergistic effect.

Table 10 – Chou-Talalay analysis to show concentration of Romidepsin and DNMTi that gave the greatest level of synergy.

Cell line	Drug		Schedule	Combination Index
	Romidepsin (nM)	5-Azacytidine (μM)		
RHuT78	3	12	Same time	0.96
	3	11	Romi. then Aza.	0.95
	3	9	Aza. then Romi.	0.85

Cell line	Drug		Schedule	Combination Index
	Romidepsin (nM)	Decitabine (μM)		
RHuT78	3	10	Same time	1.0
	3	4	Romi. then Dec.	0.68
	3	2	Dec. then Romi.	0.55

Romi., Romidepsin; Aza., 5-Azacytadine; Dec., Decitabine. Combination Index <1 indicates these concentrations are synergistic.

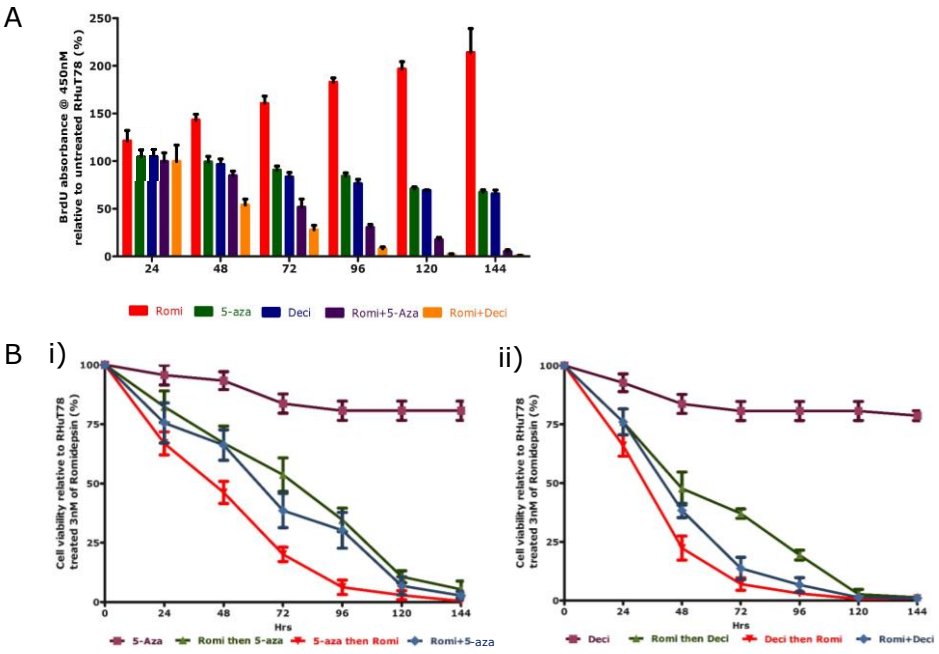

Figure 6.10 – Time course showing proliferation and apoptosis induced in RHuT78 cells after combination of Romidepsin with DNMTi's.

A) Proliferation in RHuT78 cells by BrdU ELISA assay. Romidepsin and each DNMTi were added at the same time. Results are made relative to untreated RHuT78 at each timepoint (error bars are from assay performed once in triplicate). **B)** Apoptosis induced in RHuT78 cells after treatment with each DNMTi **i)** 5-Azacytadine (5-aza) or **ii)** Decitabine (Deci), either alone or in combination with Romidepsin. Apoptosis induced by DNMTi alone or after regimen 1 (green), regimen 2 (red) or regimen 3 (blue) are all made relative to apoptosis induced by Romidepsin alone (error bars are from assay performed once in triplicate).

6.2.10 Gene expression changes in RHuT78 cells after treatment with DNMTi's and Romidepsin

Having established that treatment with DNMTis re-sensitises RHuT78 cells to Romidepsin, changes in epigenetic gene expression were investigated. Cells were again treated with the three different regimen and mRNA expression of HDAC8, DNMT3A, DNMT3B and KDM5A was quantified by qRT-PCR after 24hrs.

As can be seen in **Figure 6.11**, treatment with Romidepsin induced expression of these genes as expected. However, treatment with 5-Azacytadine or Decitabine abolished induction of these epigenetic genes by Romidepsin. Decitabine produced the greatest effect on gene expression and decreased responses to Romidepsin were more pronounced when cells were first pre-treated with DNMTi and then treated with Romidepsin.

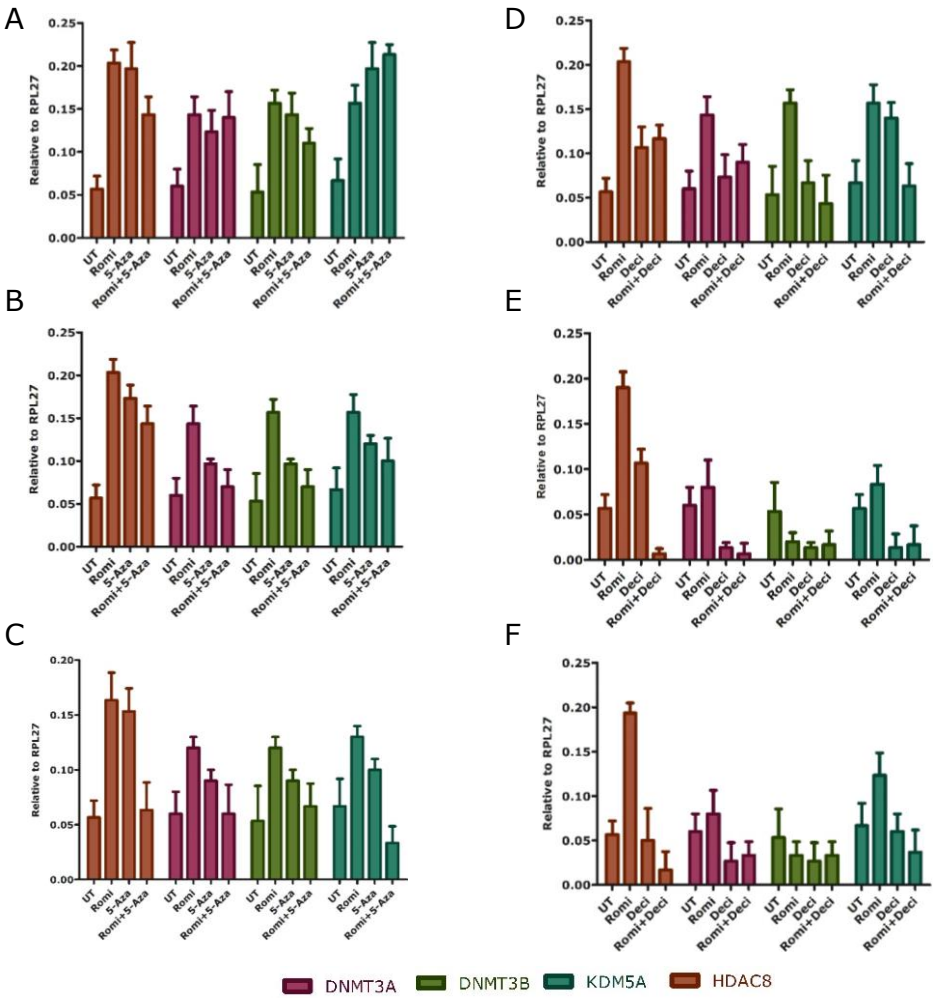

Figure 6.11 – Gene expression changes upon treatment with DNMTi and Romidepsin.

RHuT78 cells were treated with regimen 1 (Romidepsin first then DNMTi; **A** and **D**), regimen 2 (DNMTi then Romidepsin; **B** and **E**) or regimen 3 (same time; **C** and **F**), harvested 24hrs later and mRNA quantified by qRT-PCR for the DNMT3A, DNMT3B, KDM5A and HDAC8 (error bars are from assay performed once in triplicate).

6.3 Discussion

The aim of this chapter was to identify potential epigenetic drivers of Romidepsin resistance and Romidepsin-induced proliferation. Synergistic drug combinations and schedules that could overcome resistance mechanisms were also investigated.

In order to identify potential epigenetic genes that could be regulating resistance and/or proliferation in response to Romidepsin, RHuT78 cells were initially screened for mRNA changes after treatment with a range of HDACis and HATis. RHuT78 and RMEC1 cells were shown in **Chapter 5** to be apoptotic resistant and induced proliferation in response to other HDACis, but not to HATis. It was therefore hypothesised that genes which changed in mRNA expression upon treatment with HDACis, but remained the same or had opposite responses to HATis were potential genes of interest. This strategy led to the identification of HDAC8, HDAC9 and NEK6. All three of these genes were upregulated more in resistant cells than both their parental and drug holiday counterpart cells upon treatment with Romidepsin. Also, these genes are involved in, or are associated with, cell cycle regulation and could potentially be driving apoptotic resistance or proliferation in response to HDACis.

Knockdown studies showed that RHuT78 cells could maintain enhanced proliferation and resistance to Romidepsin even in the absence of HDAC9, concluding that up-regulation of this gene was probably not the responsible for these phenomenon. Also, NEK6 lost expression differences in cell cycle arrested RMEC1 cultures before and after stimulation with Romidepsin suggesting that up-regulation of NEK6 may be a consequence of enhanced proliferation and not vice versa. In contrast to these genes, HDAC8 mRNA was consistently up-regulated in both resistant cell lines even when cells were arrested in the cell cycle. An increase in HDAC8 mRNA coincided with an increase in HDAC8 protein in RHuT78 cells and knockdown of this protein caused death and/or cell cycle arrest. Furthermore, overexpression studies in HuT78 parental cells showed that enhanced HDAC8 protein expression (similar to elevated levels seen in RHuT78 cells after treatment with Romidepsin) was associated with increased proliferation and enhanced resistance to Romidepsin. Furthermore, enhanced proliferation in response to overexpression of HDAC8 could be abolished in the presence of the HDAC8 inhibitor PCI-34051. Although additional experiments need to be performed to prove the involvement of HDAC8 in proliferation and resistance in RHuT78 cells, current results strongly implicate HDAC8 in the process.

DNMTs were another set of enzymes that showed potential to overcome resistance to Romidepsin in RHuT78 cells. During the epigenetic gene expression profiling of changes upon treatment with HDACis, levels of DNMT3A and 3B mRNA consistently increased in RHuT78 more than parental and drug holiday cells. As DNMTi can synergise and enhance effects of HDACis[246-250], and because RHuT78 cells remain sensitive to Romidepsin at higher concentrations of the drug (see **Chapter 5**), it was hypothesised that combination treatment with DNMTi and Romidepsin may overcome resistance to HDACis in RHuT78 cells. Using two different DNMTis it was shown that these class of drugs can overcome resistance to Romidepsin, strongly induce apoptosis and cause cell cycle arrest in RHuT78 cells. This synergistic effect was even seen when lower concentrations of 3nM Romidepsin were used. It is unclear how DNMTis synergise with HDACis to induce apoptosis. One study shows that loss of methylation marks caused by incubation with DNMTis aids the action of Romidepsin at gene promotors and increases gene expression of pro-apoptotic and anti-proliferative genes[246,249,251]. Our study showed synergy even at early time points of 24hrs, before methylation may have had time to alter in RHuT78 cells, suggesting that alternative mechanisms may also be present. Interestingly, incubation with

DNMTi inhibited Romidepsin induced transcription of epigenetic genes that were normally overexpressed in resistant cells. This could suggest that certain pro-survival and/or pro-proliferation genes that would normally increase in expression in RHuT78 cells upon addition of Romidepsin, have their expression blocked in the presence of DNMTi. The mechanism for this is currently unclear and is discussed further in the next chapter.

Importantly, these studies also shed light on the importance of drug scheduling to fully utilise synergistic interactions in the clinical setting. We believe that current combination therapies do not pay adequate attention to the rational and sequential timing and scheduling of individual drug components.

Chapter 7

Conclusions and Future Work

7.1 Major conclusions of the thesis

This thesis aimed to address if epigenetic reprogramming occurred in established cell line models that have previously shown sensitivity to HDACis. In addition, we wish to examine if such perturbation of the epigenetic landscape was responsible in the acquisition of resistance and could be exploited for therapeutic gain. The study primarily focussed on the CTCL cell line HuT78 and its responses to Romidepsin as this HDACi is currently licensed for relapsed cases of the disease.

This thesis draws four major conclusions:

- HuT78 and MEC1 resistance cells lines can be developed from the persistently growing cells present after treatment with the 48hrs IC_{50} drug concentrations. Continual exposure of these cells to Romidepsin causes an altered morphology and a faster growth rate than their parental counterparts.
- Romidepsin can cause changes in global histone modifications, particularly H3K4me3, and this is more

pronounced in the HuT78 parental than resistant cell line.

- The transcriptional activities of a broad range of genes that influence the chromatin landscape are changed upon treatment with Romidepsin. Resistance to Romidepsin causes the drug's effects on epigenetic gene expression to be altered (but not all genes are effected), with responses of HDAC8, HDAC9, DNMT3A and 3B, and NEK6 genes being notably perturbed.
- In the right context, pan HDACi treatment can promote proliferation of cells that have acquired resistance. The proliferative advantage in response to Romidepsin can be replicated in HuT78 cells by exposure to a narrow concentration range of around 0.3nM. Faster proliferation is likely to be caused by a quicker transition through the S-phase of the cell cycle and this enhanced rate of mitosis can be inhibited using HATis.

Common changes in epigenetic gene expression can be seen in sensitivity/resistance cell lines in response to other panHDACis. HDAC8 was consistently up regulated in both resistant cell lines and showed potential as a gene that could drive HDACi-resistance and cause HDACi-induced proliferation. Combination therapy of DNMTi plus Romidepsin may provide increased

efficacy for Romidepsin-only therapies. Combining DNMTi with HDACi diminishes resistance-specific gene expression changes in response to HDACi, potentially causing the avoidance of resistance development in patients treated with Romidepsin. This study further establishes that attention to sequencing/scheduling of these synergistic drugs is critical for greater therapeutic gain; in particularly, pre-treatment of cell lines with DNMTi and HDACis showed that greater therapeutics gains could potentially be achieved by treating with the DNA methylase inhibitor first followed by HDAC inhibition.

7.2 Possible avenues for further investigation

1. All the experiments in the current study were performed in cell line models. The work requires validation in primary samples from CTCL patients that are sensitive to Romidepsin (or indeed other HDACis) or who have acquired resistance. Hence, the work will need to be extended to examine primary patient samples.
2. The changes in histone modification patterns were examined at a global level but not at specific gene resolution. It will be important to examine if the specific changes in histone modifications correlate with changes in transcriptional output of individual genes such as

DNMTs, HDAC8 and 9, NEK6 etc. This could be a potential avenue for further work

3. To see if the epigenetic changes are co-ordinated with wider changes in gene expression. Therefore, it would be important to look at DNA methylation (Infinium HumanMethylation450 BeadChip Kit) *vs* mRNA levels *vs* microRNA levels (RNA next generation sequencing using Illumina Hi-Seq). These experiments and subsequent bioinformatic analysis are currently ongoing.
4. To establish the mechanism of proliferation induced by HDACis. The current hypothesis is that low levels of Romidepsin inside the cells leads to enhanced proliferation. Therefore, RHuT78 cells that are treated with 6nM of the drug reduce Romidepsin levels inside the cell by efflux mechanisms to a concentration that induces proliferation (~0.3nM). A small number of cells in the original HuT78 culture which can up-regulate efflux mechanisms and have an intracellular concentration of ~0.3nM Romidepsin have a proliferative advantage and outgrow those of the surrounding culture and predominate during later passages. This hypothesis is illustrated in **Figure 7.1**. If this hypothesis is correct then genes that promote cell cycle progression should be

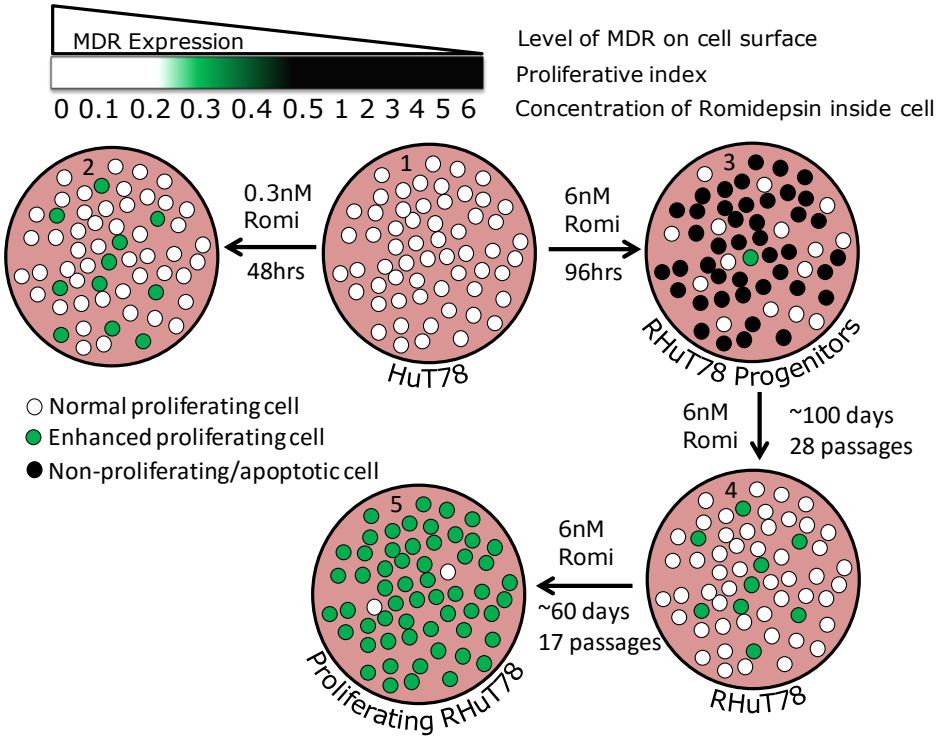

Figure 7.1 – Hypothesis explaining the Romidepsin-induced development of a faster proliferating RHuT78 cell line.

Parental HuT78 (culture dish 1) can be treated with 0.3nM of Romidepsin (Romi) and increased proliferation is detected (green circles; dish 2). Alternatively, cells are treated with 6nM of drug, causing a large number of cells to undergo cell cycle arrest and apoptosis (black circles; dish 3). A variable increase in MDR produces a low range of intracellular drug concentrations that can either have little or no effect (<0.25nM; white circles) or induce proliferation (~0.3nM; green circle). Over time, apoptotic cells are passaged out of the culture (dish 4) and faster proliferating cells become predominant (dish 5).

in higher abundance than those that cause cell cycle arrest at lower concentrations of Romidepsin. For example, HDAC8 is induced which promotes cell cycle progression at 0.3nM, but p21 is not. All of these changes may be single-cell specific and so expression analysis needs to be performed in an appropriate way (e.g. flow cytometry).

5. To establish if HDAC8 is truly responsible for the enhanced proliferation and tolerance in the presence of HDACis. This could be proven by firstly, establishing whether HDAC8 expression increases in parental HuT78 cells when treated with 0.3nM Romidepsin – at least in a proportion of the cells. Secondly, removal of Romidepsin from RHuT78 cells cause protein expression of HDAC8 to return to levels similar to that observed in parental cells. Thirdly, treatment of RHuT78 cells with the HDAC8 inhibitor, or partial knockdown of HDAC8 expression by siRNA abolishes increases in proliferation caused by Romidepsin.
6. Another interesting avenue of research would be to understand how Romidepsin resistance is overcome in RHuT78 cells by combining DNMTis with Romidepsin. Previous studies showed that DNMTis can increase

sensitivity to HDACis in cells that were not resistant[131,247,249]. This was at least partly due to DNMTi reducing DNA methylation and enhancing HDACi-induced pro-apoptotic/anti-proliferative gene expression. It would be interesting to see whether the synergistic effect of DNMTis on HDAC inhibition was affected by cell cycle arrest of the cells prior to treatment. This would inform whether incorporation of the cytidine analog into DNA was required for increased sensitivity to HDACi or if the DNMTi was acting via an alternative mechanism. If DNMTis do enhance HDACi efficacy, then possibly those cells that do not normally induce pro-apoptotic, cell cycle arresting genes are forced to do so.

Appendix

Table A1 – List of Antibodies

Antibody	Source	Host	Dilution	MW (kDa)
ChiPAb+ Acetyl-Histone H3 monoclonal (17-615)	MerckMillipore, UK	Rabbit	1:20000	17
ChiPAb+ Me3-Histone H3 (Lys4) monoclonal (17-614)	MerckMillipore, UK	Rabbit	1:10000	17
ChIPAb+ Trimethyl-Histone H3 (Lys27) polyclonal (17-622)	MerckMillipore, UK	Rabbit	1:15000	17
Cyclin A2 (4656) monoclonal	Cell signalling technology, UK	Mouse	1:10000	55
Cyclin B1 (12231) monoclonal	Cell signalling technology, UK	Rabbit	1:10000	55
Cyclin D1 (2978) monoclonal	Cell signalling technology, UK	Rabbit	1:10000	36
Cyclin D3 (2936) monoclonal	Cell signalling technology, UK	Mouse	1:10000	31
Cyclin E2 (4132) monoclonal	Cell signalling technology, UK	Rabbit	1:10000	48
HDAC8 (ab187139)	Abcam, UK	Rabbit	1:10000	42
HDAC9 (ab109446) monoclonal	Abcam, UK	Rabbit	1:5000	111
Histone H3 symmetric-dimethyl Arg2 (NB21-1002)	NOVUS biological, UK	Rabbit	1:500	15
Histone H3 asymmetric-dimethyl Arg2	ErnestoGuccione Institute of Molecular and Cell Biology, Singapore	Rabbit	1:500	15
KDM3B (5377) monoclonal	Cell signalling technology, UK	Mouse	1:5000	220
KDM4A (5328) monoclonal	Cell signalling technology, UK	Rabbit	1:5000	150
KDM5A (3876) monoclonal	Cell signalling technology, UK	Rabbit	1:5000	200
KDM5C (5361) monoclonal	Cell signalling technology, UK	Rabbit	1:5000	180
p21WAF1/Cip1 (2947) monoclonal	Cell signalling technology, UK	Rabbit	1:5000	21
PHF2 (3497) monoclonal	Cell signalling technology, UK	Rabbit	1:2000	150
Anti-GAPDH antibody - Loading Control polyclonal (ab9485)	Abcam, UK	Rabbit	1:2500	37
Anti-beta Actin antibody monoclonal (mAbcam 8226)	Abcam, UK	Rabbit	1:5000	42

Table A2 – Sources for the chemicals that were used for the buffers preparations

Chemicals	Name of supplier	Chemicals	Name of supplier
Betaine	SigmaAldrich,UK	$CaCl_2$	Fisher Thermo Sceintific, UK
β-glycerolphosphate		Glycine	
β- mercaptoethanol		KCl	
Bromophenol blue dye		KOH	
BSA		$MgCl_2$	
DTT		NaCl	
EDTA		NaOH	
Ethanol		SDS	
Ficoll-400		Sodium deoxycholate	
Glycerol		Tris acetate	
IGEPAL®CA-630		Tris borate	
Imidazole		Tris-HCl	
LiCL		Tween-20	
$NaHCO_3$		Paraformaldehyde	
Orange G			
Sodium fluoride			
Sodium orthovanadate			
Sodium pyrophosphate			
Sodium Tartarate			
Spermine			
Spermidine			
Tritron-×100			

Table A3 – Drugs and Reagents used

Manufacturer	Catalog no	Product Name
Merck Chemicals Ltd.	382110-10MG	Histone Acetyltransferase Inhibitor II
Merck Chemicals Ltd.	382113-10MG	Histone Acetyltransferase p300 Inhibitor, C646
Newmarket Scientific	08-25-00001	5x HOT FIREPol EvaGreen® qPCR Mix Plus (NO ROX)
Stratech Scientific Ltd	S1047 – 200mg	Vorinostat (SAHA)
Sigma-Aldrich Company Ltd	303410-100G	Sodium butyrate
Celgene Ltd		Romidepsin
Sigma-Aldrich Company Ltd.	D6546-6X500ML	Dulbecco's Modified Eagle's Medium - high glucose
Promega UK	M1705	M-MLV Reverse Transcriptase 50,000u
QIAGEN HOUSE	79654	QIAshredder (50)
QIAGEN HOUSE	74104	RNeasy Mini Kit (50)
Perbio Science UK Ltd	PA5-16190	PAN ACETYLATED-LYSINE POLYCLONAL
New England Biolabs	9717S	Histone H3 (3H1) Rabbit mAb #9717 100 ul (10 western blots)
vwr	732-3038	Transfer membranes, BioTrace™ PVDF 300 mm × 3 m

Table A4– Equipment used

Equipment	Manufacturer	Purpose
AccuBlock Digital Dry Bath	Labnet	Heating block
Bag Sealer	Parker	Seal the blot in a bag
Bench top centrifuge (1.5mL)	Sigma	Centrifugation of 1.5 mL Eppendorf tubes
Biomat class II cabinet	Medical air technology	Culturing cell lines
Biorupture Sonicator System	Diagenode	Sonicate the samples for western blot
Cell counter	Nexcelcom	Cell count and viability
Centrifuge Avanti® J-26 XP	Beckman CoulterTM	Centrifugation of ≥ 15 ml
Dark Box II	Fujifilm LAS1000	UV-camera for gels
Electronic balance	Fisher Scientific	Weighing chemicals
FACS Calibur	BD Bioscence	Apoptosis and Selection of stable cell lines
Fluorescence Reader	Biotek	Protein determination, BrdU assay
Infros AG CH-4103 bottmingen	Tamro	Shaker
Inverted microscope	Leica	Counting cells
LAS-4000	UVITEC cambridge	Western blot Luminescent Image analyzer
Light Microscope	Olympus V PMTVC	Examine cells
Magnetic stirrer	Fisher Scientific	Mixing the solutions
Microfuge® 22R refrigerated centrifuge	Beckman CoulterTM	Centrifugation of 1.5 mL Eppendorf tubes
Mx3000P qPCR System	Agilent technologies	qRT-PCR
pH meter	Mettler Toledo	Buffers preparation
Powerpack300/1000	Biorad	Western blot and agarose gel electrophoresis
Rocker	Stuart	Western blot
Rotator SB3	Stuart	Tube rotator
Shaker	Skyline	culturing bacteria with plasmid
Spectrophotometer ND-1000	Saveen Werner	Nucleic acid measurements
T-100 PCR machine	BioRAD	Thermo cycler
Thermal cycler	Applied Biosystems	amplify segments of DNA
Thermomixer	Eppendorf	RNA and cDNA preparation
Vortex mixer	Corning LSE	mix small vials of liquid
Water bath	Grant	incubate samples and warm media
Water jacketed incubator	Panasonic	Humidified CO_2-incubator

Table A5 – Software used for data analysis

Software	Purpose
Aida image analyzer	Densitometry
Alliance	Capture images of western blots and agarose gel
ImageJ	Densitometry
Graphpadv6	Plot the graphs
GeneE	Plot heat map
Qiagen data analysis software	Analysis gene array plate
Xlstat	Principle component analysis (PCA)

Table A6 – Molecular markers used

Molecular marker	Manufacturer	Purpose
1kb Plus DNA ladder	Invitrogen	Agarose gel electrophoresis
Precision Plus Protein™ Kaleidoscope™ Prestained Protein Standards #1610375	Biorad	Western blot

Table A7 – Buffers and solutions used in this study

Buffers and solutions	Manufacturer/Contents	Purpose
1xPBS	Biochrom, powder dissolved in dH_2O, pH 7.4	Human cell culture
1X TBS (Tris Buffered saline)	20mM Tris, 150mM NaCl, pH 8	Western Blot
Sample buffer	150mM sodium chloride 1.0% Triton X-100 50 mM Tris pH 8.0	SDS-PAGE lysate preparation
5X loading sample buffer	5% SDS, 625mM Tris pH6.8, and 50% glycerol, 5% β-mercaptoethanol and 0.04% bromophenol blue	SDS-PAGE lysate preparation
10x SDS-PAGE running buffer	1% w/v SDS, 250mM glycine, 1.92M Tris and Working dilution 1:10	
TBST	TBS with 0.1% v/v Tween-20	Western Blot
10x Washing buffer	100mM Tris HCl pH 8, 150mM NaCl, 121.1g Tris, 87.7g NaCl and dH_2O up to 1L. Working dilution 1:10	Western Blot
Ponceau S staining	0.2% w/v Ponceau S 5% glacial acetic acid	Western Blot
Stripping Buffer	20ml 10% SDS, 12.5mL 0.5M Tris HCl, 8.8mL β-mercaptoethanol 67.5mL dH2O	Western Blot
1x TE Buffer (pH 8.0)	100mM Tris/10mM EDTA	Plasmid DNA purification/DNA storage
Blocking buffer	5% w/v low fat milk powder in TBST	Western blot
Blotting buffer	5.8g Tris base, 29g glycine, 200mL methanol and 800mL dH_2O	Western blot
50x TAE (Tris Acetate EDTA)	242g Tris base, 57.1mL glacial acetic acid, 100mL 0.5M EDTA (pH 8.0), dH2O up to 1L. Working dilution 1:50.	Agarose gel electrophoresis
6x Loading buffer	0.25% bromophenol blue, 40% sucrose	Agarose gel electrophoresis
Trypsin/ EDTA	Lonza 0.25% trypsin in PBS and 0.05% Na_2-EDTA	Cell culture
96% Ethanol	Sigma-Aldrich	Plasmid DNA purification
Isopropanol	Arcus	Plasmid DNA purification
Solubilization solution	Roche Applied Science	Cell viability assay
Stop solution	100mL isopropanol, 330µl 37% HCl	Cell viability assay
BrdU	Roche Applied Science	Cell proliferation assay

Table A8 – qPCR primers used

Gene Symbol	Forward	Reverse	Base Pairs	T
ATF2	GAA TCT CGA CCG CAG TCA TTA	CCG ACG ACC ACT TGT ACT TT	105	62
AURKC	CGC ACA GCC ACG ATA ATA GA	CAG CAG GTT CTC TGG CTT AAT A	96	62
CBP	AGT CAT CGC AGC AAC AGC CG	CCG AGG AGG GGG TAG GGA CT	175	57
CIITA	CTG TGC CTC TAC CAC TTC TAT G	GTC GCA GTT GAT GGT GTC T	97	62
DNMT3A	GCC CAT TCG ATC TGG TGA TT	GGC GGT AGA ACT CAA AGA AGA G	114	56
DNMT3B	AGA CAG TGG AGA TGG AGA CA	CAG GAG AAG CCC TTG ATC TTT	94	62
HDAC11	GTC TAC AAC CGC CAC ATC TAC	TCT CCA CCT TAT CCA GGT ACT C	147	56
HDAC8	GAA GTC CCA TCC ATT CCT TCA	TGG TCA ACA TTC CCT CCT ATT C	83	58
HDAC4	GGA ATG TAC GAC GCC AAA GA	TCG GCC ACT TTC TGC TTT AG	95	62
HDAC5	GAA TAC CAC ACC CTG CTC TAT G	CAG CAT ACA TCT TCT GGC TGA T	97	62
HDAC9	CTC AGC TTC AGG AGC ATA TCA A	GCC TCT CTA CTT CCT GTT CTT G	158	56
KDM1A	GCC TCC TTT GAA TGA CCT AGA G	CAC ACA CCA AGG GAC TAA GAT G	123	58
KDM2B	CTG AAG GAG AAG CAG ACA GAA G	CGA TGT GGA AGT CGG TGA AA	112	56
KDM4C	GAG CGC AAG TAC TGG AAG AA	GAC TGT ATT GAG GCG AGC TAT G	117	58
KDM5A	CTC GAG AAT GGA CCG CTA AA	TCA AGA CGC ACA GGA ATA GG	112	62
KDM6A	CGC ACT CAC TCT ACC TCA TAA C	GAG AGA GGT CGT TCA CCA TTA G	144	62
KDM6B	CCA GTC TGT GAA ACC GAA GAT	CCG TTT GCT CTC CAG ATA GAT G	93	62
MLL3	CCC TAT ATG CCT GCG TCT AAT G	CAC ACA CCA TCC TGG GTA TAA G	122	62
NCOA3	CCT GAA ATG CGC CAG AGA TA	CGT GCC ACA CAG ATC ATA CA	109	62
NEK6	GAT CCA TGA GAA CGG CTA CAA	GTA GTC ACA CTG CTC GAT CTT C	145	62
PRMT2	CTC GGT CTA CCC TGA CAT TTG	CAG GAC ATC TTG AAG CCA TAG A	110	62
RPL27	ATC GCC AAG AGA TCA AAG ATA A	TCT GAA GAC ATC CTT ATT GAC G	123	60
SETD6	GAA GAG GGA GCC TTT GTG ATA G	CCA TCC TGG TCT TTA AGC TCT C	119	62

Forward and reverse indicate the specific primers; base pairs, the product length and T, the annealing temperature given as ^{o}C.

Table A9 – Cell lines used in this study

Cell -line	Origin	Cell type	Purpose
HuT78	Human 53yr male	Cutaneous T lymphocyte	Transfection, gene expression and proliferation studies
MEC1	Human 61yr male	Chronic B cell leukemia	Transfection and proliferation studies
THP-1	Human 1yr male	Acute monocytic leukemia monocyte	Proliferation studies
MCF-7	Human 69yr female	Adenocarcinoma epithelial	Proliferation studies
Daudi	Human 16yr male	Burkitt's lymphoma B lymphoblast	Apoptosis
Raji	Human 11yr male	Burkitt's lymphoma B lymphocyte	Apoptosis

Table A10 – Growth media used in this study

Growth media	Media composition	Manufacturer/ Contents	Purpose	Doubling Time
DMEM	10% FBS (50mL)+5mL L-Glutamine+ 10mL P/S	Sigma-Aldrich/Standard Dulbecco's modified Eagle's medium	MEC1, MCF-7	40hrs 33hrs
IMDM	20% FBS (50mL)+5mL L-Glutamine+ 10mL P/S	Sigma-Aldrich/ Iscove's Modified Dulbecco's Medium	HuT78	30hrs
RPMI-1640	10% FBS (50mL)+5mL L-Glutamine+ 10mL P/S	Sigma-Aldrich / Roswell Park Memorial Institute 1640	THP-1, Daudi and Raji	30hrs 29hrs 33hrs
FBS		Gibco®/ Heat inactivated Foetal Bovine Serum	10% DMEM 20% IMDM 10% RPMI-1640	

A

Layout	01	02	03	04	05	06	07	08	09	10	11	12
A	ASH1L -1.18	ATF2 1.50	AURKA 1.07	AURKB 1.24	AURKC -2.47	CARM1 -1.05	CDYL 1.27	CIITA 1.58	CSRP2BP -1.05	DNMT1 -1.12	DNMT3A 1.80	DNMT3B 1.72
B	DOT1L 1.14	DZIP3 1.27	EHMT2 1.03	ESCO1 -1.19	ESCO2 -1.32	HAT1 -1.49	HDAC1 -1.04	HDAC10 1.42	HDAC11 1.89	HDAC2 -1.24	HDAC3 1.25	HDAC4 -1.51
C	HDAC5 2.86	HDAC6 1.03	HDAC7 1.44	HDAC8 1.02	HDAC9 3.06	KAT2A 1.01	KAT2B -1.47	KAT5 1.19	KAT6A -1.21	KAT6B -1.12	KAT7 -1.56	KAT8 -1.22
D	KDM1A 1.22	KDM4A -1.00	KDM4C 1.22	KDM5B 1.11	KDM5C 1.19	KDM6B 1.60	MBD2 -1.29	KMT2A 1.19	KMT2C 2.47	KMT2E -1.17	MYSM1 -1.42	NCOA1 -1.18
E	NCOA3 1.53	NCOA6 -1.26	NEK6 1.60	NSD1 1.32	PAK1 1.08	PRMT1 -1.07	PRMT2 1.02	PRMT3 -1.66	PRMT5 -1.47	PRMT6 1.29	PRMT7 -1.08	PRMT8 1.04
F	RNF2 -1.01	RNF20 1.29	RPS6KA3 -1.05	RPS6KAS -1.08	SETD1A 1.35	SETD1B 1.35	SETD2 1.04	SETD3 -1.17	SETD4 -1.32	SETD5 1.25	SETD6 -1.77	SETD7 -1.94
G	SETD8 1.20	SETDB1 -1.07	SETDB2 1.29	SMYD3 -1.05	SUV39H1 1.24	SUV420H1 1.15	UBE2A -1.20	UBE2B -1.16	USP16 -1.37	USP21 -1.16	USP22 1.44	WHSC1 -1.40

B

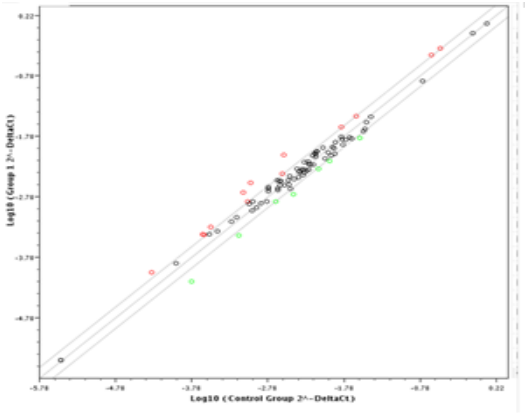

Figure A1 – Results from epigenetic qRT-PCR array plate

A) qRT-PCR array results showing fold change of 84 epigenetic modifiers genes between untreated and Romidepsin treated RHuT78 cells. Genes expression was made relative to RPL27 mRNA **B)** Linear regression analysis of $2^{-\Delta Ct}$ between group 1 (Romidepsin treated) and group 2 (untreated) RHuT78 cells. Genes Up and down regulated >1.5 fold are highlighted in red and green respectively.

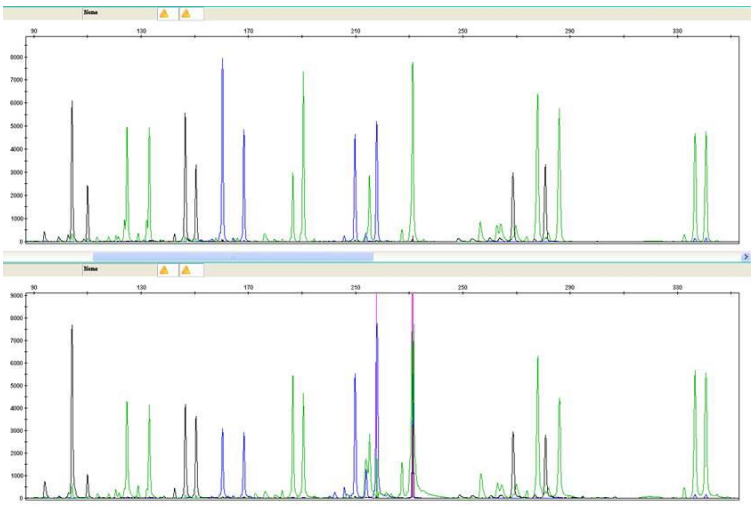

HuT78

RHuT78

STR Locus	Alleles
TH01	6,8
D2S11	27,29
D5S818	10,12
D13S317	12,12 (homozygous)
D7S820	11,11 (homozygous)
D16539	9,11
CSF1PO	11,12
AMEL	X,Y
vWA	16,17
TPOX	8,11

Figure A2 – Analysis of HuT78 and RHuT78 using the GenePrint 10 System

A single-source DNA template (10ng) was amplified using the GenePrint 10 System. Amplification products were mixed with Internal Lane Standard 600 and analyzed using an Applied Biosystems® 3130 Genetic Analyzer and a 3.0kV, 4-second injection. The results were analyzed using GeneMapper® ID-X software.

Bibliography

1. Holliday R. The inheritance of epigenetic defects. *Science*. 1987;238(4824):163-170.
2. Blackledge NP, Klose R. CpG island chromatin: a platform for gene regulation. *Epigenetics*. 2011;6(2):147-152.
3. Frederiks F, Stulemeijer IJ, Ovaa H, van Leeuwen F. A modified epigenetics toolbox to study histone modifications on the nucleosome core. *Chembiochem*. 2011;12(2):308-313.
4. Cairns BR. The logic of chromatin architecture and remodelling at promoters. *Nature*. 2009;461(7261):193-198.
5. Glenn M, Duckworth, Andrew, Kalakonda, Nagesh. DNA Methylation Abnormalities in Mature B-cell Lymphoid Neoplasms. *Academic Journal*. 2012;20(4):109.
6. Bestor TH. The DNA methyltransferases of mammals. *Hum Mol Genet*. 2000;9(16):2395-2402.
7. Wu SC, Zhang Y. Active DNA demethylation: many roads lead to Rome. *Nat Rev Mol Cell Biol*. 2010;11(9):607-620.
8. Tomatsu S, Orii KO, Bi Y, et al. General implications for CpG hot spot mutations: methylation patterns of the human iduronate-2-sulfatase gene locus. *Hum Mutat*. 2004;23(6):590-598.
9. Jones PL, Veenstra GJ, Wade PA, et al. Methylated DNA and MeCP2 recruit histone deacetylase to repress transcription. *Nat Genet*. 1998;19(2):187-191.
10. Nan X, Ng H-H, Johnson CA, et al. Transcriptional repression by the methyl-CpG-binding protein MeCP2 involves a histone deacetylase complex. *Nature*. 1998;393(6683):386-389.
11. Costello JF, Plass C. Methylation matters. *J Med Genet*. 2001;38(5):285-303.
12. Baylin SB. Resistance, epigenetics and the cancer ecosystem. *Nat Med*. 2011;17(3):288-289.
13. Bestor T, Laudano A, Mattaliano R, Ingram V. Cloning and sequencing of a cDNA encoding DNA methyltransferase of mouse cells: The carboxyl-terminal domain of the mammalian enzymes is related to bacterial

restriction methyltransferases. *Journal of Molecular Biology*. 1988;203(4):971-983.
14. Okano M, Bell DW, Haber DA, Li E. DNA methyltransferases Dnmt3a and Dnmt3b are essential for de novo methylation and mammalian development. *Cell*. 1999;99(3):247-257.
15. Chen ZX, Mann JR, Hsieh CL, Riggs AD, Chedin F. Physical and functional interactions between the human DNMT3L protein and members of the de novo methyltransferase family. *J Cell Biochem*. 2005;95(5):902-917.
16. Robertson KD, Uzvolgyi E, Liang G, et al. The human DNA methyltransferases (DNMTs) 1, 3a and 3b: coordinate mRNA expression in normal tissues and overexpression in tumors. *Nucleic Acids Res*. 1999;27(11):2291-2298.
17. Robertson KD. DNA methylation, methyltransferases, and cancer. *Oncogene*. 2001;20(24):3139-3155.
18. Beard C, Li E, Jaenisch R. Loss of methylation activates Xist in somatic but not in embryonic cells. *Genes Dev*. 1995;9(19):2325-2334.
19. Li E, Bestor TH, Jaenisch R. Targeted mutation of the DNA methyltransferase gene results in embryonic lethality. *Cell*. 1992;69(6):915-926.
20. Klose RJ, Bird AP. Genomic DNA methylation: the mark and its mediators. *Trends Biochem Sci*. 2006;31(2):89-97.
21. Otani J, Nankumo T, Arita K, Inamoto S, Ariyoshi M, Shirakawa M. Structural basis for recognition of H3K4 methylation status by the DNA methyltransferase 3A ATRX-DNMT3-DNMT3L domain. *EMBO Rep*. 2009;10(11):1235-1241.
22. Yang LB, Rau R, Goodell MA. DNMT3A in haematological malignancies. *Nature Reviews Cancer*. 2015;15(3):152-165.
23. Clark SJ, Melki J. DNA methylation and gene silencing in cancer: which is the guilty party? *Oncogene*. 2002;21(35):5380-5387.
24. De Smet C, Loriot A. DNA hypomethylation in cancer: epigenetic scars of a neoplastic journey. *Epigenetics*. 2010;5(3):206-213.

25. Laird PW. Cancer epigenetics. *Hum Mol Genet*. 2005;14 Spec No 1:R65-76.
26. Garcia-Manero G, Jeha S, Daniel J, et al. Aberrant DNA methylation in pediatric patients with acute lymphocytic leukemia. *Cancer*. 2003;97(3):695-702.
27. Roll JD, Rivenbark AG, Jones WD, Coleman WB. DNMT3b overexpression contributes to a hypermethylator phenotype in human breast cancer cell lines. *Mol Cancer*. 2008;7:15.
28. Ribeiro AF, Pratcorona M, Erpelinck-Verschueren C, et al. Mutant DNMT3A: a marker of poor prognosis in acute myeloid leukemia. *Blood*. 2012;119(24):5824-5831.
29. Bojang P, Jr., Ramos KS. The promise and failures of epigenetic therapies for cancer treatment. *Cancer Treat Rev*. 2014;40(1):153-169.
30. Goffin J, Eisenhauer E. DNA methyltransferase inhibitors-state of the art. *Ann Oncol*. 2002;13(11):1699-1716.
31. Leone G, Teofili L, Voso MT, Lubbert M. DNA methylation and demethylating drugs in myelodysplastic syndromes and secondary leukemias. *Haematologica*. 2002;87(12):1324-1341.
32. Lyko F, Brown R. DNA methyltransferase inhibitors and the development of epigenetic cancer therapies. *J Natl Cancer Inst*. 2005;97(20):1498-1506.
33. Garcia-Manero G. Demethylating agents in myeloid malignancies. *Curr Opin Oncol*. 2008;20(6):705-710.
34. Flotho C, Claus R, Batz C, et al. The DNA methyltransferase inhibitors azacitidine, decitabine and zebularine exert differential effects on cancer gene expression in acute myeloid leukemia cells. *Leukemia*. 2009;23(6):1019-1028.
35. Hagemann S, Heil O, Lyko F, Brueckner B. Azacytidine and decitabine induce gene-specific and non-random DNA demethylation in human cancer cell lines. *PLoS One*. 2011;6(3):e17388.
36. Gros C, Fahy J, Halby L, et al. DNA methylation inhibitors in cancer: Recent and future approaches. *Biochimie*. 2012;94(11):2280-2296.
37. Christiansen DH, Andersen MK, Pedersen-Bjergaard J. Methylation of p15INK4B is common, is associated with deletion of genes on chromosome arm 7q and predicts a

poor prognosis in therapy-related myelodysplasia and acute myeloid leukemia. *Leukemia*. 2003;17(9):1813-1819.
38. Uchida T, Kinoshita T, Nagai H, et al. Hypermethylation of the p15INK4B gene in myelodysplastic syndromes. *Blood*. 1997;90(4):1403-1409.
39. Cihak A. Biological effects of 5-azacytidine in eukaryotes. *Oncology*. 1974;30(5):405-422.
40. Glover AB, Leyland-Jones BR, Chun HG, Davies B, Hoth DF. Azacitidine: 10 years later. *Cancer Treat Rep*. 1987;71(7-8):737-746.
41. Momparler RL, Rossi M, Bouchard J, Vaccaro C, Momparler LF, Bartolucci S. Kinetic interaction of 5-AZA-2'-deoxycytidine-5'-monophosphate and its 5'-triphosphate with deoxycytidylate deaminase. *Mol Pharmacol*. 1984;25(3):436-440.
42. Li LH, Olin EJ, Fraser TJ, Bhuyan BK. Phase specificity of 5-azacytidine against mammalian cells in tissue culture. *Cancer Res*. 1970;30(11):2770-2775.
43. Vesely J. Mode of action and effects of 5-azacytidine and of its derivatives in eukaryotic cells. *Pharmacol Ther*. 1985;28(2):227-235.
44. Momparler RL, Cote S, Eliopoulos N. Pharmacological approach for optimization of the dose schedule of 5-Aza-2'-deoxycytidine (Decitabine) for the therapy of leukemia. *Leukemia*. 1997;11 Suppl 1:S1-6.
45. Hollenbach PW, Nguyen AN, Brady H, et al. A comparison of azacitidine and decitabine activities in acute myeloid leukemia cell lines. *PLoS One*. 2010;5(2):e9001.
46. Momparler RL, Momparler LF, Samson J. Comparison of the antileukemic activity of 5-AZA-2'-deoxycytidine, 1-beta-D-arabinofuranosylcytosine and 5-azacytidine against L1210 leukemia. *Leuk Res*. 1984;8(6):1043-1049.
47. Fang MZ, Wang Y, Ai N, et al. Tea polyphenol (-)-epigallocatechin-3-gallate inhibits DNA methyltransferase and reactivates methylation-silenced genes in cancer cell lines. *Cancer Res*. 2003;63(22):7563-7570.
48. Mund C, Brueckner B, Lyko F. Reactivation of epigenetically silenced genes by DNA methyltransferase

inhibitors: basic concepts and clinical applications. *Epigenetics*. 2006;1(1):7-13.
49. Lao VV, Grady WM. Epigenetics and colorectal cancer. *Nat Rev Gastroenterol Hepatol*. 2011;8(12):686-700.
50. Santos-Rosa H, Caldas C. Chromatin modifier enzymes, the histone code and cancer. *European Journal of Cancer*. 2005;41(16):2381-2402.
51. Allfrey VG, Faulkner R, Mirsky AE. ACETYLATION AND METHYLATION OF HISTONES AND THEIR POSSIBLE ROLE IN THE REGULATION OF RNA SYNTHESIS. *Proc Natl Acad Sci U S A*. 1964;51:786-794.
52. Yap KL, Zhou MM. Structure and function of protein modules in chromatin biology. *Results Probl Cell Differ*. 2006;41:1-23.
53. Kouzarides T. Chromatin modifications and their function. *Cell*. 2007;128(4):693-705.
54. Martin C, Zhang Y. The diverse functions of histone lysine methylation. *Nat Rev Mol Cell Biol*. 2005;6(11):838-849.
55. Thompson PR, Fast W. Histone citrullination by protein arginine deiminase: is arginine methylation a green light or a roadblock? *ACS Chem Biol*. 2006;1(7):433-441.
56. Zhang Y, Reinberg D. Transcription regulation by histone methylation: interplay between different covalent modifications of the core histone tails. *Genes Dev*. 2001;15(18):2343-2360.
57. Marmorstein R. Structure and function of histone acetyltransferases. *Cell Mol Life Sci*. 2001;58(5-6):693-703.
58. Robey RW, Chakraborty AR, Basseville A, et al. Histone deacetylase inhibitors: emerging mechanisms of resistance. *Mol Pharm*. 2011;8(6):2021-2031.
59. Tambaro FP, Dell'Aversana C, Carafa V, et al. Histone deacetylase inhibitors: clinical implications for hematological malignancies. *Clin Epigenetics*. 2010;1(1-2):25-44.
60. Blanco-Garcia N, Asensio-Juan E, de la Cruz X, Martinez-Balbas MA. Autoacetylation regulates P/CAF nuclear localization. *J Biol Chem*. 2009;284(3):1343-1352.

61. Parthun MR. Hat1: the emerging cellular roles of a type B histone acetyltransferase. *Oncogene*. 0000;26(37):5319-5328.
62. Sun XJ, Man N, Tan Y, Nimer SD, Wang L. The Role of Histone Acetyltransferases in Normal and Malignant Hematopoiesis. *Front Oncol*. 2015;5:108.
63. Giles RH, Peters DJM, Breuning MH. Conjunction dysfunction: CBP/p300 in human disease. *Trends in Genetics*;14(5):178-183.
64. Puttagunta R, Tedeschi A, Sória MG, et al. PCAF-dependent epigenetic changes promote axonal regeneration in the central nervous system. *Nat Commun*. 2014;5.
65. Zhang S, Sun G, Wang Z, Wan Y, Guo J, Shi L. PCAF-mediated Akt1 acetylation enhances the proliferation of human glioblastoma cells. *Tumour Biol*. 2015;36(3):1455-1462.
66. Khan SN, Khan AU. Role of histone acetylation in cell physiology and diseases: An update. *Clinica Chimica Acta*. 2010;411(19–20):1401-1411.
67. Rekowski M, Giannis A. Histone acetylation modulation by small molecules: a chemical approach. *Biochim Biophys Acta*. 2010;1799(10-12):760-767.
68. Manzo F, Tambaro FP, Mai A, Altucci L. Histone acetyltransferase inhibitors and preclinical studies. *Expert Opin Ther Pat*. 2009;19(6):761-774.
69. Dekker FJ, Haisma HJ. Histone acetyl transferases as emerging drug targets. *Drug Discov Today*. 2009;14(19-20):942-948.
70. Furdas SD, Kannan S, Sippl W, Jung M. Small molecule inhibitors of histone acetyltransferases as epigenetic tools and drug candidates. *Arch Pharm (Weinheim)*. 2012;345(1):7-21.
71. Balasubramanyam K, Swaminathan V, Ranganathan A, Kundu TK. Small molecule modulators of histone acetyltransferase p300. *J Biol Chem*. 2003;278(21):19134-19140.
72. Sun Y, Jiang X, Chen S, Price BD. Inhibition of histone acetyltransferase activity by anacardic acid sensitizes tumor cells to ionizing radiation. *FEBS Letters*. 2006;580(18):4353-4356.

73. Balasubramanyam K, Varier RA, Altaf M, et al. Curcumin, a novel p300/CREB-binding protein-specific inhibitor of acetyltransferase, represses the acetylation of histone/nonhistone proteins and histone acetyltransferase-dependent chromatin transcription. *J Biol Chem*. 2004;279(49):51163-51171.
74. Ott M, Verdin E. HAT Trick: p300, Small Molecule, Inhibitor. *Chemistry & Biology*. 2010;17(5):417-418.
75. Gao XN, Lin J, Ning QY, et al. A histone acetyltransferase p300 inhibitor C646 induces cell cycle arrest and apoptosis selectively in AML1-ETO-positive AML cells. *PLoS One*. 2013;8(2):e55481.
76. Hess-Stumpp H, Bracker TU, Henderson D, Politz O. MS-275, a potent orally available inhibitor of histone deacetylases—The development of an anticancer agent. *The International Journal of Biochemistry & Cell Biology*. 2007;39(7–8):1388-1405.
77. de Ruijter AJ, van Gennip AH, Caron HN, Kemp S, van Kuilenburg AB. Histone deacetylases (HDACs): characterization of the classical HDAC family. *Biochem J*. 2003;370(Pt 3):737-749.
78. Johnstone RW. Histone-deacetylase inhibitors: novel drugs for the treatment of cancer. *Nat Rev Drug Discov*. 2002;1(4):287-299.
79. Yang WM, Tsai SC, Wen YD, Fejer G, Seto E. Functional domains of histone deacetylase-3. *J Biol Chem*. 2002;277(11):9447-9454.
80. Falkenberg KJ, Johnstone RW. Histone deacetylases and their inhibitors in cancer, neurological diseases and immune disorders. *Nat Rev Drug Discov*. 2014;13(9):673-691.
81. Marquard L, Gjerdrum LM, Christensen IJ, Jensen PB, Sehested M, Ralfkiaer E. Prognostic significance of the therapeutic targets histone deacetylase 1, 2, 6 and acetylated histone H4 in cutaneous T-cell lymphoma. *Histopathology*. 2008;53(3):267-277.
82. Giannini G, Cabri W, Fattorusso C, Rodriquez M. Histone deacetylase inhibitors in the treatment of cancer: overview and perspectives. *Future Med Chem*. 2012;4(11):1439-1460.
83. Ropero S, Fraga MF, Ballestar E, et al. A truncating mutation of HDAC2 in human cancers confers resistance

to histone deacetylase inhibition. *Nat Genet*. 2006;38(5):566-569.
84. Lee H, Sengupta N, Villagra A, Rezai-Zadeh N, Seto E. Histone deacetylase 8 safeguards the human ever-shorter telomeres 1B (hEST1B) protein from ubiquitin-mediated degradation. *Mol Cell Biol*. 2006;26(14):5259-5269.
85. Buggy JJ, Sideris ML, Mak P, Lorimer DD, McIntosh B, Clark JM. Cloning and characterization of a novel human histone deacetylase, HDAC8. *Biochem J*. 2000;350 Pt 1:199-205.
86. Van den Wyngaert I, de Vries W, Kremer A, et al. Cloning and characterization of human histone deacetylase 8. *FEBS Lett*. 2000;478(1-2):77-83.
87. Wilson BJ, Tremblay AM, Deblois G, Sylvain-Drolet G, Giguere V. An acetylation switch modulates the transcriptional activity of estrogen-related receptor alpha. *Mol Endocrinol*. 2010;24(7):1349-1358.
88. Sengupta N, Seto E. Regulation of histone deacetylase activities. *J Cell Biochem*. 2004;93(1):57-67.
89. Lee H, Rezai-Zadeh N, Seto E. Negative regulation of histone deacetylase 8 activity by cyclic AMP-dependent protein kinase A. *Mol Cell Biol*. 2004;24(2):765-773.
90. Oehme I, Deubzer HE, Lodrini M, Milde T, Witt O. Targeting of HDAC8 and investigational inhibitors in neuroblastoma. *Expert Opin Investig Drugs*. 2009;18(11):1605-1617.
91. Balasubramanian S, Ramos J, Luo W, Sirisawad M, Verner E, Buggy JJ. A novel histone deacetylase 8 (HDAC8)-specific inhibitor PCI-34051 induces apoptosis in T-cell lymphomas. *Leukemia*. 2008;22(5):1026-1034.
92. Nakagawa M, Oda Y, Eguchi T, et al. Expression profile of class I histone deacetylases in human cancer tissues. *Oncol Rep*. 2007;18(4):769-774.
93. Yang XJ, Gregoire S. Class II histone deacetylases: from sequence to function, regulation, and clinical implication. *Mol Cell Biol*. 2005;25(8):2873-2884.
94. Fischle W, Kiermer V, Dequiedt F, Verdin E. The emerging role of class II histone deacetylases. *Biochem Cell Biol*. 2001;79(3):337-348.
95. McKinsey TA, Zhang CL, Olson EN. Identification of a signal-responsive nuclear export sequence in class II

histone deacetylases. *Mol Cell Biol*. 2001;21(18):6312-6321.
96. McKinsey TA, Zhang CL, Olson EN. Activation of the myocyte enhancer factor-2 transcription factor by calcium/calmodulin-dependent protein kinase-stimulated binding of 14-3-3 to histone deacetylase 5. *Proc Natl Acad Sci U S A*. 2000;97(26):14400-14405.
97. Li X, Song S, Liu Y, Ko SH, Kao HY. Phosphorylation of the histone deacetylase 7 modulates its stability and association with 14-3-3 proteins. *J Biol Chem*. 2004;279(33):34201-34208.
98. Kao HY, Verdel A, Tsai CC, Simon C, Juguilon H, Khochbin S. Mechanism for nucleocytoplasmic shuttling of histone deacetylase 7. *J Biol Chem*. 2001;276(50):47496-47507.
99. Grozinger CM, Schreiber SL. Regulation of histone deacetylase 4 and 5 and transcriptional activity by 14-3-3-dependent cellular localization. *Proc Natl Acad Sci U S A*. 2000;97(14):7835-7840.
100. Fischle W, Dequiedt F, Hendzel MJ, et al. Enzymatic activity associated with class II HDACs is dependent on a multiprotein complex containing HDAC3 and SMRT/N-CoR. *Mol Cell*. 2002;9(1):45-57.
101. Sjoblom T, Jones S, Wood LD, et al. The consensus coding sequences of human breast and colorectal cancers. *Science*. 2006;314(5797):268-274.
102. Witt O, Deubzer HE, Milde T, Oehme I. HDAC family: What are the cancer relevant targets? *Cancer Letters*. 2009;277(1):8-21.
103. Witt O, Deubzer HE, Milde T, Oehme I. HDAC family: What are the cancer relevant targets? *Cancer Lett*. 2009;277(1):8-21.
104. Khan O, La Thangue NB. HDAC inhibitors in cancer biology: emerging mechanisms and clinical applications. *Immunol Cell Biol*. 2012;90(1):85-94.
105. Marquard L, Poulsen CB, Gjerdrum LM, et al. Histone deacetylase 1, 2, 6 and acetylated histone H4 in B- and T-cell lymphomas. *Histopathology*. 2009;54(6):688-698.
106. Fischer DD, Cai R, Bhatia U, et al. Isolation and characterization of a novel class II histone deacetylase, HDAC10. *J Biol Chem*. 2002;277(8):6656-6666.

107. Guardiola AR, Yao TP. Molecular cloning and characterization of a novel histone deacetylase HDAC10. *J Biol Chem*. 2002;277(5):3350-3356.
108. Zhou X, Marks PA, Rifkind RA, Richon VM. Cloning and characterization of a histone deacetylase, HDAC9. *Proceedings of the National Academy of Sciences*. 2001;98(19):10572-10577.
109. Okudela K, Mitsui H, Suzuki T, et al. Expression of HDAC9 in lung cancer--potential role in lung carcinogenesis. *Int J Clin Exp Pathol*. 2014;7(1):213-220.
110. Zhao YX, Wang YS, Cai QQ, Wang JQ, Yao WT. Up-regulation of HDAC9 promotes cell proliferation through suppressing p53 transcription in osteosarcoma. *Int J Clin Exp Med*. 2015;8(7):11818-11823.
111. Bradbury CA, Khanim FL, Hayden R, et al. Histone deacetylases in acute myeloid leukaemia show a distinctive pattern of expression that changes selectively in response to deacetylase inhibitors. *Leukemia*. 2005;19(10):1751-1759.
112. Schwer B, Verdin E. Conserved Metabolic Regulatory Functions of Sirtuins. *Cell Metabolism*. 2008;7(2):104-112.
113. Butler KV, Kozikowski AP. Chemical origins of isoform selectivity in histone deacetylase inhibitors. *Curr Pharm Des*. 2008;14(6):505-528.
114. Casimiro MC, Crosariol M, Loro E, Li Z, Pestell RG. Cyclins and Cell Cycle Control in Cancer and Disease. *Genes & Cancer*. 2012;3(11-12):649-657.
115. Marks PA, Richon VM, Rifkind RA. Histone deacetylase inhibitors: inducers of differentiation or apoptosis of transformed cells. *J Natl Cancer Inst*. 2000;92(15):1210-1216.
116. Ng HH, Bird A. Histone deacetylases: silencers for hire. *Trends Biochem Sci*. 2000;25(3):121-126.
117. Glaser KB, Li J, Staver MJ, Wei RQ, Albert DH, Davidsen SK. Role of class I and class II histone deacetylases in carcinoma cells using siRNA. *Biochem Biophys Res Commun*. 2003;310(2):529-536.
118. Haberland M, Johnson A, Mokalled MH, Montgomery RL, Olson EN. Genetic dissection of histone deacetylase requirement in tumor cells. *Proc Natl Acad Sci U S A*. 2009;106(19):7751-7755.

119. Bhaskara S, Chyla BJ, Amann JM, et al. Deletion of histone deacetylase 3 reveals critical roles in S phase progression and DNA damage control. *Mol Cell*. 2008;30(1):61-72.
120. Zupkovitz G, Grausenburger R, Brunmeir R, et al. The cyclin-dependent kinase inhibitor p21 is a crucial target for histone deacetylase 1 as a regulator of cellular proliferation. *Mol Cell Biol*. 2010;30(5):1171-1181.
121. Hagelkruys A, Sawicka A, Rennmayr M, Seiser C. The biology of HDAC in cancer: the nuclear and epigenetic components. *Handb Exp Pharmacol*. 2011;206:13-37.
122. Grausenburger R, Bilic I, Boucheron N, et al. Conditional deletion of histone deacetylase 1 in T cells leads to enhanced airway inflammation and increased Th2 cytokine production. *J Immunol*. 2010;185(6):3489-3497.
123. Montgomery RL, Davis CA, Potthoff MJ, et al. Histone deacetylases 1 and 2 redundantly regulate cardiac morphogenesis, growth, and contractility. *Genes Dev*. 2007;21(14):1790-1802.
124. Montgomery RL, Potthoff MJ, Haberland M, et al. Maintenance of cardiac energy metabolism by histone deacetylase 3 in mice. *J Clin Invest*. 2008;118(11):3588-3597.
125. Yamaguchi T, Cubizolles F, Zhang Y, et al. Histone deacetylases 1 and 2 act in concert to promote the G1-to-S progression. *Genes Dev*. 2010;24(5):455-469.
126. Senese S, Zaragoza K, Minardi S, et al. Role for histone deacetylase 1 in human tumor cell proliferation. *Mol Cell Biol*. 2007;27(13):4784-4795.
127. Huang BH, Laban M, Leung CH, et al. Inhibition of histone deacetylase 2 increases apoptosis and p21Cip1/WAF1 expression, independent of histone deacetylase 1. *Cell Death Differ*. 2005;12(4):395-404.
128. Wilson AJ, Byun DS, Popova N, et al. Histone deacetylase 3 (HDAC3) and other class I HDACs regulate colon cell maturation and p21 expression and are deregulated in human colon cancer. *J Biol Chem*. 2006;281(19):13548-13558.
129. Mottet D, Pirotte S, Lamour V, et al. HDAC4 represses p21(WAF1/Cip1) expression in human cancer cells through a Sp1-dependent, p53-independent mechanism. *Oncogene*. 2009;28(2):243-256.

130. Ueda H, Manda T, Matsumoto S, et al. FR901228, a novel antitumor bicyclic depsipeptide produced by Chromobacterium violaceum No. 968. III. Antitumor activities on experimental tumors in mice. *J Antibiot (Tokyo)*. 1994;47(3):315-323.
131. Mercurio C, Minucci S, Pelicci PG. Histone deacetylases and epigenetic therapies of hematological malignancies. *Pharmacol Res*. 2010;62(1):18-34.
132. Weeks KL, Avkiran M. Roles and post-translational regulation of cardiac class IIa histone deacetylase isoforms. *J Physiol*. 2015;593(8):1785-1797.
133. Marks PA. The clinical development of histone deacetylase inhibitors as targeted anticancer drugs. *Expert Opin Investig Drugs*. 2010;19(9):1049-1066.
134. Ueda H, Nakajima H, Hori Y, et al. FR901228, a novel antitumor bicyclic depsipeptide produced by Chromobacterium violaceum No. 968. I. Taxonomy, fermentation, isolation, physico-chemical and biological properties, and antitumor activity. *J Antibiot (Tokyo)*. 1994;47(3):301-310.
135. Grant C, Rahman F, Piekarz R, et al. Romidepsin: a new therapy for cutaneous T-cell lymphoma and a potential therapy for solid tumors. *Expert Rev Anticancer Ther*. 2010;10(7):997-1008.
136. Xiao JJ, Byrd J, Marcucci G, Grever M, Chan KK. Identification of thiols and glutathione conjugates of depsipeptide FK228 (FR901228), a novel histone protein deacetylase inhibitor, in the blood. *Rapid Commun Mass Spectrom*. 2003;17(8):757-766.
137. Hideshima T, Anderson KC. Histone deacetylase inhibitors in the treatment for multiple myeloma. *International Journal of Hematology*. 2013;97(3):324-332.
138. Furumai R, Matsuyama A, Kobashi N, et al. FK228 (depsipeptide) as a natural prodrug that inhibits class I histone deacetylases. *Cancer Res*. 2002;62(17):4916-4921.
139. Yu X, Guo ZS, Marcu MG, et al. Modulation of p53, ErbB1, ErbB2, and Raf-1 expression in lung cancer cells by depsipeptide FR901228. *J Natl Cancer Inst*. 2002;94(7):504-513.

140. Woo S, Gardner ER, Chen X, et al. Population pharmacokinetics of romidepsin in patients with cutaneous T-cell lymphoma and relapsed peripheral T-cell lymphoma. *Clin Cancer Res*. 2009;15(4):1496-1503.
141. Batty N, Malouf GG, Issa JP. Histone deacetylase inhibitors as anti-neoplastic agents. *Cancer Lett*. 2009;280(2):192-200.
142. Belinsky SA, Klinge DM, Stidley CA, et al. Inhibition of DNA methylation and histone deacetylation prevents murine lung cancer. *Cancer Res*. 2003;63(21):7089-7093.
143. Klisovic MI, Maghraby EA, Parthun MR, et al. Depsipeptide (FR 901228) promotes histone acetylation, gene transcription, apoptosis and its activity is enhanced by DNA methyltransferase inhibitors in AML1/ETO-positive leukemic cells. *Leukemia*. 2003;17(2):350-358.
144. Cameron EE, Bachman KE, Myohanen S, Herman JG, Baylin SB. Synergy of demethylation and histone deacetylase inhibition in the re-expression of genes silenced in cancer. *Nat Genet*. 1999;21(1):103-107.
145. Codd R, Braich N, Liu J, Soe CZ, Pakchung AA. Zn(II)-dependent histone deacetylase inhibitors: suberoylanilide hydroxamic acid and trichostatin A. *Int J Biochem Cell Biol*. 2009;41(4):736-739.
146. Stimson L, Wood V, Khan O, Fotheringham S, La Thangue NB. HDAC inhibitor-based therapies and haematological malignancy. *Ann Oncol*. 2009;20(8):1293-1302.
147. Minucci S, Pelicci PG. Histone deacetylase inhibitors and the promise of epigenetic (and more) treatments for cancer. *Nat Rev Cancer*. 2006;6(1):38-51.
148. Codd R. Traversing the coordination chemistry and chemical biology of hydroxamic acids. *Coordination Chemistry Reviews*. 2008;252(12–14):1387-1408.
149. Ma X, Ezzeldin HH, Diasio RB. Histone deacetylase inhibitors: current status and overview of recent clinical trials. *Drugs*. 2009;69(14):1911-1934.
150. Bolden JE, Peart MJ, Johnstone RW. Anticancer activities of histone deacetylase inhibitors. *Nat Rev Drug Discov*. 2006;5(9):769-784.
151. West AC, Johnstone RW. New and emerging HDAC inhibitors for cancer treatment. *J Clin Invest*. 2014;124(1):30-39.

152. Sawas A, Radeski D, O'Connor OA. Belinostat in patients with refractory or relapsed peripheral T-cell lymphoma: a perspective review. *Ther Adv Hematol*. 2015;6(4):202-208.
153. Duvic M, Dummer R, Becker JC, et al. Panobinostat activity in both bexarotene-exposed and -naive patients with refractory cutaneous T-cell lymphoma: results of a phase II trial. *Eur J Cancer*. 2013;49(2):386-394.
154. George P, Bali P, Annavarapu S, et al. Combination of the histone deacetylase inhibitor LBH589 and the hsp90 inhibitor 17-AAG is highly active against human CML-BC cells and AML cells with activating mutation of FLT-3. *Blood*. 2005;105(4):1768-1776.
155. Kalff A, Shortt J, Farr J, et al. Laboratory tumor lysis syndrome complicating LBH589 therapy in a patient with acute myeloid leukaemia. *Haematologica*. 2008;93(1):e16-17.
156. Tsuji N, Kobayashi M, Nagashima K, Wakisaka Y, Koizumi K. A new antifungal antibiotic, trichostatin. *J Antibiot (Tokyo)*. 1976;29(1):1-6.
157. Yoshida M, Nomura S, Beppu T. Effects of trichostatins on differentiation of murine erythroleukemia cells. *Cancer Res*. 1987;47(14):3688-3691.
158. Yatouji S, El-Khoury V, Trentesaux C, et al. Differential modulation of nuclear texture, histone acetylation, and MDR1 gene expression in human drug-sensitive and -resistant OV1 cell lines. *Int J Oncol*. 2007;30(4):1003-1009.
159. Canani RB, Costanzo MD, Leone L, Pedata M, Meli R, Calignano A. Potential beneficial effects of butyrate in intestinal and extraintestinal diseases. *World J Gastroenterol*. 2011;17(12):1519-1528.
160. Terao Y, Nishida J, Horiuchi S, et al. Sodium butyrate induces growth arrest and senescence-like phenotypes in gynecologic cancer cells. *Int J Cancer*. 2001;94(2):257-267.
161. Gilbert J, Baker SD, Bowling MK, et al. A phase I dose escalation and bioavailability study of oral sodium phenylbutyrate in patients with refractory solid tumor malignancies. *Clin Cancer Res*. 2001;7(8):2292-2300.
162. Mai A, Altucci L. Epi-drugs to fight cancer: From chemistry to cancer treatment, the road ahead. *The*

International Journal of Biochemistry & Cell Biology. 2009;41(1):199-213.
163. Yamada H, Arakawa Y, Saito S, Agawa M, Kano Y, Horiguchi-Yamada J. Depsipeptide-resistant KU812 cells show reversible P-glycoprotein expression, hyper-acetylated histones, and modulated gene expression profile. *Leuk Res*. 2006;30(6):723-734.
164. Dedes KJ, Dedes I, Imesch P, von Bueren AO, Fink D, Fedier A. Acquired vorinostat resistance shows partial cross-resistance to 'second-generation' HDAC inhibitors and correlates with loss of histone acetylation and apoptosis but not with altered HDAC and HAT activities. *Anticancer Drugs*. 2009;20(5):321-333.
165. Fiskus W, Rao R, Fernandez P, et al. Molecular and biologic characterization and drug sensitivity of pan-histone deacetylase inhibitor-resistant acute myeloid leukemia cells. *Blood*. 2008;112(7):2896-2905.
166. Callaghan R, Luk F, Bebawy M. Inhibition of the Multidrug Resistance P-Glycoprotein: Time for a Change of Strategy? *Drug Metabolism and Disposition*. 2014;42(4):623-631.
167. Dannenberg JH, Berns A. Drugging drug resistance. *Cell*. 2010;141(1):18-20.
168. Vijayaraghavalu S, Dermawan JK, Cheriyath V, Labhasetwar V. Highly synergistic effect of sequential treatment with epigenetic and anticancer drugs to overcome drug resistance in breast cancer cells is mediated via activation of p21 gene expression leading to G2/M cycle arrest. *Mol Pharm*. 2013;10(1):337-352.
169. Segura-Pacheco B, Perez-Cardenas E, Taja-Chayeb L, et al. Global DNA hypermethylation-associated cancer chemotherapy resistance and its reversion with the demethylating agent hydralazine. *J Transl Med*. 2006;4:32.
170. Klose RJ, Zhang Y. Regulation of histone methylation by demethylimination and demethylation. *Nat Rev Mol Cell Biol*. 2007;8(4):307-318.
171. Lan F, Shi Y. Epigenetic regulation: methylation of histone and non-histone proteins. *Sci China C Life Sci*. 2009;52(4):311-322.

172. Rice KL, Hormaeche I, Licht JD. Epigenetic regulation of normal and malignant hematopoiesis. *Oncogene*. 2007;26(47):6697-6714.
173. Barth TK, Imhof A. Fast signals and slow marks: the dynamics of histone modifications. *Trends in Biochemical Sciences*;35(11):618-626.
174. Mozzetta C, Boyarchuk E, Pontis J, Ait-Si-Ali S. Sound of silence: the properties and functions of repressive Lys methyltransferases. *Nat Rev Mol Cell Biol*. 2015;16(8):499-513.
175. Dawson Mark A, Kouzarides T. Cancer Epigenetics: From Mechanism to Therapy. *Cell*;150(1):12-27.
176. Varier RA, Timmers HT. Histone lysine methylation and demethylation pathways in cancer. *Biochim Biophys Acta*. 2011;1:75-89.
177. Kooistra SM, Helin K. Molecular mechanisms and potential functions of histone demethylases. *Nat Rev Mol Cell Biol*. 2012;13(5):297-311.
178. Torres IO, Kuchenbecker KM, Nnadi CI, Fletterick RJ, Kelly MJ, Fujimori DG. Histone demethylase KDM5A is regulated by its reader domain through a positive-feedback mechanism. *Nat Commun*. 2015;6:6204.
179. Agger K, Cloos PA, Rudkjaer L, et al. The H3K27me3 demethylase JMJD3 contributes to the activation of the INK4A-ARF locus in response to oncogene- and stress-induced senescence. *Genes Dev*. 2009;23(10):1171-1176.
180. Di Lorenzo A, Bedford MT. Histone arginine methylation. *FEBS Lett*. 2011;585(13):2024-2031.
181. Migliori V, Muller J, Phalke S, et al. Symmetric dimethylation of H3R2 is a newly identified histone mark that supports euchromatin maintenance. *Nat Struct Mol Biol*. 2012;19(2):136-144.
182. Yang Y, Bedford MT. Protein arginine methyltransferases and cancer. *Nat Rev Cancer*. 2013;13(1):37-50.
183. Mujtaba S, Zeng L, Zhou MM. Structure and acetyl-lysine recognition of the bromodomain. *Oncogene*. 0000;26(37):5521-5527.
184. Yap KL, Zhou M-M. Structure and Mechanisms of Lysine Methylation Recognition by the Chromodomain in

Gene Transcription. *Biochemistry*. 2011;50(12):1966-1980.
185. Lachner M, O'Carroll D, Rea S, Mechtler K, Jenuwein T. Methylation of histone H3 lysine 9 creates a binding site for HP1 proteins. *Nature*. 2001;410(6824):116-120.
186. Kia SK, Gorski MM, Giannakopoulos S, Verrijzer CP. SWI/SNF Mediates Polycomb Eviction and Epigenetic Reprogramming of the INK4b-ARF-INK4a Locus. *Molecular and Cellular Biology*. 2008;28(10):3457-3464.
187. Peterson CL. Chromatin remodeling enzymes: taming the machines: Third in review series on chromatin dynamics. *EMBO Reports*. 2002;3(4):319-322.
188. Schuettengruber B, Chourrout D, Vervoort M, Leblanc B, Cavalli G. Genome Regulation by Polycomb and Trithorax Proteins. *Cell*. 2007;128(4):735-745.
189. Campos EI, Reinberg D. Histones: annotating chromatin. *Annu Rev Genet*. 2009;43:559-599.
190. Migliori V, Müller J, Phalke S, et al. Symmetric dimethylation of H3R2 is a newly identified histone mark that supports euchromatin maintenance. *Nat Struct Mol Biol*. 2012;19(2):136-144.
191. Guenova E, Hoetzenecker W, Rozati S, Levesque MP, Dummer R, Cozzio A. Novel therapies for cutaneous T-cell lymphoma: what does the future hold? *Expert Opin Investig Drugs*. 2014;23(4):457-467.
192. Chang MB, Weaver AL, Brewer JD. Cutaneous T-cell lymphoma in patients with chronic lymphocytic leukemia: clinical characteristics, temporal relationships, and survival data in a series of 14 patients at Mayo Clinic. *Int J Dermatol*. 2014;53(8):966-970.
193. Jawed SI, Myskowski PL, Horwitz S, Moskowitz A, Querfeld C. Primary cutaneous T-cell lymphoma (mycosis fungoides and Sezary syndrome): part I. Diagnosis: clinical and histopathologic features and new molecular and biologic markers. *J Am Acad Dermatol*. 2014;70(2):205 e201-216; quiz 221-202.
194. DeSimone JA, Sodha P, Ignatova D, Dummer R, Cozzio A, Guenova E. Recent advances in primary cutaneous T-cell lymphoma. *Curr Opin Oncol*. 2015;27(2):128-133.

195. McGraw AL. Romidepsin for the treatment of T-cell lymphomas. *Am J Health Syst Pharm*. 2013;70(13):1115-1122.
196. Wang L, Ni X, Covington KR, et al. Genomic profiling of Sezary syndrome identifies alterations of key T cell signaling and differentiation genes. *Nat Genet*. 2015;47(12):1426-1434.
197. da Silva Almeida AC, Abate F, Khiabanian H, et al. The mutational landscape of cutaneous T cell lymphoma and Sezary syndrome. *Nat Genet*. 2015;47(12):1465-1470.
198. Foss F. Overview of cutaneous T-cell lymphoma: prognostic factors and novel therapeutic approaches. *Leuk Lymphoma*. 2003;44 Suppl 3:S55-61.
199. Fantin VR, Richon VM. Mechanisms of resistance to histone deacetylase inhibitors and their therapeutic implications. *Clin Cancer Res*. 2007;13(24):7237-7242.
200. Gottesman MM, Fojo T, Bates SE. Multidrug resistance in cancer: role of ATP-dependent transporters. *Nat Rev Cancer*. 2002;2(1):48-58.
201. Ni X, Li L, Pan G. HDAC inhibitor-induced drug resistance involving ATP-binding cassette transporters (Review). *Oncol Lett*. 2015;9(2):515-521.
202. Luqmani YA. Mechanisms of drug resistance in cancer chemotherapy. *Med Princ Pract*. 2005;14 Suppl 1:35-48.
203. Chakraborty AR, Robey RW, Luchenko VL, et al. MAPK pathway activation leads to Bim loss and histone deacetylase inhibitor resistance: rationale to combine romidepsin with an MEK inhibitor. *Blood*. 2013;121(20):4115-4125.
204. To KK, Polgar O, Huff LM, Morisaki K, Bates SE. Histone modifications at the ABCG2 promoter following treatment with histone deacetylase inhibitor mirror those in multidrug-resistant cells. *Mol Cancer Res*. 2008;6(1):151-164.
205. Robey RW, Zhan Z, Piekarz RL, Kayastha GL, Fojo T, Bates SE. Increased MDR1 expression in normal and malignant peripheral blood mononuclear cells obtained from patients receiving depsipeptide (FR901228, FK228, NSC630176). *Clin Cancer Res*. 2006;12(5):1547-1555.

206. Kim YK, Kim NH, Hwang JW, et al. Histone deacetylase inhibitor apicidin-mediated drug resistance: involvement of P-glycoprotein. *Biochem Biophys Res Commun*. 2008;368(4):959-964.
207. Xiao JJ, Foraker AB, Swaan PW, et al. Efflux of depsipeptide FK228 (FR901228, NSC-630176) is mediated by P-glycoprotein and multidrug resistance-associated protein 1. *J Pharmacol Exp Ther*. 2005;313(1):268-276.
208. Mann DL, O'Brien SJ, Gilbert DA, et al. Origin of the HIV-susceptible human CD4+ cell line H9. *AIDS Res Hum Retroviruses*. 1989;5(3):253-255.
209. Klein E, Klein G, Nadkarni JS, Nadkarni JJ, Wigzell H, Clifford P. Surface IgM-kappa specificity on a Burkitt lymphoma cell in vivo and in derived culture lines. *Cancer Res*. 1968;28(7):1300-1310.
210. Tsuchiya S, Kobayashi Y, Goto Y, et al. Induction of maturation in cultured human monocytic leukemia cells by a phorbol diester. *Cancer Res*. 1982;42(4):1530-1536.
211. Sugarman BJ, Aggarwal BB, Hass PE, Figari IS, Palladino MA, Jr., Shepard HM. Recombinant human tumor necrosis factor-alpha: effects on proliferation of normal and transformed cells in vitro. *Science*. 1985;230(4728):943-945.
212. Koeffler HP, Golde DW. Human myeloid leukemia cell lines: a review. *Blood*. 1980;56(3):344-350.
213. Hallek M, Cheson BD, Catovsky D, et al. Guidelines for the diagnosis and treatment of chronic lymphocytic leukemia: a report from the International Workshop on Chronic Lymphocytic Leukemia updating the National Cancer Institute-Working Group 1996 guidelines. *Blood*. 2008;111(12):5446-5456.
214. Stacchini A, Aragno M, Vallario A, et al. MEC1 and MEC2: two new cell lines derived from B-chronic lymphocytic leukaemia in prolymphocytoid transformation. *Leukemia Research*. 1999;23(2):127-136.
215. de Jonge HJM, Fehrmann RSN, de Bont E, et al. Evidence Based Selection of Housekeeping Genes. *PLoS ONE*. 2007;2(9).
216. Heider U, Rademacher J, Lamottke B, et al. Synergistic interaction of the histone deacetylase inhibitor SAHA with the proteasome inhibitor bortezomib in

cutaneous T cell lymphoma. *Eur J Haematol*. 2009;82(6):440-449.
217. Piotrowska H, Jagodzinski PP. Trichostatin A, sodium butyrate, and 5-aza-2'-deoxycytidine alter the expression of glucocorticoid receptor α and β isoforms in Hut-78 T- and Raji B-lymphoma cell lines. *Biomedicine & Pharmacotherapy*. 2007;61(7):451-454.
218. Shi H, Guo J, Duff DJ, et al. Discovery of novel epigenetic markers in non-Hodgkin's lymphoma. *Carcinogenesis*. 2006;28(1):60-70.
219. Piekarz RL, Robey RW, Zhan Z, et al. T-cell lymphoma as a model for the use of histone deacetylase inhibitors in cancer therapy: impact of depsipeptide on molecular markers, therapeutic targets, and mechanisms of resistance. *Blood*. 2004;103(12):4636-4643.
220. Hemshekhar M, Sebastin Santhosh M, Kemparaju K, Girish KS. Emerging Roles of Anacardic Acid and Its Derivatives: A Pharmacological Overview. *Basic & Clinical Pharmacology & Toxicology*. 2012;110(2):122-132.
221. Eliseeva ED, Valkov V, Jung M, Jung MO. Characterization of novel inhibitors of histone acetyltransferases. *Mol Cancer Ther*. 2007;6(9):2391-2398.
222. Sung B, Pandey MK, Ahn KS, et al. Anacardic acid (6-nonadecyl salicylic acid), an inhibitor of histone acetyltransferase, suppresses expression of nuclear factor-kappaB-regulated gene products involved in cell survival, proliferation, invasion, and inflammation through inhibition of the inhibitory subunit of nuclear factor-kappaBalpha kinase, leading to potentiation of apoptosis. *Blood*. 2008;111(10):4880-4891.
223. Bertino EM, Otterson GA. Romidepsin: a novel histone deacetylase inhibitor for cancer. *Expert Opin Investig Drugs*. 2011;20(8):1151-1158.
224. Frye R, Myers M, Axelrod KC, et al. Romidepsin: a new drug for the treatment of cutaneous T-cell lymphoma. *Clin J Oncol Nurs*. 2012;16(2):195-204.
225. Kim M, Thompson LA, Wenger SD, O'Bryant CL. Romidepsin: a histone deacetylase inhibitor for refractory cutaneous T-cell lymphoma. *Ann Pharmacother*. 2012;46(10):1340-1348.

226. Lee JH, Choy ML, Marks PA. Mechanisms of resistance to histone deacetylase inhibitors. *Adv Cancer Res*. 2012;116:39-86.
227. Lyseng-Williamson KA, Yang LP. Romidepsin: a guide to its clinical use in cutaneous T-cell lymphoma. *Am J Clin Dermatol*. 2012;13(1):67-71.
228. Hauswald S, Duque-Afonso J, Wagner MM, et al. Histone deacetylase inhibitors induce a very broad, pleiotropic anticancer drug resistance phenotype in acute myeloid leukemia cells by modulation of multiple ABC transporter genes. *Clin Cancer Res*. 2009;15(11):3705-3715.
229. Huang Y, Nayak S, Jankowitz R, Davidson NE, Oesterreich S. Epigenetics in breast cancer: what's new? *Breast Cancer Res*. 2011;13(6):225.
230. Lee MG, Wynder C, Schmidt DM, McCafferty DG, Shiekhattar R. Histone H3 lysine 4 demethylation is a target of nonselective antidepressive medications. *Chem Biol*. 2006;13(6):563-567.
231. Nightingale KP, Gendreizig S, White DA, Bradbury C, Hollfelder F, Turner BM. Cross-talk between histone modifications in response to histone deacetylase inhibitors: MLL4 links histone H3 acetylation and histone H3K4 methylation. *J Biol Chem*. 2007;282(7):4408-4416.
232. Lee YH, Ma H, Tan TZ, et al. Protein arginine methyltransferase 6 regulates embryonic stem cell identity. *Stem Cells Dev*. 2012;21(14):2613-2622.
233. Banelli B, Carra E, Barbieri F, et al. The histone demethylase KDM5A is a key factor for the resistance to temozolomide in glioblastoma. *Cell Cycle*. 2015;14(21):3418-3429.
234. Sharma SV, Lee DY, Li B, et al. A chromatin-mediated reversible drug-tolerant state in cancer cell subpopulations. *Cell*. 2010;141(1):69-80.
235. He J, Liu H, Chen Y. Effects of trichostatin A on HDAC8 expression, proliferation and cell cycle of Molt-4 cells. *J Huazhong Univ Sci Technolog Med Sci*. 2006;26(5):531-533.
236. Wu J, Du C, Lv Z, et al. The up-regulation of histone deacetylase 8 promotes proliferation and inhibits apoptosis in hepatocellular carcinoma. *Dig Dis Sci*. 2013;58(12):3545-3553.

237. Song S, Wang Y, Xu P, et al. The inhibition of histone deacetylase 8 suppresses proliferation and inhibits apoptosis in gastric adenocarcinoma. *Int J Oncol*. 2015;47(5):1819-1828.
238. Chakrabarti A, Oehme I, Witt O, et al. HDAC8: a multifaceted target for therapeutic interventions. *Trends in Pharmacological Sciences*. 2015;36(7):481-492.
239. Moreno D, Salomão KD, Cruzeiro GA, et al. 953: HDAC9 inhibition decreases cell proliferation in acute lymphoblastic leukemia. *European Journal of Cancer*. 2014;50, Supplement 5:S232.
240. Zhao Y-X, Wang Y-S, Cai Q-Q, Wang J-Q, Yao W-T. Up-regulation of HDAC9 promotes cell proliferation through suppressing p53 transcription in osteosarcoma. *International Journal of Clinical and Experimental Medicine*. 2015;8(7):11818-11823.
241. Lapierre M, Linares A, Dalvai M, et al. Histone deacetylase 9 regulates breast cancer cell proliferation and the response to histone deacetylase inhibitors. *Oncotarget*. 2016.
242. Majumdar G, Adris P, Bhargava N, Chen H, Raghow R. Pan-histone deacetylase inhibitors regulate signaling pathways involved in proliferative and pro-inflammatory mechanisms in H9c2 cells. *BMC Genomics*. 2012;13:709.
243. Newbold A, Salmon JM, Martin BP, Stanley K, Johnstone RW. The role of p21(waf1/cip1) and p27(Kip1) in HDACi-mediated tumor cell death and cell cycle arrest in the Emu-myc model of B-cell lymphoma. *Oncogene*. 2014;33(47):5415-5423.
244. Benedetti R, Conte M, Altucci L. Targeting Histone Deacetylases in Diseases: Where Are We? *Antioxid Redox Signal*. 2015;23(1):99-126.
245. Mensah AA, Kwee I, Gaudio E, et al. Novel HDAC inhibitors exhibit pre-clinical efficacy in lymphoma models and point to the importance of CDKN1A expression levels in mediating their anti-tumor response. *Oncotarget*. 2015;6(7):5059-5071.
246. Yi TZ, Li J, Han X, et al. DNMT inhibitors and HDAC inhibitors regulate E-cadherin and Bcl-2 expression in endometrial carcinoma in vitro and in vivo. *Chemotherapy*. 2012;58(1):19-29.

247. Pfeiffer MM, Burow H, Schleicher S, Handgretinger R, Lang P. Influence of Histone Deacetylase Inhibitors and DNA-Methyltransferase Inhibitors on the NK Cell-Mediated Lysis of Pediatric B-Lineage Leukemia. *Front Oncol*. 2013;3:99.
248. Xu W, Li Z, Yu B, et al. Effects of DNMT1 and HDAC inhibitors on gene-specific methylation reprogramming during porcine somatic cell nuclear transfer. *PLoS One*. 2013;8(5):e64705.
249. Susanto JM, Colvin EK, Pinese M, et al. The epigenetic agents suberoylanilide hydroxamic acid and 5AZA2' deoxycytidine decrease cell proliferation, induce cell death and delay the growth of MiaPaCa2 pancreatic cancer cells in vivo. *Int J Oncol*. 2015;46(5):2223-2230.
250. Xu P, Hu G, Luo C, Liang Z. DNA methyltransferase inhibitors: an updated patent review (2012-2015). *Expert Opin Ther Pat*. 2016;26(9):1017-1030.
251. Stintzing S, Kemmerling R, Kiesslich T, Alinger B, Ocker M, Neureiter D. Myelodysplastic syndrome and histone deacetylase inhibitors: "to be or not to be acetylated"? *J Biomed Biotechnol*. 2011;2011:214143.